The Hong Kong Polytechnic University

Department of Industrial Systems and Engineering

Optimization of Titanium Nitride and Chromium Nitride PVD Coating Process for Toolings

By

YIM Siu Lan

A thesis submitted in partial fulfillment of the requirements for
the Degree of Master of Philosophy at
The Hong Kong Polytechnic University

March   2006

CERTIFICATE OF ORIGINALITY

I hereby declare that this thesis is my own work and that, to the best of my knowledge and belief, it reproduces no material previously published or written nor material which has been accepted for the award of any other degree or diploma, except where due acknowledgements has been made in the text.

_____

YIM Siu Lan (嚴少蘭)

ABSTRACT

In the last two decades, Cathodic Arc Physical Vapour Deposition (CAPVD) coating is widely used in cutting tools such as endmills, drills and cutting inserts. Many researches pointed out the advantages of using coated cutting tools for interrupting cutting. Some researches were carried out to investigate the influence of the bias voltage, arc current, and nitrogen pressure to coating structure, hardness, and surface morphology of coating for mainly cutting tool materials like tungsten carbide and high speed steel (HSS).

However, no study was carried out to obtain the optimization windows for different kinds of CAPVD coating for moulds and dies. From previous researches, the optimization parameters of CAPVD were bias voltage, nitrogen pressure, acetylene pressure, coating thickness, and target composition. Two most popular coatings, titanium nitride (TiN) and chromium nitride (CrN) for Hong Kong moulds and dies industry, were selected for this study.

The main apparatus was the PLATIT PL 50 of PLATIT AG cathodic arc deposition system. Ball crater was used to find the substrate coating thickness. And a surface profilometer was used for finding the mean roughness value (R_a). The Daimler-Benz Rockwell-C adhesion test method was used to investigate the adhesion of coating. After that, Scanning Electron Microscope was used to analyze the surface morphology of the coating.

This study was aimed to find the optimal region for surface roughness of TiN and CrN coating. By using cause-and-effect diagram, the coating parameters that affect the coatings were identified. They are bias voltage, arc current, nitrogen pressure, and coating time.

In this study, Taguchi method was used as screening experiment to find the near optimum region. For further optimization, the Response Surface Method (RSM) was used to help finding out the optimal region. First, a first-order model was determined. Then, steepest ascent experiments were used to obtain the middle point of the first-order regression model. After that a new first-order model was found. And finally, the second-order model was obtained.

From Taguchi analysis of TiN coating, roughness test had been conducted for optimization. It was found that the bias voltage was the most critical factor to affect the roughness value whereas the arc current shows less interaction. For CrN coating, the nitrogen pressure was the most critical factor to affect roughness value whereas the coating time shows less interaction.

From RSM analysis, for TiN coating, the optimal point was at (0.384, 0.091), where bias voltage = -115V and nitrogen pressure = 9.54 x 10E-03 mbar. And this point was a minimum point. For CrN coating, the optimal point was at (1.061, -0.063), where bias voltage = -121V and nitrogen pressure = 9.46 x 10E-03 mbar. And this was a minimum point.

For future work, evolutionary solution is suggested to run RSM in a real production size and practice. Furthermore, a multi-characteristic response method using Taguchi method and utility concept together may help to find out the optimal condition when several characteristics are needed to consider at the same time.

LIST OF PUBLICATION

Journal Paper

S.L. Yim, K.M. Yu, D. Kwok and T.C. Lee, "Taguchi methods to optimize TiN coating surface roughness", Materials Science Forum, Vol. 471 - 472, p.891- 894, 2003.

S.L. Yim, K.M. Yu, D. Kwok, L.C. Chan and T.C. Lee, "Optimizing TiN coating surface roughness with RSM", "Materials Science Forum, Vol. 532 - 533, p.424- 427, 2006.

Conference Paper

S.L. Yim, K.M. Yu, D. Kwok and T.C. Lee, "Taguchi methods to optimize TiN coating surface roughness", 11th International Manufacturing Conference (IMCC2004), September 18th – 20th 2004, Jinan, China.

S.L. Yim, K.M. Yu, D. Kwok, L.C. Chan and T.C. Lee, "Optimizing TiN coating surface roughness with RSM", 12th International Manufacturing Conference (IMCC2006), September 21st – 23rd 2006, Xian, China.

ACKNOWLEDGEMENTS

I would like to take the opportunity here to express my sincere thanks to my chief supervisor, Dr. K.M. Yu, for his valuable guidance and assistance throughout the study. Thanks also go to my co-supervisors, Prof. T.C. Lee and Dr. L.C. Chan, for their professional suggestions and comments.

The work described in this research is supported by a grant from the Techmart Platit Limited, The Hong Kong Polytechnic University, and the Innovation and Technology Commission (ITC) of the government Hong Kong Special Administrative Region (HKSAR).

I would also like to acknowledge Mr. David Kwok, the President of Techmart Platit Limited for providing valuable assistances and supports. Also, I would like to thank my colleagues in Techmart Platit Limited and PLATIT AG for their thoughtful discussions and assistances.

Last but not the least, I would like to thank my family and my schoolmates in the Department of Industrial and Systems Engineering for their support throughout the study.

TABLE OF CONTENTS

LIST OF FIGURES

LIST OF TABLES

LIST OF ABBREVIATIONS

%	**Percentage**
°C	**Degree Celsius**
μm	**Micron / micrometer**
AFM	**Atomic force microscope**
Al	**Aluminum**
AlTiN	**Aluminum titanium nitride**
ANOVA	**Analysis of variance**
at. %	**Atomic percentage**
C	**Carbon**
C_2H_2	**Acetylene**
CAPVD	**Cathodic arc physical vapor deposition**
CBC	**Carbon Based Coating**
CNC	**Computer numerical control**
Cr	**Chromium**
CrN	**Chromium nitride**
CrN-CBC	**Chromium nitride + Carbon based coating**
CVD	**Chemical vapor deposition**
DC	**Direct current**
DLC	**Diamond like carbon**
DOE	**Design of experiments**
EDM	**Electrical discharge machining**
HRC	**Hardness Rockwell C**
HSS	**High speed steel**
A	**Ampere**
IAD	**Ion assisted deposition**
IBAD	**Ion beam assisted deposition**
IVD	**Ion vapor deposition**
L_9	**(3^4) Orthogonal array**
min/s	**Minutes per second**
mbar	**Millibar**
Mn	**Manganese**

Mo	Molybdenum
N_2	Nitrogen
Off-line QC	Off-line quality control
On-line QC	On-line quality control
PVD	Physical vapor deposition
QC	Quality control
R	Regression ratio
R_{adj}	Adjusted regression ratio
R_a	Mean roughness value
RP	Rapid prototype
S/N	Signal-to-noise
sccm	Second / centimeter^3
SEM	Scanning electron microscope
Si	Silicon
TEPA	Tetrapentyl-Ammonium
Ti	Titanium
Ti/Al	Titanium aluminum
TiAlCN	Titanium aluminum carbon nitride
TiAlN	Titanium aluminum nitride
TiCN	Titanium carbon nitride
TiCN-MP	Titanium carbon nitride – Multipurpose
TiN	Titanium nitride
TiN-CBC	Titanium + Carbon based coating
V	Voltage
V	Vanadium
Zr	Zirconium
ZrN	Zirconium nitride

CHAPTER 1 INTRODUCTION

1.1 Background of Study

Environmental protection is an essential and emergent task in today's manufacturing industry. Many organizations and regulations are founded to protect and maintain our world natural. 'Clean' technologies in all aspects of industrial manufacturing today is encouraged and initiated by environmental law and different countries all over the world.

In manufacturing, metal finishing operation including electroless and electroplating process produces high ratio of toxic wastes. To reduce pollution to our environment, there are many available 'clean' technologies to replace the plating technology. The highest consideration has been focused on physical vapor deposition (PVD), chemical vapor deposition (CVD), and thermal spraying. Although these technologies are not waste free processes, their pollution to our environment is much less than electroless and electroplating.

Techmart Platit Limited, founded in 2001, is the first functional PVD coating center in Hong Kong. It provides technical support of equipments and coating services to Hong Kong, China, and South East Asia customers. Techmart Platit Limited is the Asia representative of Plait AG, which is part of Blösch Corporated Inc. (BCI) Group, founded in 1947 Switzerland.

Since 1947, the main business of BCI group is to provide different coatings like

electroplating, CVD and PVD to different industries, such as watch industry and optical industry. The applications are mainly for decorative purposes.
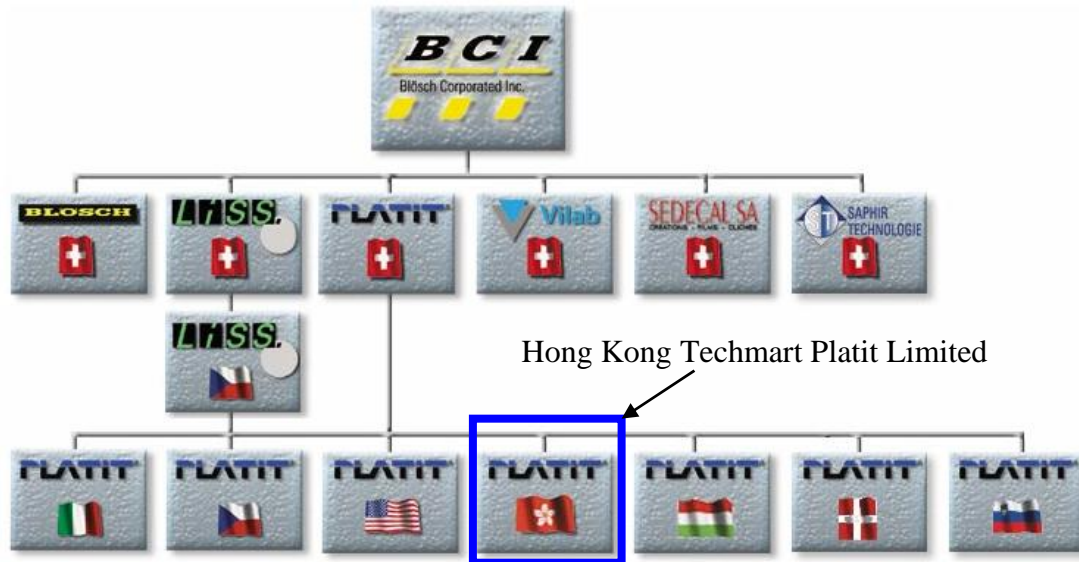
Figure 1.1: Organization chart of BCI group, Platit AG, and Hong Kong Techmart Platit Limited.

Platit AG (Switzerland)

In 1993, Platit AG was founded to provide hard PVD coating for industrial applications. Their main focus is on toolings. Cutting tools like end mills, drills, cutting inserts, taps and saw cutters, moulds and components that require high wear resistances are the main coating substrates.

Figure 1.2: End mills coated with titanium nitride.

Figure 1.3: Drills coated with titanium aluminum nitride.

Figure 1.4: Bearings, gears, and shafts coated with carbon based coating for lubrication purpose.

Figure 1.5: Cutting inserts coated with titanium nitride and titanium aluminum nitride.
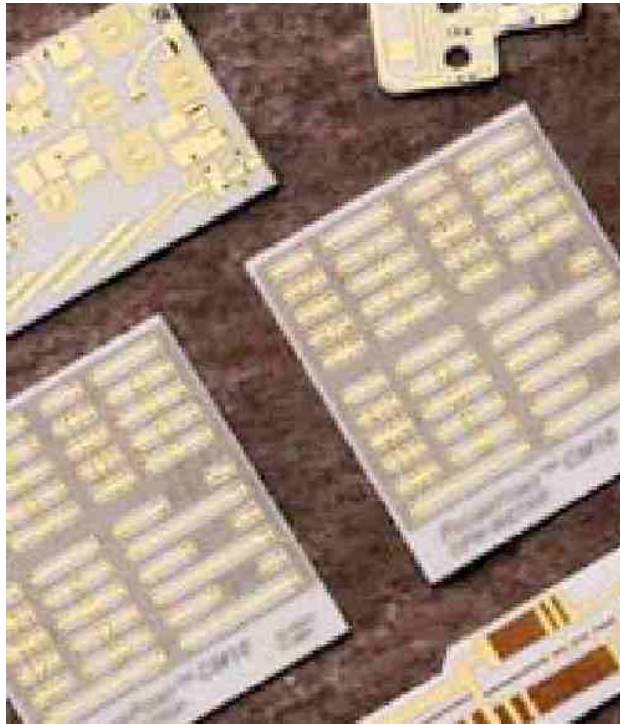
Figure1.6: Coating applies to electronic parts.

Figure1.7: Coating can increase the wear resistance of the implant materials or to provide an implant surface (Zircotec).

Techmart Platit Limited (Hong Kong)

Associated with Switzerland Platit AG, Techmart Platit is the first functional PVD coating center in Hong Kong. Since 2001, the Hong Kong operation has been providing coating equipment and coating services to mould and die and cutting tool industries in Hong Kong and China. For example, punches and die, plastic injection moulds, forming dies, die cast mould, drills, end mills, etc.

The customers of Platit AG and Techmart Platit are different since industrial development of Switzerland, are dissimilar in Hong Kong and China. The former customers mainly come from the watch industry and cutting tool manufacturers but the latter customers come from different industries like watch bands and casing manufacturers, mould making manufacturers, plastic product manufacturers, etc. The information and problems solving solutions that can be shared from Platit AG to Techmart Platit is not enough due to the market gap between them. Today, Techmart Platit has to solve problems and find the best solutions themselves for their customers who are mainly coating plastic injection moulds, die-casting moulds, stamping punches and dies, and cutting tools.

Techmart Platit provides mainly eleven standard coatings for their customers. Each coating has its own properties for different working purpose. The coatings are:

a. Titanium nitride (TiN)

Titanium nitride (TiN) is a common and the "oldest" coating being used for toolings. It provides an attractive "golden" color. When a titanium (Ti) target material is evaporated in vacuum chamber, nitrogen (N_2) is injected into the chamber. The Ti^{+2} ions are then reacted with N_2 to form TiN.

b. Chromium nitride (CrN)

Chromium nitride, which has better corrosion resistance than other coatings, is in grey color. Again, Cr^{+2} ions will react with nitrogen to form chromium nitride. It usually coats plastic injection mould for preventing corrosion.

c. Titanium carbon nitride (TiCN)

Titanium carbon nitride is a blue-grey multi-layer coating. In coating chamber, titanium ions will react with two reactive gases, nitrogen (N_2) and acetylene (C_2H_2) to form titanium carbon nitride coating. It provides high wear resistance to toolings and high toughness. Therefore, this coating is usually used in mould and die applications like forming, deep drawing, and stamping processes.

d. Titanium carbon nitride – multipurpose (TiCN-MP)

Titanium carbon nitride – multipurpose (TiCN-MP) is an adjusted coating from titanium carbon nitride. Both Titanium carbon nitride and titanium carbon nitride-multipurpose is around 0.2 in coefficient (fretting) of friction. The hardness of titanium carbon nitride is higher than that of TiCN-MP but the toughness of TiCN-MP is better than that of titanium carbon nitride.

e. Titanium aluminum nitride (TiAlN)

Titanium aluminum nitride coating is another titanium based coating that is mainly applied to cutting tools like endmills, drills, saw blades and cutting inserts. The atomic percentage (at. %) of titanium/aluminum (Ti/Al) target is 50% titanium (Ti) and 50% aluminum (Al).

f. Titanium aluminum carbon nitride (TiAlCN)

The atomic percentage (at. %) of titanium/aluminum (Ti/Al) target is 25% Ti and 75% Al. It is usually used for metal mould and cutting tools.

g. Aluminum titanium nitride (AlTiN)

The atomic percentage (at. %) ratio of aluminum/titanium (Al/Ti) target is 67% aluminum and 33% titanium. The high aluminum content coating provides an extremely high heat resistance function (maximum usage temperature is 800°C).

Therefore, this coating is usually applied for high-speed cutting in computer numerical control (CNC) machines.

h. Titanium nitride + carbon based coating (TiN - CBC)

This is a multilayer coating. The first deposited coating is titanium and the outer layer is carbon-based coating (CBC). This coating provides a smooth surface and the friction of coefficient is low.

i. Chromium nitride + carbon based coating (CrN-CBC)

Chromium nitride + carbon based coating (CrN-CBC) is also a multilayer coating. The base coating is chromium nitride and the CBC layer is deposited on the CrN layer. This coating has an anti-corrosion property and the surface is smooth.

j. Zirconium Nitride (ZrN)

Zirconium Nitride (ZrN) coating is in pale yellow color. The properties are similar to titanium nitride. Not many coating centre provides this type of coating as the coating becomes popular only in these few years.

k. Nano-composite Coating (nACo)

In nano-composite coatings, nano-crystalline grains like aluminum titanium nitride and titanium aluminum nitride can be embedded into an amorphous matrix like Si_3N_4, which realizes an enormously compact and resistant structure like that of a beehive.
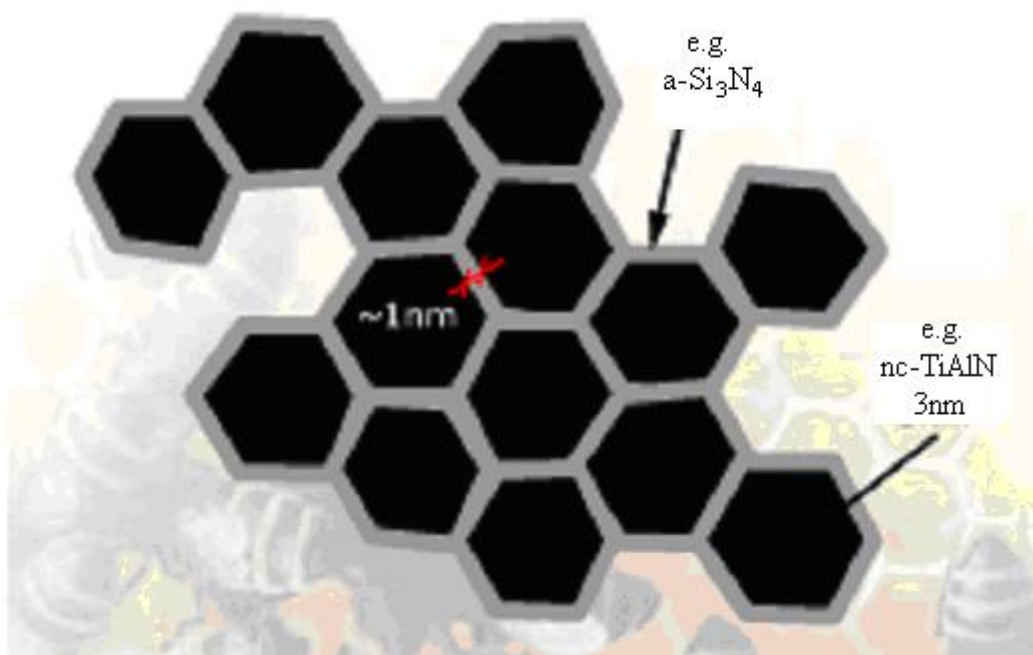
Figure 1.8 Example of nano-composite coating structure (PLATIT AG).

In 2005, Techmart Platit introduces the nano-composites coating to Hong Kong and China market. The nano-composites coating is mainly applied to cutting tools for increasing the tool life and cutting performance.

Figure 1.9: PLATIT PL 50 Cathodic Arc Physical Vapor Deposition (CAPVD) system

(PLATIT AG).

1.2 Coating Applications and Their Properties

Thin film deposition process being applied included the following application:

a. Metal electrical conductor films, such as in PCB and semiconductor industry;

b. Optical films for transmission and reflection, e.g. glasses and plastics;

c. Decorative films such as coating watch band, door handles, and glass frame;

d. Corrosion resistant films;

e. Wear and erosion resistant coatings for cutting tools and mould;

f. Dry film lubricants such as coating on bearings and shaft for lubrication.

Coatings have many useful applications that depend on the actual requirements of the working conditions. Moreover, different coatings have different physical properties. The different general properties of coatings are listed in Table 1.2.

Properties of coatings	Coatings									
	TiN	TiCN	TiCN-MP	TiAlN	AlTiN	ZrN	CrN	TiN-CBC & CrN-CBC	TiAlCN	nACo
Nano-hardness (GPa)	24	37	32	35	38	28	18	20	28	45
Friction (fretting) coefficient	0.55	0.2	0.2	0.5	0.7	0.5	0.3	0.15	0.25	0.45
Maximum working temperature (°C)	600	400	400	800	800	600	700	400	500	1200
Coating color	Golden yellow	Blue-ray	Light red	Violet	Blue-black	Pale yellow	Silver	Charcoal gray	Reddish copper	Violet-blue

Table 1.1:General properties of different coatings (PLATIT AG and Techmart Platit).

Advanced Coatings Applied Research Laboratory

Advanced Coatings Applied Research Laboratory (ACARL), was established in 2000. It occupies an area of approximately 110 m^2 in the Manufacturing Engineering Laboratories of the Department of Manufacturing Engineering & Engineering Management, City University of Hong Kong. ACARL uses a different PVD coating technique from Techmart Platit. A Closed Field Unbalanced Magnetron Sputter Ion Plating (CFUMSIP) system is used to provide coating service to Hong Kong and China customers. Their technique is mainly for decorative and tooling purposes. ACARL provides five main kinds of coating: titanium nitride (TiN), titanium aluminum nitride (TiAlN), titanium doped diamond-like carbon (Ti-DLC), Graphit-IC^{TM} (Cr-DLC) and MoST^{TM}. By comparing with Techmart Platit, the selections of coatings are fewer.

Figure 1.10: Coating laboratory of Advanced Coatings Applied Research Laboratory.

The Advanced Surface Technology Development Centre of the Hong Kong Productivity Council

The Advanced Surface Technology Development Centre of the Hong Kong Productivity Council (HKPC) provides manufacturing supports and consultancy services of ion plating technology. This technology is mainly applied to decorative coating for watch and clock parts, spectacle frames, imitation jewellery, and functional coating for toolings and mechanical parts.

The Advanced Surface Technology Development Centre is a multi-institutional centre to promote advanced surface technologies to the local industry. The Centre, funded by the Innovation and Technology Fund of the Hong Kong SAR Government, serves as: 1) a virtual centre connecting various institutions to effectively promote advanced surface technologies to the industry; 2) a bridge between academics and manufacturers; 3) a framework to stimulate future market-driven research and development work and to deliver results in a timely manner to the industry.

Figure 1.11: Some coating samples from ASDC (Hong Kong Productivity Council).

Figure 1.12: Ion plating uses in decorative purpose such as door handles and watch dials (PLATIT, AG).

HKPC provides both ion plating coating services and equipment services for Hong Kong customers. Their coatings applications are divided into two groups. The first group is decorative coating. The coatings include titanium (Ti), titanium nitride (TiN), titanium nitride + gold (TiN+Au), titanium carbide (TiC), titanium aluminum nitride (TiAlN) and titanium aluminum carbon nitride (TiAlCN). The second group is functional coating: TiN and TiAlCN for toolings.

Jing Mei Group of Companies

Jing Mei Group of Companies provides mainly electroplating services and low temperature Arc Vapor Deposition in TiN coating. Coating that can be coated for tooling are fewer than Techmart Platit and the other competitors.

Their low temperature Arc Vapor Deposition (LTAVD) is suitable for plastics and low temperature tolerant metal substrates. This thin coating is usually from 0.3 to 0.5 micrometers. By comparing to Techmart Platit, their coating thickness varies from one to five micrometers. Therefore, Techmart Platit coatings provide better performance in resistant to abrasion.

Figure 1.13: TiN coating sample coated by Jing Mei (Jing Mei Group of Companies).

To increase the competence and to maintain the leadership, Techmart Platit has to increase the satisfactions of their customers by increasing the qualities of services and products.

As a young company, Techmart Platit faces the following problems:

a. what are the best or optimal coating parameters or conditions for the surface finishing especially in plastic injection moulds;

b. any effective and easy way to obtain the optimal conditions in order to improve the existing processes or new coatings.

1.3 Aims and Scope of Study

The main objective of the research is to investigate practically feasible means to optimize parameter settings in the Techmart Platit CAPVD coating for toolings. The contribution of the study is:

- to standardize and control the coating process,
- to maintain quality and characteristic of coatings and
- to decrease rejection and rework of substrates during production.

The workflow of the research is outlined in Figure1.14.

```
┌─────────────────────────────────────┐
│ Define the controllable factors for  │
│        design of experiments          │
└─────────────────────────────────────┘
                  │
                  ▼
┌─────────────────────────────────────┐
│        Carry out experiments          │
└─────────────────────────────────────┘
                  │
                  ▼
┌─────────────────────────────────────┐
│  Working out windows for optimal      │
│      process parameter settings       │
└─────────────────────────────────────┘
                  │
                  ▼
┌─────────────────────────────────────┐
│          Verify findings              │
└─────────────────────────────────────┘
```
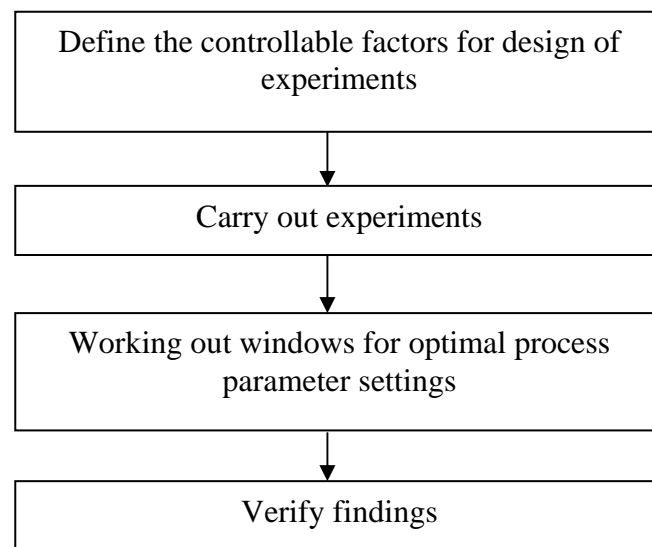
Figure 1.14: Workflow of the research.

In the study, Techmart Platit's standard CAPVD coatings, TiN and CrN are investigated to get the optimal conditions under different parameters.

1.4 Thesis Outline

In Chapter 1, an introduction covers the background of study, aims and scope of study.

In Chapter 2, a comprehensive literature review is provided, which is relevant to the research work in this dissertation, including more detailed background information of the study as well as the previous work on the coating methods. Also, clear statements of the problem to be tackled are presented.

In Chapter 3, the chosen research methodology is described in detail.

In Chapter 4, the implementation tools would be described.

In Chapter 5, the experimental results and analysis of the research are given.

In Chapter 6, the main problems encountered and future work are discussed.

Finally, conclusion is drawn in Chapter 7.

CHAPTER 2 LITERATURE SURVEY

In this chapter, coating techniques, coating parameters, coating materials and applications, and adhesion testing methods are reviewed in Section 2.1, Section 2.2, Section 2.3, and Section 2.4 respectively. Then, optimization method, problems in optimizing PVD coating and the major achievements of current research are summarized in Sections 2.5 and 2.6.

2.1 Coatings

Coatings are widely applied in many industries. Apart from tools, it can be used in electronic industries (Gupta, 2003), decorative purpose, and even of biological and surgical implants (Li *et al.*, 2003 and Mudali *et al.*). Coatings can vary from a few to several hundred microns. It can be deposited by different means. The coating, its thickness, and means of deposition will depend on the final use of the components and the environment it has to resist.

A wide variety of surface coatings are available in today industry or market. But, the most commonly used coatings are the following four:

a. Physical Vapour Deposition (PVD)

- Arc Vapour Deposition (AVD)
- Vacuum Deposition
- Sputter Deposition
- Ion plating

b.	Chemical Vapour Deposition (CVD)

c.	Electroplating, Electroless Plating, and Displacement Plating

d.	Plasma Spraying

2.1.1 Physical Vapour Deposition (PVD)

Physical Vapour Deposition (PVD) process, often just called thin film process, is an atomistic deposition process. Material is transported from solid or liquid form to atoms or molecules or transported in the form of vapour through vacuum or low pressure gaseous or plasma environment. It condenses when it contacts with the substrates. In PVD process, the deposition rate is from 1 to 10 nanometers per second (Donald, 1998; Gupta *et al.*, 2003 and Nalwa *et al.*, 2002).

PVD process can be used to deposit films of elements and alloys as well as compounds using reactive deposition processes. In case of reactive deposition, the deposition material reacts with a gaseous environment of co-deposited material to form a film of compound material, such as a nitride, oxide, carbide or carbonitride (Donald, 1998; Gupta *et al.*, 2003 and Nalwa, 2002).

The main categories of PVD processes are: arc vapour deposition, vacuum deposition, sputter deposition and ion plating. Each PVD technology generates and deposits material in a different manner and requiring equipment unique to each process. However, all processes utilize the same three essential steps to develop a coating. It includes (Donald, 1998; Jeffrey *et al.*, 2000 and John, 2000):

a. vapour phase generation from coating material stock by evaporation, sputtering, arc vaporization or chemical vapours and gases.

b. transfer of the vapour phase from source to substrate by molecular flow or vapour ionization by creating a plasma.

c. deposition and film growth on the substrates.

These steps can be independent or superimposed on each other depending on the desired coating characteristics. The result of the coating or substrate composite is a function of each material's individual property, the interaction of the materials and process constraints that may exist (Donald, 1998). Figure 2.1 shows the phase change diagram of PVD coating process.
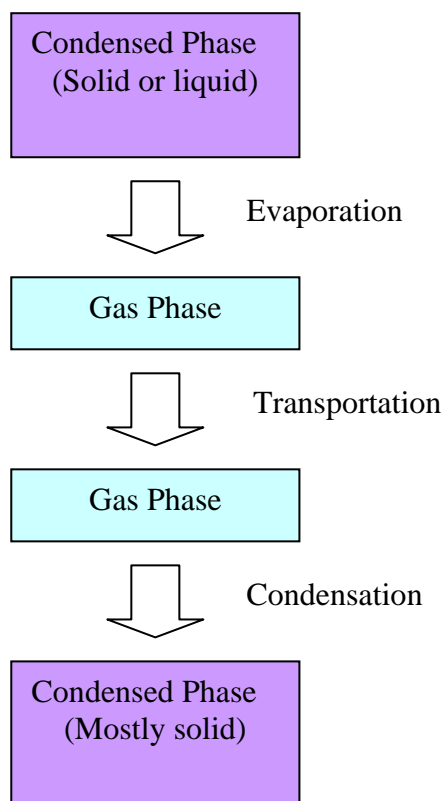
Figure 2.1: Phase change diagram of PVD coating process.

2.1.1.1 Arc Vapour Deposition (AVD)

Arc Vapour Deposition uses a high current, low–voltage arc to vaporize a cathodic electrode (cathodic arc) or anodic electrode (anodic arc) and deposit the vaporized material on a substrate. The vaporized material is highly ionized and usually the substrate is biased to accelerate the ions to the substrate surface. The extremely high ionization rate of arc vapour deposition, the cathodic arc process, deposits a very dense film with excellent adhesion to the substrate (Donald, 1998; Gupta *et al.*, 2003 and Nalwa, 2002). Therefore, this technique is mainly used to deposit material on cutting tools such as endmills, drills, inserts, moulds, and wear resistant tribology components.
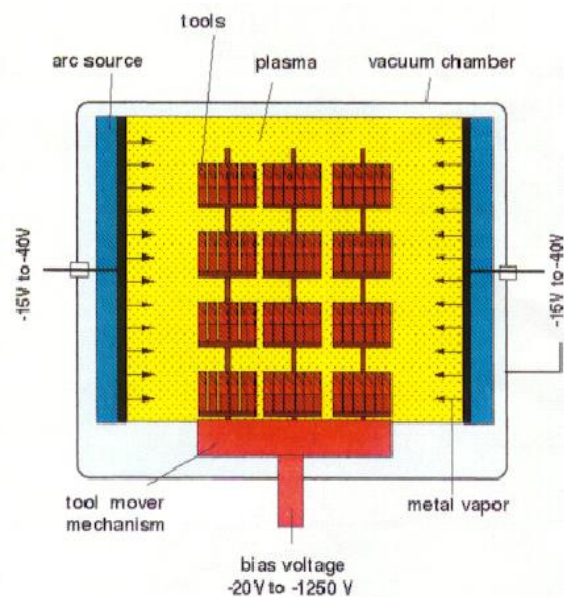
Figure 2.2: Schematic diagram of Arc Vapour Deposition (AVD).

2.1.1.2 Vacuum Deposition

Vacuum Deposition, which is sometimes called vacuum evaporation, is a PVD process in which material from a thermal vaporization source reaches the substrates with little or no collisions with gas molecules in the space between the source and substrates. The vacuum environment provides the ability to reduce gaseous contamination in the deposition system to a low level. It takes place in the gas pressure range from 0.13 E-03 mbar to 1.33 E-08 mbar depending on the level of gaseous contamination that can be tolerated in the deposition system (Donald, 1998 and Nalwa, 2002). The thermal vaporization rate can be very high compared to other vaporization method.

The material vaporized from the source has a composition, which is in proportion to the relative vapour pressure of the material in the molten source material. Thermal evaporation is generally done using thermally heated source such as tungsten wire coils or by high-energy electron beam heating of the source material itself. Generally, the substrates are mounted at an appreciable distance away from the evaporation source to reduce radiant heating of the substrate by the vaporization source (Donald, 1998 and Nalwa, 2002).

2.1.1.3 Sputter Deposition

Sputter deposition is the deposition of particles vaporized from a surface (target) by the physical sputtering process. Physical sputtering is a non-thermal vaporization process where surface atoms are physically ejected from a solid surface by momentum transfer from an atomic-sized energetic bombarding particle which is usually a gaseous ion accelerated from a plasma. This PVD process is sometimes just called sputtering (Nalwa, 2002 and John, 2000).

Comparing with vacuum deposition, the distance from source to substrate is short. Sputter deposition can be performed by energetic ion bombardment of a solid surface (sputtering target) in a vacuum using an ion gun or low-pressure plasma (<6.66E-03 mbar) where the sputtered particles suffer few or no gas phase collisions in the space between the target and the substrate (Nalwa, 2002 and John, 2000). Sputtering can also be done in a higher plasma pressure (6.66E-03 – 33.33E-03 mbar) where energetic particles sputtered or reflected from the sputtering target are "thermalized" by gas phase collisions before they reach the substrate surface. The plasma used in sputtering can be confined near the sputtering surface or may fill the region between the source and substrates (Nalwa, 2002 and John, 2000).

The sputtering source can be an element, alloy, mixture, or a compound and the material is vaporized with the bulk composition of the target. The sputtering target provides a long-lived vaporization source that can be mounted to vaporize in any direction. The presence of the plasma activates the reactive gas making it more chemically reactive.
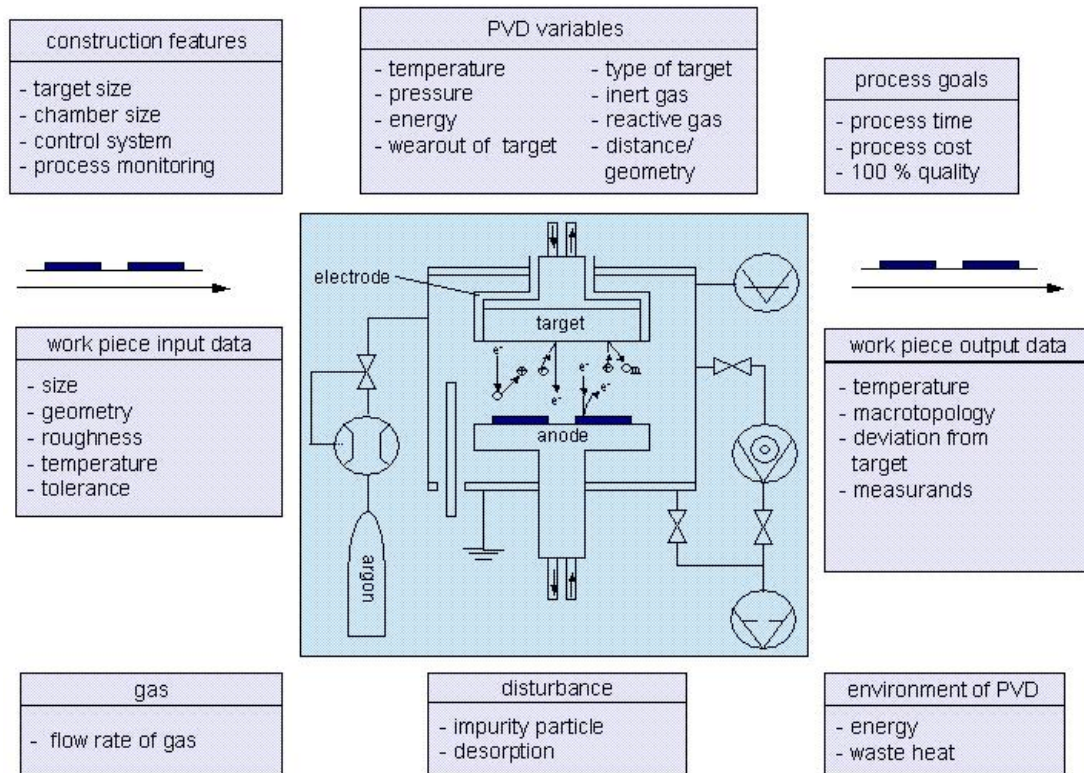
Figure 2.3: Schematic diagram for sputtering.

2.1.1.4 Ion Plating

Ion plating, which is often known as Ion Assisted Deposition (IAD) or Ion Vapour Deposition (IVD), utilizes concurrent or periodic modifies and controls the properties of the deposition film. In ion plating, the energy, flux and mass of the bombarding species along with the ratio of bombarding particles to depositing particles are important processing variables. The depositing material may be vaporized either by evaporation, sputtering, arc erosion or by decomposition of a chemical vapour precursor. The energetic particles used for bombardment are usually ions of an inert or reactive gas, or, in some cases, ions of the condensing film material ("film ions") (Donald, 1998; Gupta, 2003; Nalwa, 2002 and John, 2000).

Ion plating can be done in plasma or it may be done in a vacuum environment where ions for bombardment are formed in a separate "ion gun". The latter ion plating configuration is often called Ion Beam Assisted Deposition (IBAD). By using a reactive gas in the plasma, films of compound materials can be deposited. Ion plating can provide dense coatings at relatively high gas pressure where gas scattering can enhance surface coverage (Donald, 1998; Gupta, 2003; Jeffrey, 2000; John, 2000 and Nalwa, 2002).

2.1.2 Chemical Vapour Deposition (CVD)

Chemical Vapour Deposition (CVD) is a high temperature process (1000°C) which is carried out in vacuum chamber where gases disassociate and then react at the workpiece surface to form a solid coating. This is the process by which diamond like carbon (DLC), also called carbon based coating (CBC) coatings, are produced. The greatest problem with the technique is that high temperatures are required (Donald, 1998 and Kelly *et al.*, 1998).
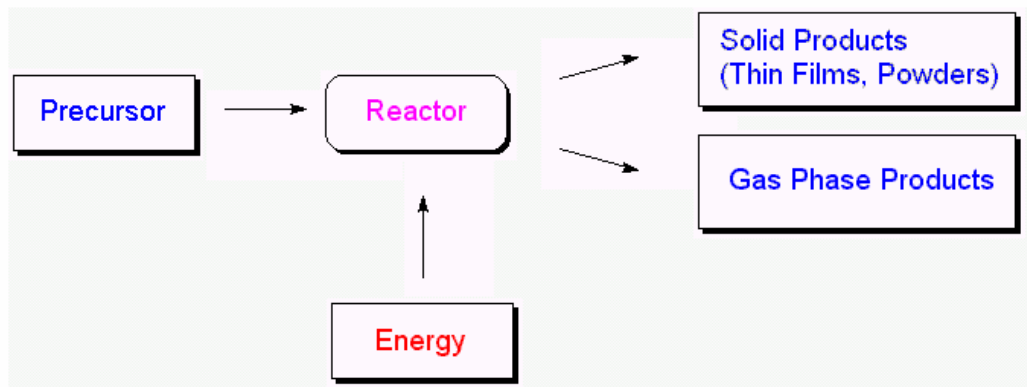
Figure 2.4: Essential elements in CVD.

2.1.3 Electroplating, Electroless Plating and Displacement Plating

Electroplating is the deposition on the cathode metallic ions from the electrolyte of an electrolytic cell. Elements such as chromium, nickel, zinc, and sliver are deposited from aqueous solutions. A thin film of material deposition by electroplating is often called a "flash". The anode of the electrolytic cell is of the material being deposited and is not consumed in the deposition processes (Nalwa, 2002 and Villiger, 1999).
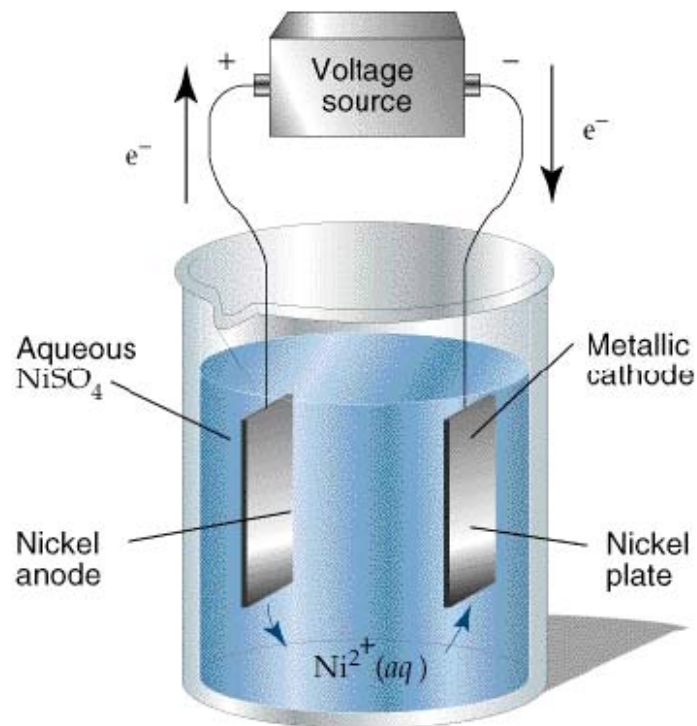
Figure 2.5: The basic working principle of electroplating.

In electroless or autocatalytic plating, no external voltage or current source is required. The voltage or current is supplied by the chemical reduction of an agent at the deposition face. The reduction reaction is catalyzed by a material, which is often

boron or phosphorous. Materials that are commonly deposited by electroless deposition are nickel, copper, gold, etc.

Displacement plating is the deposition of ions in solution on a surface and results from the difference in electronegativity of the surface and the ions (Villiger, 1999).

2.1.4 Plasma Spraying

This system, as the name implies, uses an electric arc as the heat source, which is much hotter than the temperature produced by an oxy-acetylene flame. This means that higher melting point materials can be deposited at higher velocities (200-400 min/s) leading to moderate bond strength in air plasma spraying and high bond strength in vacuum plasma sprays. In addition, porosity contents are lower, especially in the case of vacuum plasma spraying. Disadvantages are that the process requires more expensive equipment and that it is not suitable for manual operation, i.e. some form of manipulation or robotic system is required (Jeffrey, 2000 and Nalwa, 2002).
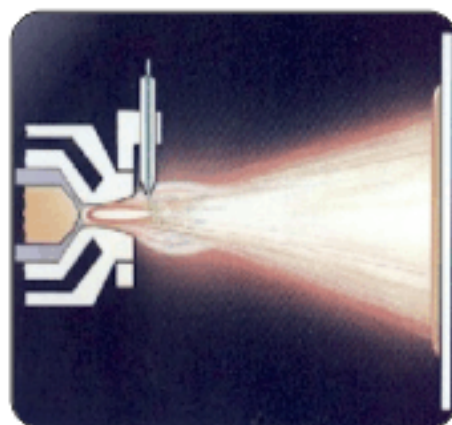
Figure 2.6: Schematic of plasma spraying [Dynamic Ceramic].

2.2 Controlling Parameters for Coatings Processes

For different coating processes or methods, the factors influencing the coatings vary. For example, the factors in CVD would be the substrate temperature, carrier gas (mostly hydrogen) flow, the water flow, etc. For PVD coating, bias voltage, nitrogen pressure/flow rate, acetylene pressure/flow rate, and arc current would be the factors that affect the final coatings properties. In Figure 2.7, different controllable factors are listed out.

2.2.1 Controlling Parameters for CVD

For CVD coating, Hu (Hu, 2003) optimized hot-wire-CVD process by considering the filament arrangement. Another research (Mouche, 2002) used screening and experimental design modeling to optimize the CVD process. This study considered the influence of substrates temperature, carrier gas (hydrogen), water flow, water injection time, and bubbler pressure to the coating process.

2.2.2 Controlling Parameters for Electroplating

For electroplating, Hu *et al.* (2003) optimized zinc-nickel deposition by using fractional factorial design and central composite design coupled with the response surface methodology. The study optimized the key variables of deposition temperature, current density, pH value, Zn/Ni ionic ratio, and tetrapentyl-ammonium (TePA) concentration in electroplating.

2.2.3 Controlling Parameters for Plasma Spraying

For plasma spraying, Kelly *et al.* (1998) carried out a research to vary different parameters: current intensity, argon and hydrogen flow rates. In the experiment, DPV2000 diagnostic system was used to measure the velocity, temperature, and diameter of the in-flight particles in order to search for a process window. The research found that the temperatures of the particles are directly related to the amount of unmelted particles, oxides and delamination in the microstructure. Tensile strength measurements also show a clear correlation to the amount of delamination in the coating and therefore to the in-flight particle temperature.

2.2.4 Controlling Parameters for PVD coating

Vacuum Deposition

For PVD coating, Zhitomirsky *et al.* (2000) has studied the effects of bias voltage and incidence angle effects to structure and properties of vacuum deposited titanium nitride (TiN) coating. However, optimizing method was proposed to find the critical factors of vacuum deposition.

Sputtering

Chou *et al.* (2003) optimized sputtering process in titanium nitride (TiN) and zirconium nitride (ZrN) coating by selecting factors: direct current (DC) power, nitrogen (N_2) flow rate, specimen-target distance, and specimens' height. He found

that the DC power and specimen height was the most sensitive parameters in the sputtering process when coating both TiN and ZrN.

Kelly and Arnell (1998) experimented on closed-field unbalanced magnetron sputtering (CFUBMS) process for Al, Zr, and W coatings. Deposition parameters, such as target current (over the range 2A to 8A), substrate bias (-30 V to -70 V), coating pressure (0.6E-3 to 4E-3 mbar), and substrate-to-target separation (80 mm to 150 mm) are investigated. Their work, based on Taguchi method, showed that the relationship between deposition parameters varied in a systematic manner.

Hajjaji *et al.* (2000) optimized magnetron-sputtered parameters in titanium + diamond like carbon (Ti-DLC) coating. The process parameters included substrate bias voltage, acetylene flow rate, and argon and nitrogen partial pressures. The results indicated that bias voltages in the range -20 to -60 V had little or no influence on the mechanical properties. The acetylene flow rate, which controlled the titanium content in the Ti-DLC layers, exhibited the most significant effect. An explanation based on the relationship between relative film thickness and critical applied loads was provided for the coating failure mechanisms.

2.2.4.1 Ion Plating

Guzman *et al.* (1998) optimized ion beam assisted deposition (IBAD) in ion plating process parameters for TiN and TiC coatings. He optimized the nitrogen pressure (for TiN), acetylene pressure (for TiC), ion current density, and deposition rate in IBAD

pressure. However, he optimized the process without using statistical method and simply used trial-and-error type method.

2.2.4.2 Arc Vapour Deposition

Lin *et al.* (1999) optimized cathodic arc plasma deposition system with TiAlN coating. They found that the bias voltage, nitrogen pressure, and target composition were the most influential variables to wear resistance of TiAlN coating among the eight parameters. The eight parameters were target atomic ratio (Ti/Al), substrate bias, nitrogen pressure, titanium aluminum (TiAl) deposition time, titanium aluminum nitrides (TiAlN) deposition time, surface condition, and sputter cleaning time.

Another research (Sato *et al.*, 2003) only found the influence of changing bias voltage when coating aluminum titanium nitride (AlTiN). It discovered that carbide drills deposited with lower bias voltage showed better cutting performance in the machining of carbon steel compared with those deposited with coating under high bias voltage.

2.2.5 Summary of Coating Parameter Settings

Different coating techniques have their own process parameters that will affect the coating. Coating is very sensitive to its process environment like temperature and concentration of reactive gases. Therefore, optimal parameters or to find the best parameter settings are important to the process.

In PVD coating, the most effective coating parameters summarized from previous work and researches (Chou, 2003; Kelly and Arnell, 1998; Lin *et al.*, 1999; Sato, 2003; Schulz, 1997; Villiger *et al.*, 1999 and Zhitomirsky, 2000;) are bias voltage, target or arc current, nitrogen pressure, acetylene pressure, coating thickness, and target composition.
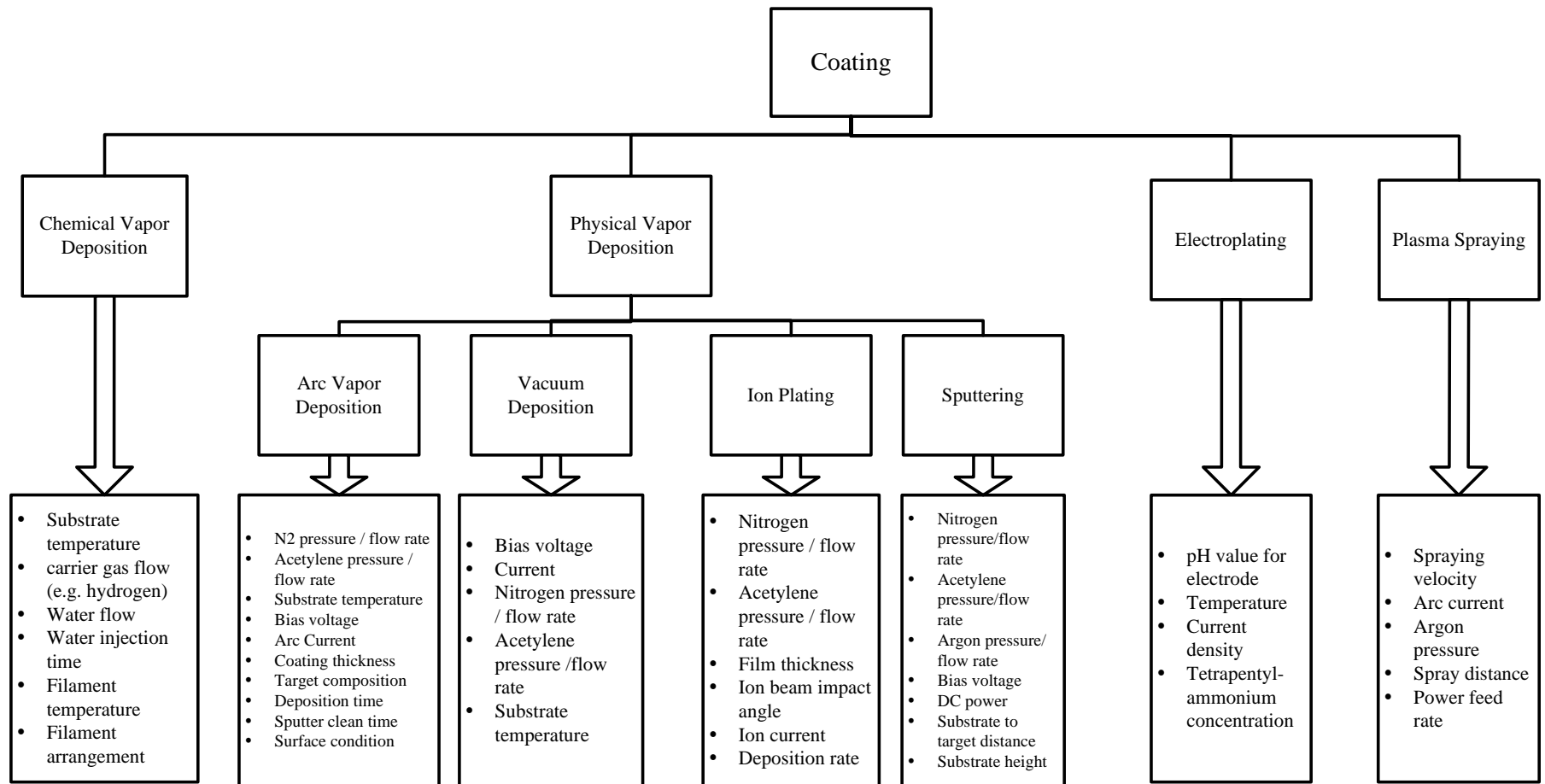
Figure 2.7: Controllable factors for different coating techniques (Chou, 2003; Kelly and Arnell, 1998; Lin *et al.*, 1999; Sato, 2003; Schulz, 1997; Villiger *et al.*, 1999 and Zhitomirsky, 2000).

2.3 Substrate Material and Application Consideration for PVD Coating Techniques

2.3.1 Coating for Cutting Tools

By considering the substrate materials, most researches (Ghani *et al.*, 2003; Hofmann *et al.*, 1993 and Sarwar *et al.*, 1997) carried out experiments with cutting tool materials like tungsten carbide and high-speed steel. Moreover, the above researches had not investigated the relationship between the substrate materials and the coating parameters.

2.3.2 Coating for Die Casting Mould Steels

Hajjaji's *et al.* (2000) presented their results obtained with Cr-based PVD coating, which led to substantially increased tool lives. In their research, a hot-worked steel AISI H13 was used for the magnetron-sputtering ion plating process. However, the method is restricted to die casting moulds. Other mould like plastic injection, forming, and drawing had not been considered. Moreover, the paper did not provide any method to optimize the coating of AISI H13.

2.3.3 Coating for Forming and Stamping mould steels

A low alloy cast steel (German quality 1.0443) was coated with TiN by magnetron-sputtering process in research by Schulz's *et al.* (1997). Cast steel was used in slide forming process of steel and aluminum sheets. It was found that the coefficient of

friction was reduced by coating when contact normal force was increased. Also, the tool life was increased by coating TiN.

2.3.4 Summary of Substrate Materials and Application Consideration

Most experimented substrates and techniques (Chou, 2003; Lin *et al.*, 1999; Kelly and Arnell, 1998; Sato, 2003; Schulz, 1997; Villiger *et al.*, 1999 and Zhitomirsky, 2000) were restricted to cutting tool materials like carbide and high-speed steel. Only a few researches (Knotek, 1993 and Schulz, 1997) have investigated the effects of coating to mould steels. The reason may be that moulds are not easily coated owing to large-scale material variation of physical properties (e.g. residual stress, materials deformation under high temperature treatment).

The information about substrate materials and coating parameters are still a problem to most coating processes. If the optimization windows can be worked out, the coating process can be standardized and be under control.

2.4 Adhesion Testing Method

Adhesion is one of the most important properties of thin film coating. There should be method to ensure the quality of the coating before being applied to different tools or applications. There are at least nine basic adhesion-testing methods for coating (Valli, 1986). They are: pressure sensitive tape test, acceleration (body force) test, electromagnetic stressing, shock wave testing, tensile and shear testing, laser techniques, acoustic imaging, indentation test, and scratch test. However, not all the testing methods are suitable for measuring hard coating thin film on tools and machine parts.

2.4.1 Peeling Method

Peeling method is usually called "tape test". In the test, an adhesive tape is pressed against the film and the tape will be removed. This method is to observe and measure whether the coating or film is peeled off by force during the removal. However, this method is not suitable for measuring the adhesion of hard coating and thin film. This method is only used to measure unsupported film such as coating (paint) on polymer, wood (Meijer, 2003), and plastics (Ryntz, 2003).

2.4.2 Direct Pull Method

A pin or a cylinder is bonded onto the surface of film by using soldering or cementing method. The normally applied force that required for removing the film could then be measured. The method could study the adhesion of thin film but also could measure

the strength and properties of adhesive cemented or soldered joints. The major limitation of the method is that it requires some sort of bond to the film for force transmission (Mittal, 1995 and Jacobsson, 1976).

2.4.3 Scratch Method

Scratch method consists of introducing stresses at the interface between the coating and the substrate. This is achieved by pressing a diamond stylus on the sample surface with a normal load. As the sample is displaced at constant speed, the resulting stresses at the interface cause flaking or chipping of the coating. The smallest load called the critical load at which a specific failure event is recorded (Mittal, 1995).

The critical load value L_c translates the complex intrinsic properties of a specific coating system into a very reproducible figure of great practical significance.
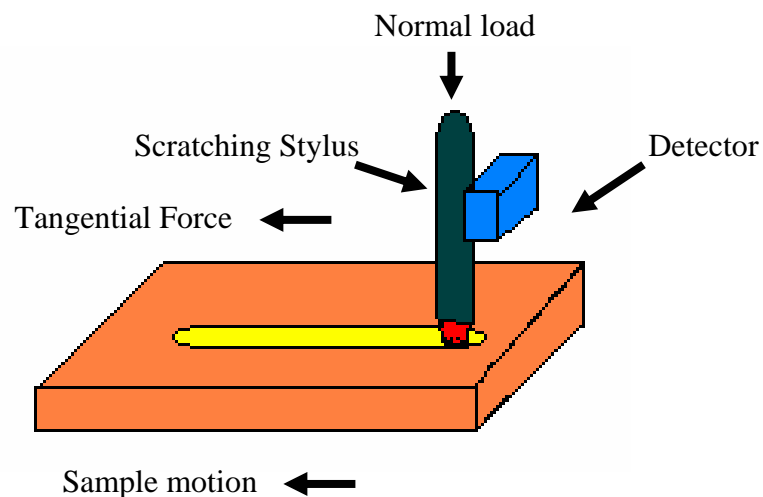
Figure 2.8: Scratch testing method.

2.4.4 Rockwell-C Indenter

Rockwell-C indentation test is a quick and convenient method developed by Mercedes-Benz (Daimler-Benz adhesion test, 1992) to measure the adhesion of hard and thin coating qualitatively. The substrates must be at least with hardness HRC 54 and the maximum coating thickness is 5μm.

A coating which well adheres on the substrate conforms to the contour of deformation and fine cracks. For those coatings with poor interfacial adhesion strengths, delamination effect will be observed around the boundary of the indentation.

Figure 2.9 shows the checking method for adhesion. If the adhesion of the coating is very good, cracking pattern of the indented point will be obtained. Figure 2.9 shows the cracking pattern of good adhesion coating. There is no peel off of coating and this is graded to class HF1 to HF3.

For bad adhesion, there is no cracking pattern and peel off coating can be seen. When there is substrate exposure after indentation, it means that the coating is in bad adhesion and this is graded to class HF4 to HF6.

Good adhesion	Bad adhesion
HF 1	HF4
HF2	HF5
HF3	HF6
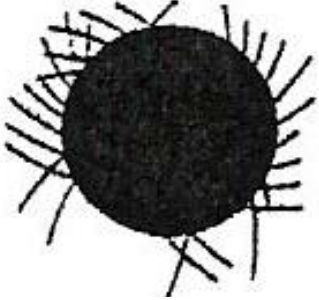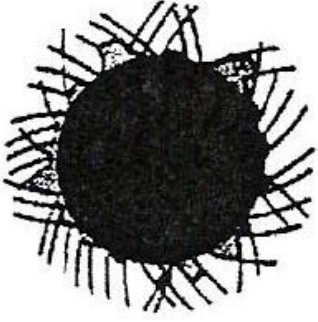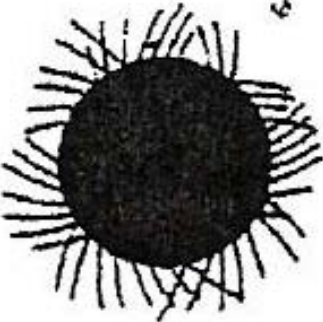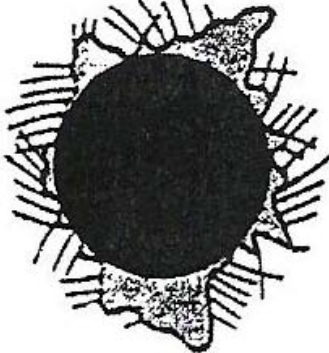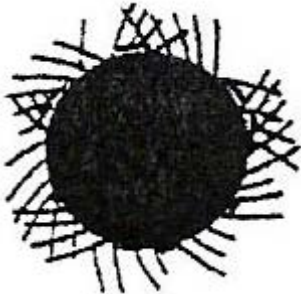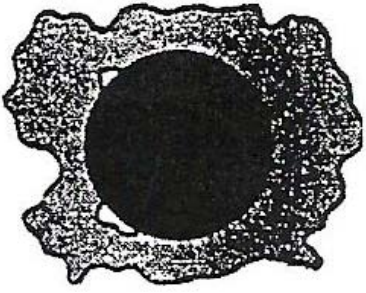
Figure 2.9: Adhesion checking method developed by Mercedes-Benz.

Figure 2.10 demonstrates the cracking pattern and the flanking after adhesion test by the Rockwell C indenter.

Cracking pattern	Flanking (substrate exposure)

Figure 2.10: Cracking pattern and flanking after adhesion test.

2.5 Optimization Methods

To optimize process or experimental conditions, there are two possible approaches. One is the statistic approach. For example, uniform design method (Lai *et al.*, 2003), fractional factorial design (Hajjaji, 2000; Hu *et al.*, 2003 and Villiger, 1999;), response surface methodology (Hu *et al.*, 2003) and Taguchi method (Cheung *et al.*, 2003; Chou, 2003; George *et al.*, 2004; Ghani *et al.*, 2003; Lin *et al.*, 1999; Lin *et al.*, 2002; Soković *et al.*, 1998; Su *et la*, 1998 and 1998; Tsao and Hong, 2000 and Zhou *et al.*, 2000). Another is the artificial intelligence approach. The ideas and concepts are different.

2.5.1 Statistic Approach

There are two methods to optimize process conditions or parameters by statistic approach. They are full factorial design and fractional design.

2.5.1.1 Factorial Design

In full factorial design, each complete trial or replicate of the experiment and all possible combinations of all levels of factors are investigated. The effect of a factor is defined as the change in response produced by a change in level of factors. The advantage is that all possible combinations of the factor levels are investigated. However, the full factorial design takes a long time to completely run all experiments because the experiments combination is too large (and usually also too expensive) to perform in practice. Table 2.1 shows some examples. For full factorial design, it is

usually used for conducting 2 levels. For more than two, it is best to use other methods.

Number of trials			
Factors	Levels	Full factorial design	Fractional design
2	2	4	4
3	2	8	4
4	2	16	8
7	2	128	8
15	2	32768	16

Table 2.1: Samples for number of trials in full factorial design and fractional design.

2.5.1.2 Fractional Design

Though a full factorial design is the most desirable design wherein one could gather information on all the main effects, two way interactions, three way interactions and other higher order interactions are very unpractical to run due to the prohibitive size of the experiments. For a design of seven factors at two levels one would have to complete 128 runs.

Fractional factorial designs are alternatives to a full factorial design. The same seven factors could be tested in either 8 runs or 16 runs or 32 runs, however, with the loss of certain information. The fractional factorial designs can be classified into three types of design:

a. Resolution III design of experiment (DOE): A design where main factor effects are confounded with two factor and higher order interactions,

b. Resolution IV DOE: A design where main effects are confounded with three factor and higher order interactions and all two factors interactions are confounded with two factor interactions and higher order interactions, and

c. Resolution V DOE: A design where main effects are confounded with four factor and higher order interactions and two factor interactions are confounded with three factor interactions and higher order interactions.

Resolution III and Resolution IV DOE are very commonly used designs in the screening of various factors during the analyze and improve phase of Six Sigma.

The problem, which one faces in utilizing these resolution designs, lies in the confounding structure of the designs, however three fundamental principles of factorial effects can be effectively utilized for the analysis of these designs.

Taguchi method is also one of the fractional designs. If a four factors and three levels experiment (3^4) is being conducted by using conventional methods, it requires us to carry out totally 81 (Appendix A) experiments. It is because only one variable is changed and the other factors are kept constant in each run. However, only 9 experiments are required to be run by using the Taguchi method. Taguchi method can reduce the trial-and-error type experiments by using a matrix design.

The using Taguchi approach can economically satisfy the needs of problem solving and product/process design optimization projects. By learning and applying this technique, engineers, scientists, and researchers can significantly reduce the time

required for experimental investigations. DOE can be highly effective when yow wish to:

    a.   optimize product and process designs, study the effects of multiple factors (i.e. variables, parameters, ingredients, etc.) on the performance, and solve production problems by objectively laying out the investigative experiments,

    b.   study influence of individual factors on the performance and determine which factor has more influence, which ones have less,

    c.   find which factor should have tighter tolerance and which tolerance should be relaxed, and

    d.   indicate whether a supplier's part causes problems or not (ANOVA data), and how to combine different factors in their proper settings to get the best results.

Further, the experimental data will allow to determine:

    a.   how to substitute a less expensive part to get the same performance,

    b.   how much money can be save the design improvement that propose by Taguchi loss function,

    c.   how to determine which factor is causing most variations in the result,

    d.   how to set up process such that it is insensitive to the uncontrollable factors,

    e.   which factors have more influence on the mean performance,

    f.   what is needed to do to reduce performance variation around the target,

    g.   how to adjust factors for a system whose response varies proportional to signal factor,

    h.   how you can adjust factor for overall satisfaction of criteria of evaluations, and

    i.   how the uncontrollable factors affect the performance.

Many experimental methods (Cheung *et al.*, 2003; Chou, 2003; George *et al.*, 2004; Ghani *et al.*, 2003; Lin *et al.*, 1999; Lin *et al.*, 2002; Tsao and Hong, 2000; Soković *et al.*, 1998; Su *et al.*, 1998 and 1998 and Zhou *et al.*, 2000) used Taguchi optimization method to obtain the dominated parameters. For examples, Taguchi method is widely used in optimizing the cutter parameters in cutting tools (Chou, 2003; Ghani *et al.*, 2003, Lin *et al.*, 2002; Soković *et al.*, 1998; Su *et al.*, 1998 and 1998 and Tsao and Hong, 2000).

Tsao and Hong (Tsao and Hong, 2000) optimized 4 factors: coatings, feed rate, spindle speed, and cutting tool materials. By measuring the width of the side flank wear of the end mills, they demonstrated that the tool materials of cutting tool is the main controlling factors that influence the milling tool life in quenched AISI 1045 carbon steel. Moreover, the TiCN hard-coated tools performed the best result than bare materials and TiAlCN coated tools. Cutting speed, feed rate, depth of cut, workpiece hardness, and cutting tool materials are variables in the cutting process. The tool life could be optimized and improved by Taguchi method.

Moreover, some researches use Taguchi method in fabricating carbon fiber electrodes (Cheng *et al.*, 2003), rapid prototyping (RP) (Zhou *et al.*, 2000) and electric discharge machining (EDM) process (George *et al.*, 2004). This shows that Taguchi method is a versatile optimization method with minimum number of trials even if there are many different and complex parameters in the experiments.

Recently, Kumar *et al.* (2000) had a new concept and idea extended on the Taguchi method. By using Taguchi method, a single response or a set of process parameters

can be optimized to find out a particular quality characteristic or response. However, the optimized settings for this particular quality characteristic or response may not be the interest of other characteristics or responses in the process. To fulfill different interests in the same process, Kumar *et al.* (2000) introduced a simplified multi-criterion methodology based on Taguchi method and the utility concept to get optimal conditions in V-processed castings of Al-7%Si alloy. By using different set of weights, a different set of optimized parameters or factors could be obtained.

2.5.2 Artificial Intelligence Approach

For the artificial intelligence approach, process modeling and prediction will be conducted.

2.5.2.1 Neural Network (NN)

Sometimes, when the derivatives are not possible to analyze or it is very time consuming or numerically inaccurate to do so, artificial intelligence approach like Neural Network (NN) can be one of the choice.

NN is an information-processing paradigm that is inspired by the way biological nervous systems process information. The definition of the NN can be regarded as a system composed of many simple processing elements operating in parallel and whose function is defined by network structure, connection strength, and the processing performed at computing elements or nodes.

NN is a massively parallel-distributed processor for storing experiment knowledge and making it a variable for use. The key element of NN paradigm is the novel structure of the information processing system. It is composed of a large number of highly interconnected processing elements (neurons) working in unison to solve specific problems. NN provides the ability to learn what happens in the process without actually modeling the physical and chemical laws that govern the system (Huang, 2004 and Montgomery, 1997).

NN can be configured for a specific application such as pattern recognition or data classification through a learning process. Learning in biological systems involves adjustments to the synaptic connections that exist between the neurons and this is true for NN as well. NN has been applied to an increasing number of real-world problems of considerable complexity (Huang, 2004 and Montgomery, 1997).

2.6 Problems in Optimizing PVD Coating

Literature surveys have been done on coating processes, coating materials, and optimization method. It is found that few optimal solutions or techniques have been used to coating processes. Also, the influence of different coating parameters to coating substrate materials, especially mould steels, have not been investigated.

Coating is still restricted to cutting tools. For example, the coating with compounds based on titanium are being applied on cutting tools (e.g., end-mill, lathe, etc.). Though coating has been used for many years (Ghani *et al.*, 2003; Hofmann *et al.*, 1993 and Sarwar *et al.*, 1997) the optimization condition for cathodic arc physical vapour deposition on different coatings and different substrate materials are still uncertain.

Therefore, this research will address the followings:

To study the controlling parameters and models for optimal settings for cathodic arc physical vapour deposition (CAPVD) process for TiN and CrN coatings which are the main and common hard coatings for plastic injection mould application. As a Teaching Company Scheme sponsored project, the result should be also practically applicable.

CHAPTER 3 RESEARCH METHODOLOGY

In this chapter, the Taguchi method will be summarized in Section 3.1. And the Response Surface Method (RSM) will be outlined in Section 3.2.

3.1 Taguchi Method

Taguchi Method, also called the Robust Design method, is pioneered by Dr. Genichi Taguchi (田口玄一), greatly improves engineering productivity. By consciously considering the noise factors (environmental variation during the product's usage, manufacturing variation and component deterioration) and the cost of failure in the field, the Robust Design method helps to ensure customer satisfactions. Robust Design focuses on improving the fundamental function of the product or process. Thus it facilitates flexible designs and concurrent engineering. Indeed, it is the most powerful method available to reduce product cost, improve quality, and simultaneously reduce development interval (Beckford, 1998).

Figure 3.1: Dr. Genichi Taguchi.

Robust Design method is central to improve engineering productivity. Pioneered by Dr. Genichi Taguchi after the end of the Second World War, the method has evolved over the last five decades. Many companies around the world have saved hundreds of millions of dollars by using the method in diverse industries: automobiles, xerography, telecommunications, electronics, software, etc. (Stuart, 1993).

3.1.1 Quality Loss Function

Dr. Taguchi defined quality as the characteristic that avoids loss to society after the time the product has been shipped (Phillip, 1996). Quality loss is the financial loss imparted to society after a product shipped. This loss is measured in monetary units (dollars) and is related to quantifiable characteristics. This definition goes much beyond the old definition of quality as simply meeting specifications. Two products designed to perform the same function may both meet specifications, but impart different losses to society. Thus, simply meeting specifications is a poor measure of quality (Phillip, 1996).

The quality loss is defined by Taguchi's loss function. This loss function relates the financial loss to the functional specification using a quadratic relationship that comes from Taylor series expansion (Taguchi, 1981 and Phillip, 1996). The quadratic equation is in the form of a parabola, Figure 3.2.

In quality improvement and design optimization, the metric plays a crucial role. Unfortunately, a single metric does not serve all stages of product delivery. It is common to use the fraction of products outside the specified limits as the measure of

quality. Though it is a good measure of the loss due to scrap, it miserably fails as a predictor of customer satisfaction. The quality loss function serves that purpose very well (Phillip, 1996).

Quality Loss Function
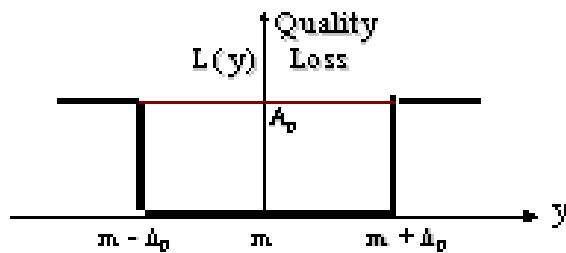
(a) Step Function
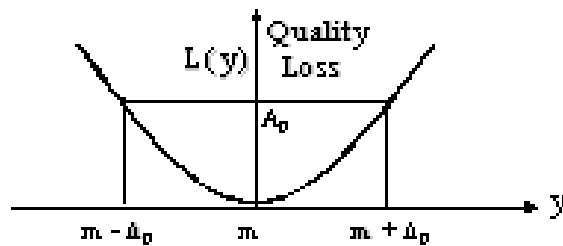
(b) Quadratic loss function
$$L(y) = k(y - m)^2$$
where $k = A_0 / \Delta_0^2$

Products that meet tolerances also inflict quality loss

Figure 3.2: The quality loss Function.

The loss function typically is of the following form:

$$L(y) = k(y - m)^2$$

where L is the loss, k is the loss constant, m is the mean target value, and y is a particular product characteristic such as weight or length.

3.1.2 The Quality Engineering

Quality engineering is a series of approaches to predict and prevent the troubles or problems. That might occur in the market after a product is sold and used by the customer when under various experimental and applying conditions for the duration of designed product life. The framework of quality engineering interrelates with both the design engineering and manufacturing. Taguchi Method encompasses and covers this overall framework rather than only deal with Design of Experiments (DOE) (Montgomery, 1997).
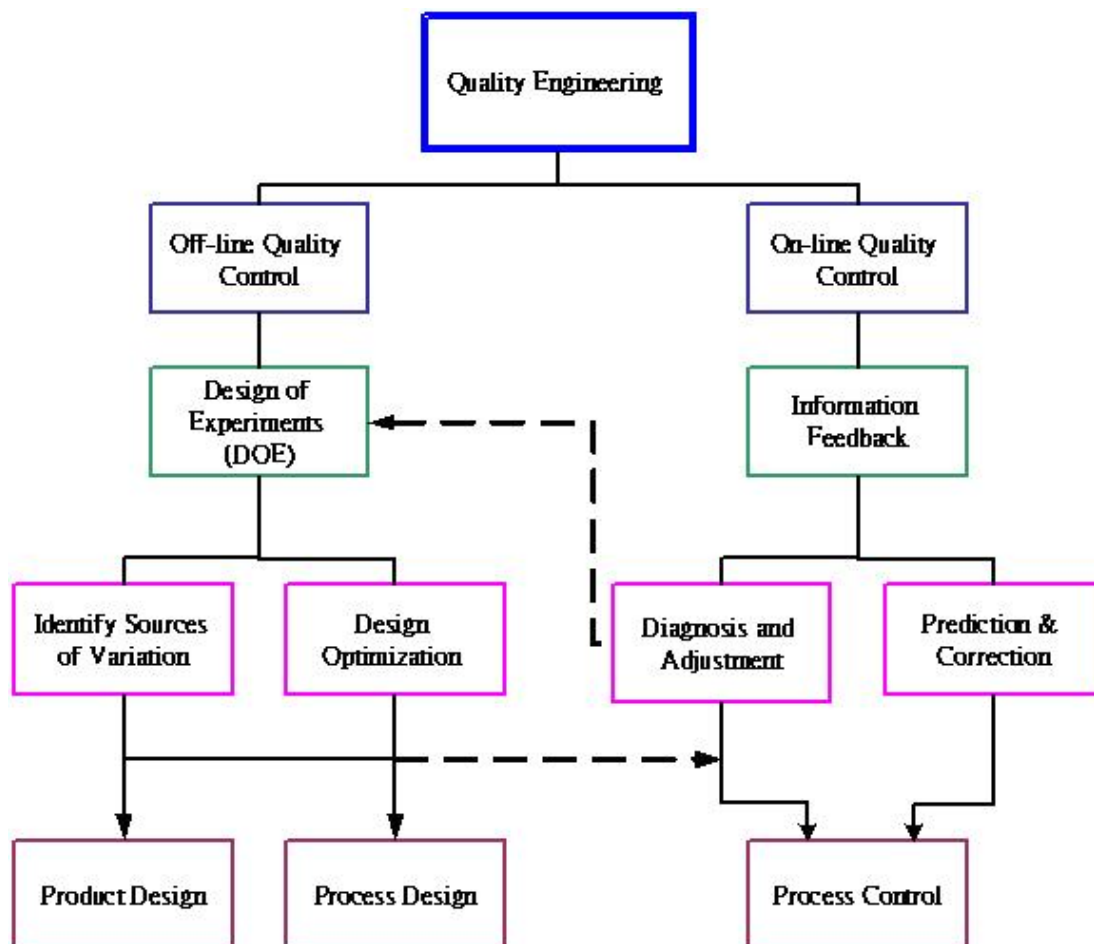
Figure 3.3: Framework of quality engineering.

There are two main areas in quality engineering, the off-line and on-line quality control (QC). Both of these areas are very cost sensitive in the decisions to the improvement of quality in the product and process development stages.

3.1.3 On-line Quality Control (On-line QC)

On-line quality control involves the actual production of the product. These are the techniques that monitor production, measure ongoing quality; provide signals of potential problems, and direct corrective action (Taguchi, 1981 and Stuart, 1993). Information feedback systems are the foundation for notifying the operator and the manufacturing supervisor of process performance. Data obtained from critical process points report the real-time status of the production.

Apart from getting raw data from production, adjustment and diagnosis is important. The information from production must be analyzed to determine if process settings are being properly maintained. Production data must be compared with the desired targets and that the desired targets are known.

If the analysis indicates that the current conditions are not acceptable, then adjustments must be made to bring the process back to within the acceptable range. The prediction and the correction functions support and react to the diagnosis inputs and adjustments. Based on historical data and capability studies, the predicted targets provide the reference for determining if the current process status is acceptable or if adjustment is required. In addition, the magnitude of adjustment can be determined for making corrections (Wu, 1993).

3.1.4 Off-line Quality Control (Off-line QC)

Off-line quality control is to optimize product and process design in support of on-line quality control. Design of experiment is the fundamental tool of off-line quality control. Some of these efforts may be accomplished on prototype lines that simulate actual production, or they could be performed on the actual manufacturing process prior to production, on-off shifts, or during production shutdown (Taguchi, 1981 and Stuart, 1993).

Experimentation techniques play two important roles in identifying sources of variation and determining design and process optimization. Identifying the principal contributors to overall variation can focus attention on the most important factors that affect functional variation and divert efforts from those factors that have minimal impact on the overall quality of the final product. The determination of the best levels of these critical factors establishes the target values for on-line quality control, activates and provides solutions to problems identified in production (Taguchi, 1981 and Stuart, 1993).

In addition, to describe a functional standpoint, off-line quality control can also be viewed as three sequential stages for optimizing a product or process. These are: (1) system design, (2) parameter design and (3) tolerance design.

3.1.5 System Design

The conceptual stage of any new product development or process innovation is system design. This is the "ideas" stage where something revolutionary or perhaps an offshoot of previous developments is conceived and tested. The concepts may be based on past experience, scientific or engineering knowledge, a new revolution, or any combination of the three. The strategy behind system design is to take these new ideas and convert into something that can be worked out (Beckford, 1998; Taguchi, 1981, and Stuart, 1993).

3.1.6 Parameter Design

The objective of parameter design is to take the innovation that has been proven to work in system design and enhance it so that it will function as intended. A major portion of Dr. Taguchi's focus has been on making the product and the process robust against the uncontrollable influences that can prevent proper functioning (Beckford, 1998; Taguchi, 1981, and Stuart, 1993).

Taguchi's parameter design can be used to make a process robust against sources of variation and hence improve field performance. If a process has robustness to noise factors that largely affects the variance of performance characteristics at the developing stage, it is highly probable for the process to have robustness against other noise factor that have not been considered at the development stage. The aim of a parameter design experiment is, then, to identify settings of the design parameters that

maximize the chosen performance measure and are insensitive to noise factors (Beckford, 1998; Taguchi, 1981, and Stuart, 1993).

Two major factors affect the quality characteristic of a product:

a. control factor (or design variables).

b. noise factor (or uncontrollable variables).

Control factors are those factors that can be controlled during the design or manufacturing stages. Noise factors are those factors whose values cannot be set and maintained.

Noise factor can be classified into three categories:

a. external noise factor (or outer noise factor).

b. internal noise factor (or inner noise factor).

c. manufacturing noise factor (or between product noise).

External noise factors are created by environmental conditions during manufacturing process or using the final product. Examples are temperature, humidity and dust (Beckford, 1998).

Internal noise factors come from product's natural ingredients. Deterioration of a product or its components can be seen as internal noise factors (Beckford, 1998).

Manufacturing noise factor refers to the differences between one completed unit and another. These differences tend to come out because of manufacturing imperfections and are often referred to as piece-to-piece variation (Beckford, 1998).

The tool for achieving parameter design objectives is the design of experiment. The strategy behind parameter design experiment is based on cost considerations. Efforts should be directed towards determining the best design at the least cost.

Taguchi's method for identifying settings of design parameters that maximize performance characteristics (e.g. yield or productivity etc) is summarized below (Beckford, 1998; Taguchi, 1981, and Stuart, 1993).

a. Identify initial and competing settings of design parameters, and identify important noise factors and their ranges.

b. Construct the design and noise matrices, and plan the parameter design experiments.

c. Conduct the parameter design experiments and evaluate the performance statistics for each test run of the design matrix.

d. Use the values of the performance statistics to predict new settings of the design matrix (if needed).

e. Confirm that the new settings indeed improve the performance statistics.

The design will be planned to determine the control factor's level that is less sensitive to noise factors. An orthogonal array containing the control factors will be arranged in the inner array, while an orthogonal array containing noise factors will be arranged in

the outer array. Taguchi suggested that parameter design using noises that are deliberately created was more effective than not, if noises can be created purposely (Taguchi, 1981 and Stuart, 1993).

The reason is that if noise is not induced deliberately, many experiments must be performed to investigate the effects of noise factors diversely on the process and it is very difficult to obtain reliable results under different noise conditions. If the experiments can be performed under various levels of noise, i.e. with positive induction of noise to the design, it can obtain a realistic level of robustness. Therefore, a characteristic of Taguchi's parameter design is the deliberate creation of noise for the identification of control factor's level that is the least sensitive to the noises (Taguchi, 1981 and Stuart, 1993).

3.1.7 Tolerance Design

The objective of tolerance design is to determine the acceptable range of variability around the nominal settings determined in parameter design. Again, design of experiments is used to study the product or process, while analysis of variance (ANOVA) provides interpretation of the experiment data. Wide tolerance parts and cheap grade raw material whose values were determined in parameter design are used (Beckford, 1998; Taguchi, 1981, and Stuart, 1993).

The strategy is to determine which tolerances and grades of materials have the greatest effect on variability. Tolerances can be tightened and materials upgraded based on tradeoffs between the cost of higher-grade parts or ingredients and the reduction in product or process variation (Beckford, 1998; Taguchi, 1981 and Stuart, 1993).

ANOVA on mean response and signal-to-noise ratio will be performed to identify significant factor effects and reduce response variability.

ANOVA employed by a researcher to whether three or more sample means are statistically significantly different from each other or instead can be regarded as derived from the same population. It is a test of the null hypothesis that population means are equal, e.g. that plumbers, electricians, and carpenters all have about the same average income. Being a test of difference among threes or more means, ANOVA is an extension of the t-test which is used to test for difference between two

means.   If we reject the null hypothesis, we still must determine which sample means differ from the others.

Regression analysis concerns the investigation of the effect of one or more continuous explanatory variables on a continuous response variable. The objective of conducting ANOVA is similar to regression analysis, except that ANOVA focuses on studying the effect of one or more categorical variables on a continuous response variable; that is, the explanatory variables are discrete in ANOVA. ANOVA can be divided into 3 groups:

1. one-way ANOVA for involving one variable,
2. two-way ANOVA for involving two variable and
3. high-order ANOVA for involving two or more variables.

Table 3.1 shows how to get the ANOVA table. One-way ANOVA are being taken as example. It constructs for the partition of sum of squares and the construction of the *F*-test.

Source	Degree of Freedom	Sum of Squares	Mean Square	*F*-value
Variable	$p-1$	SSt	$MSt = \dfrac{SSt}{p-1}$	$F = \dfrac{MSt}{MSE}$
Error	$n-\mathrm{p}$	SSE	$MSE = \dfrac{SSE}{n-p}$	
Total	$n-1$	SST		

Table 3. 1 One-way ANOVA table.

In Table 3.1, *n* is the number of observations and *p* is the number of factor levels. For the partition of sum of squares,

$$SST = \text{Total sum of squares of the data} = \sum_{i=1}^{p} \sum_{j=1}^{ni} (y_{ij} - m_{..})^2$$

$$SSE = \text{Sum of squares due to error} = \sum_{i=1}^{p} \sum_{j=1}^{ni} (y_{ij} - m_{i.})^2$$

$$SSt_i = \text{Sum of squares for } i^{th} \text{ treatment} = \sum_{j=1}^{ni} (m_{i.} - m_{..})^2$$

$$= n_i (m_{i.} - m_{..})^2$$

$$SSt = \text{Total sum of squares due to treatment} \quad = SSt_1 + SSt_2 + \ldots + SSt_p$$

$$= \sum_{i=1}^{p} \sum_{j=1}^{ni} (m_{i.} - m_{..})^2$$

$$= \sum_{i=1}^{p} n_i (m_{i.} - m_{..})^2$$

$$MSt = \text{Mean Square of treatment}$$

$$MSE = \text{Mean Square of Error}$$

where N represents the total number of data points $\sum_{i=1}^{p} n_i$;

$y_{i.}$ represents the ith treatment total $\sum_{j=1}^{ni} y_{ij}$, for $i = 1, 2 \ldots, p$;

$m_{i.}$ represents the ith treatment mean $\dfrac{1}{ni} y_{i.}$, for $i = 1, 2 \ldots, p$;

$y_{..}$ represents the grand total $\sum_{i=1}^{p} y_{i.}$ and

$m_{..}$ represents the grand mean $\dfrac{1}{N} y_{...}$

3.2 Response Surface Method (RSM)

Response surface method or methodology is a collection of mathematical and statistical techniques that are useful for the modeling and analysis of problems in which a response of interest is influenced by several variables and the objective is to optimize this response (Montgomery, 2005; Ryan, 2000).

The expected response equation is represented as:

$$E(y) = f(x_1, x_2) + \varepsilon \qquad (3\text{-}1)$$

where $E(y)$ is the response function, x_1 and x_2 are the factors that affect the function and ε represents the noise or error observed in the response y.

When the function is represented by a surface, it is called a response surface.

Response surface is usually presented by a graph such as the example shown in Figure 3.4. The expected yield $E(y) = \eta$ is plotted versus the levels of x_1 and x_2.

Usually, the contours of the response surface are plotted as shown in Figure 3.5. It helps to see the shape of a response surface. In the contour plot, lines of constant response are drawn in the $x_1 x_2 -$ plane. And each contour represents different height of the response surface.
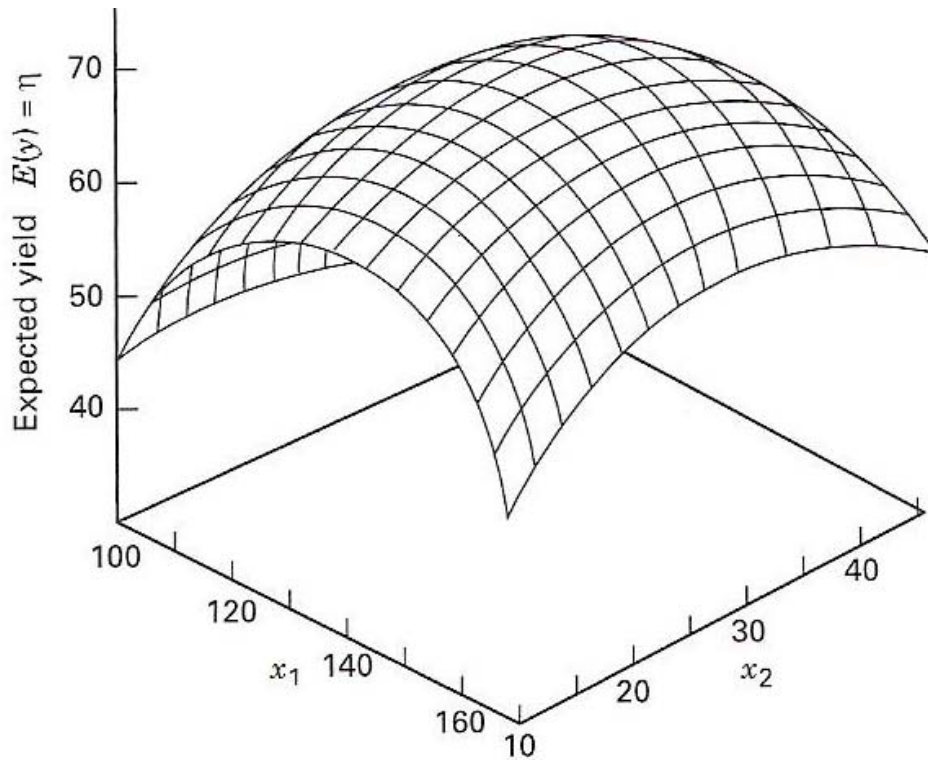
Figure 3.4: Three-dimensional response surfaces graph shows the expected yield as a

function of x_1 and x_2 (Montgomery, 2005).
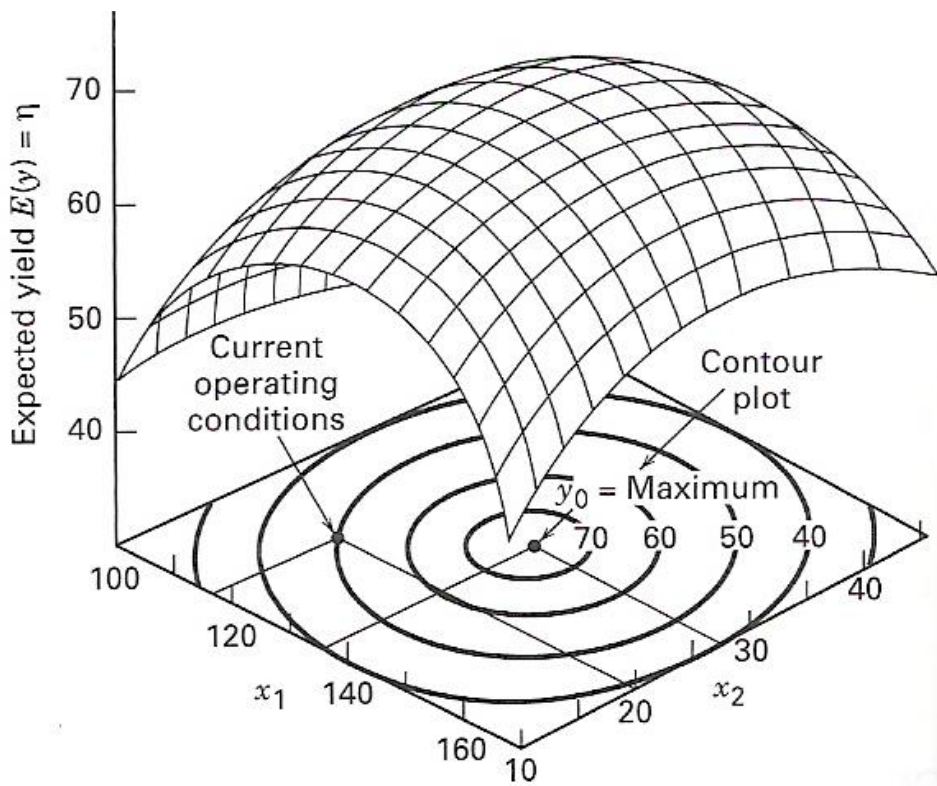
Figure 3.5: Example of contour plot of a response surface (Montgomery, 2005).

3.2.1 Defining Coded Variables

Coded variables are used to place the input variables to facilitate the construction of experimental designs. Coding removes the units of measurement of the input variables and as such, distances measured along the axes of the coded variables in a k-dimensional space are standardized (André, 1996).

A convenient coding formula for defining the coded variable, x_i, is

$$x_i = \frac{2X_i - (X_{iL} + X_{iH})}{X_{iH} - X_{iL}}, i = 1, 2, 3$$

where X_i are the levels of input variables and X_{iL} and X_{iH} are the low and high levels of X_i respectively.

Using coded variables rather than using the original input variables provides several advantages (André, 1996).

   a. Computational ease and increased accuracy in estimating the model coefficients.
   b. Enhanced interpretability of the coefficient estimates in the model.

3.2.2 First-order Response Surface

Usually, the relationship between the response and the independent variables is unfamiliar. Therefore, the first step to do when using response surface method is to find an approximation for the true functional relationship between the response and

the set of independent variables. A low-order polynomial in some region of the independent variables is used. The well-modeled response can be represented by first-order polynomial function:

$$y = \beta_0 + \beta_1 x_1 + \beta_2 x_2 + \ldots + \beta_k x_k + \varepsilon \qquad (3\text{-}2)$$

In general, Equation (3-2) can be written in a matrix form:

$$Y = \mathbf{bx} + E \qquad (3\text{-}3)$$

$$\text{where } \mathbf{x} = \begin{bmatrix} x_1 \\ x_2 \\ \vdots \\ x_k \end{bmatrix}, \ \mathbf{b} = \begin{bmatrix} b_1 \\ b_2 \\ \vdots \\ b_k \end{bmatrix}.$$

Y is defined to be a matrix of measured values, $\mathbf{x}$ to be a matrix of independent variables. The matrix $\mathbf{b}$ consists of coefficients and E consists of errors. The solution of Equation (3-3) can be obtained by matrix algebra.

The response surface analysis is then performed using the fitted surface. If the fitted surface is sufficient for approximating the true response function, then analysis of the fitted surface will be more or less equal to analysis of the actual system. The model parameters can be estimated most effectively if proper experimental designs are used to collect the data (Montgomery, 2005).

Response surface method is a sequential procedure. Often, when we are at a point on the response surface that is remote from the optimum, such as the current operating conditions in Figure 3.6, there is little curvature in the system and the first-order model will be appropriate (Montgomery, 2005).
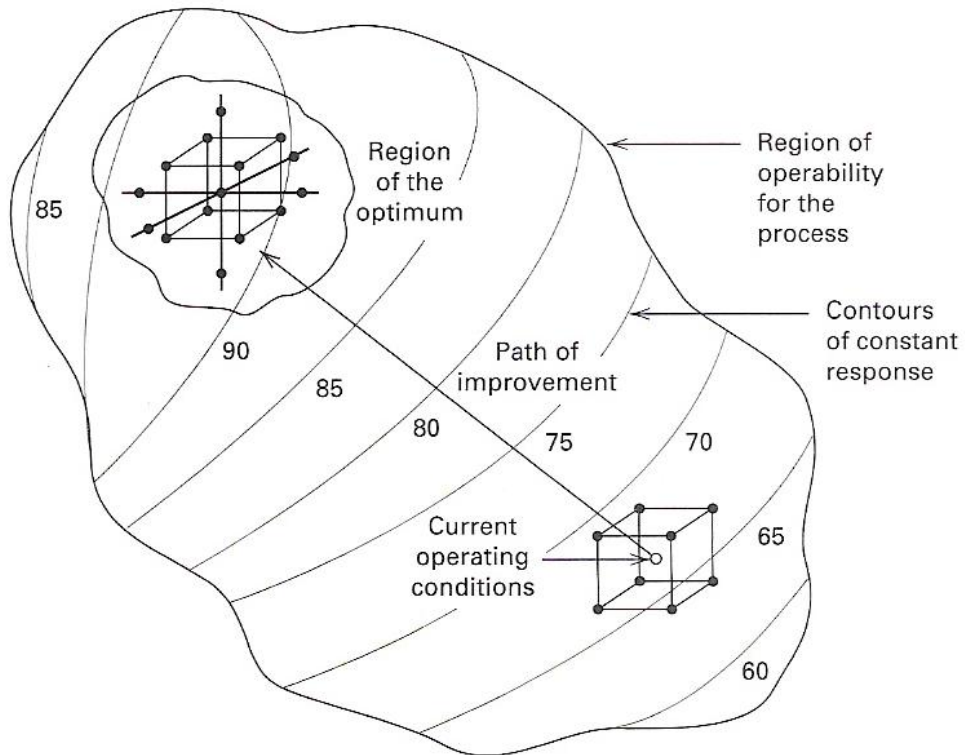
Figure 3.6: Sequential nature of response surface method (Montgomery, 2005).

3.2.3 Steepest Ascent Method in Response Surface Method

The method of steepest ascent is a procedure for moving in the direction of the maximum increase or decrease in the response. The fitted first-order model is:

$$\hat{y} = \hat{\beta}_0 + \sum_{i=1}^{k} \hat{\beta}_i x_i \qquad (3\text{-}4)$$

Frequently, the initial estimate of the optimum operating conditions for the system will be far from the actual optimum. In such circumstances, the objective of the experimenter is to move rapidly to the general vicinity of the optimum.

The first-order response surface is the contours of $\hat{y}$ which is a series of parallel lines like Figure 3.7. The direction of steepest ascent is the direction in which $\hat{y}$ increases most rapidly. This direction is parallel to the normal to the fitted response surface. The steps along the path are proportional to the regression coefficients $\left\{ \hat{\beta}_i \right\}$ and the actual step size is determined by the experimenter based on process knowledge or other practical considerations.

Experiments are conducted along the path of steepest ascent until no further increase in response is observed. Then a new first-order model may be fit, a new path of steepest ascent determined, and the procedure continued. Eventually, the experimenter will arrive in the vicinity of the optimum. This is usually indicated by a lack of fit of the first-order model. At that time, additional experiments are conducted to obtain a more precise estimate of the optimum.
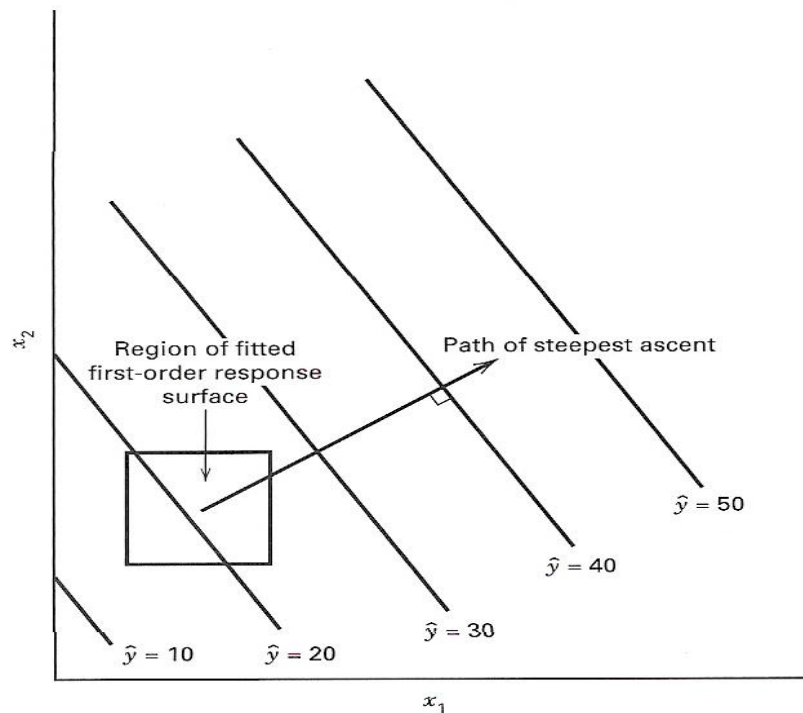
Figure 3.7: Diagram illustrates the first-order response surface and the steepest ascent

path (Montgomery, 2005).

A general algorithm can be used to determine the coordinates of a point on the path of

the steepest ascent. Assume that the point $x_1 = x_2 = \ldots x_k = 0$ is the base or origin point.

Then

    a.   chosen a step size in one of the process variables, say Δx_j. Usually, one

        will select the variable that are known or will select the variable that has

        the largest absolute regression coefficient $\left| \hat{\beta}_j \right|$.

    b.   the step size in the other variables is

$$\Delta x_i = \frac{\hat{\beta}_i}{\hat{\beta}_j / \Delta x_j}, \text{ where } i = 1, 2, \ldots, k, \, i \neq j$$

c. convert the Δx_i from coded variables to the natural variables.

3.2.4 Second-order Response Surface

When the experiments are relatively close to the optimum, a model that incorporates curvature is usually required to approximate the response. In most cases, the second-order model can be obtained. The second-order response surface can be represented by:

$$y = \beta_0 + \sum_{i=1}^{k} \beta_i x_i + \sum_{i=1} \beta_{ii} x_i^2 + \sum_i \sum_j \beta_{ij} x_i x_j + \varepsilon \qquad (3\text{-}5)$$

The second-order model can be presented in matrix notation as

$$\hat{y} = \hat{\beta}_0 + \mathbf{x}^{\mathbf{T}}\mathbf{b} + \mathbf{x}^{\mathbf{T}}\mathbf{Bx} \qquad (3\text{-}6)$$

$$\text{where } \mathbf{x} = \begin{bmatrix} x_1 \\ x_2 \\ \vdots \\ x_k \end{bmatrix}, \mathbf{b} = \begin{bmatrix} \hat{\beta}_1 \\ \hat{\beta}_2 \\ \vdots \\ \hat{\beta}_k \end{bmatrix} \text{ and } \mathbf{B} = \begin{bmatrix} \hat{\beta}_{11} & \hat{\beta}_{12}/2 & \cdots & \hat{\beta}_{1k}/2 \\ & \hat{\beta}_{22} & \cdots & \hat{\beta}_{2k}/2 \\ & & \ddots & \\ symmetrical & & & \hat{\beta}_{kk} \end{bmatrix}.$$

where **b** is a *(k*x*1)* vector of the first-order regression coefficients and **B** is a *(k*x*k)* symmetric matrix whose main diagonal elements are the pure quadratic coefficients ($\hat{\beta}_{ii}$) and the off-diagonal elements are one-half the mixed quadratic coefficients ($\hat{\beta}_{ij}$, $i \neq j$). In order to find the stationary point, the derivative of $\hat{y}$ with respect to the elements of the vector **x** is equated to **0** as:

$$\frac{\partial \hat{y}}{\partial \mathbf{x}} = \mathbf{b} + 2\mathbf{B}\mathbf{x} = \mathbf{0} \qquad (3\text{-}7)$$

or

$$\mathbf{x_s} = -\tfrac{1}{2}\,\mathbf{B}^{-1}\mathbf{b} \qquad (3\text{-}8)$$

The stationary point is the solution of Equation (3-7) or Equation (3-8). Moreover, by substituting Equation (3-8) into Equation (3-6), the predicted response at the stationary point can be found as:

$$\hat{y}_s = \hat{\beta}_0 + \frac{1}{2}\mathbf{x'}_s\mathbf{b} \qquad (3\text{-}9)$$

By fitting the second-order response surface, the stationary point for the surface can be found. Three types of stationary point can be obtained in the response surface. They are:

    a. maximum point,

    b. minimum, and

    c. saddle point.

These three possibilities are shown in Figures 3.8, 3.10, and 3.12 respectively. The contour plots of response surface can show the shape of the surface and the location of the optimal region. Three different examples are shown in Figures 3.9, 3.11, and 3.13.
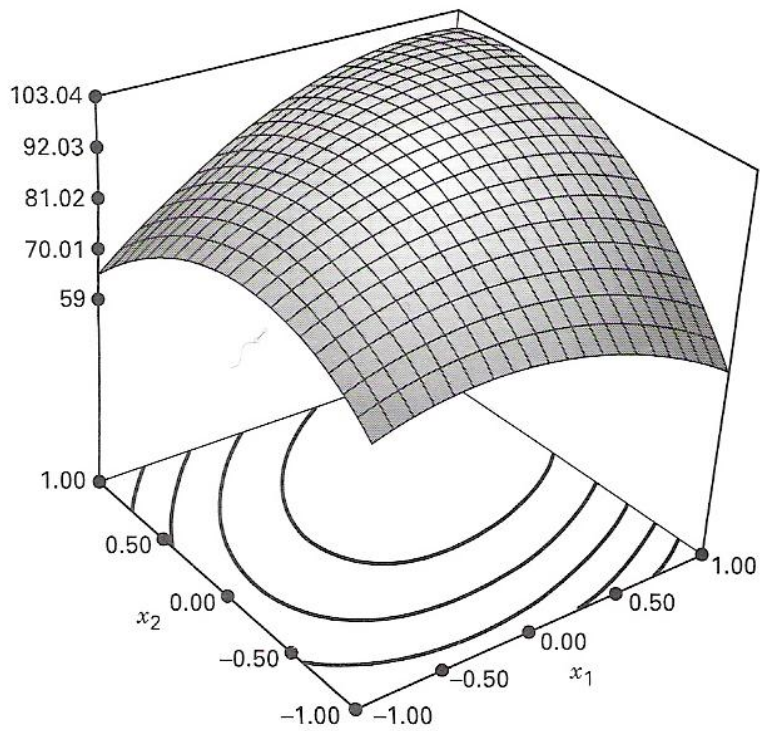
Figure 3.8: Illustration of response surface with a maximum point (Montgomery, 2005).
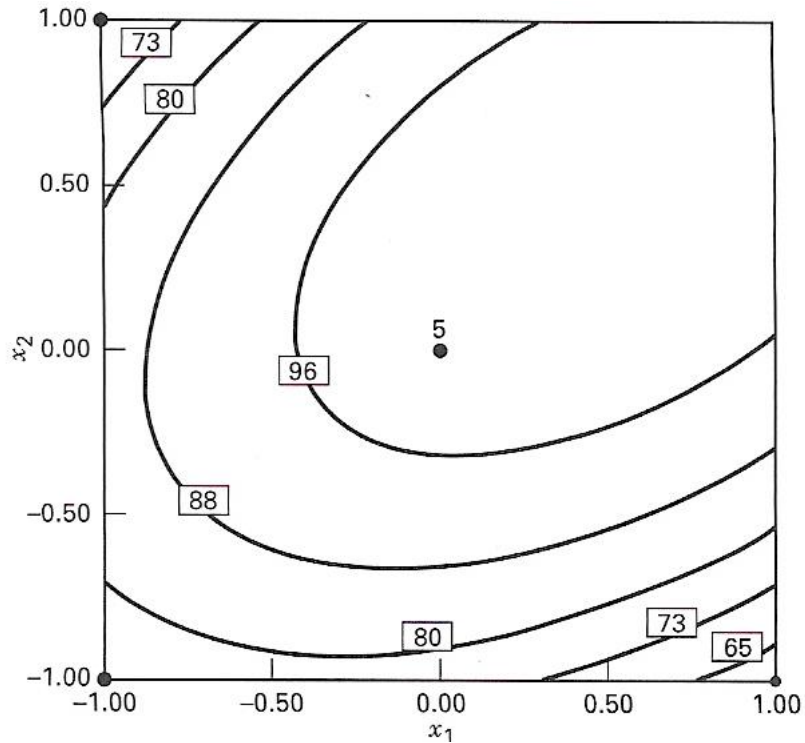
Figure 3.9: Illustration of contouring plot with a maximum point (Montgomery, 2005).
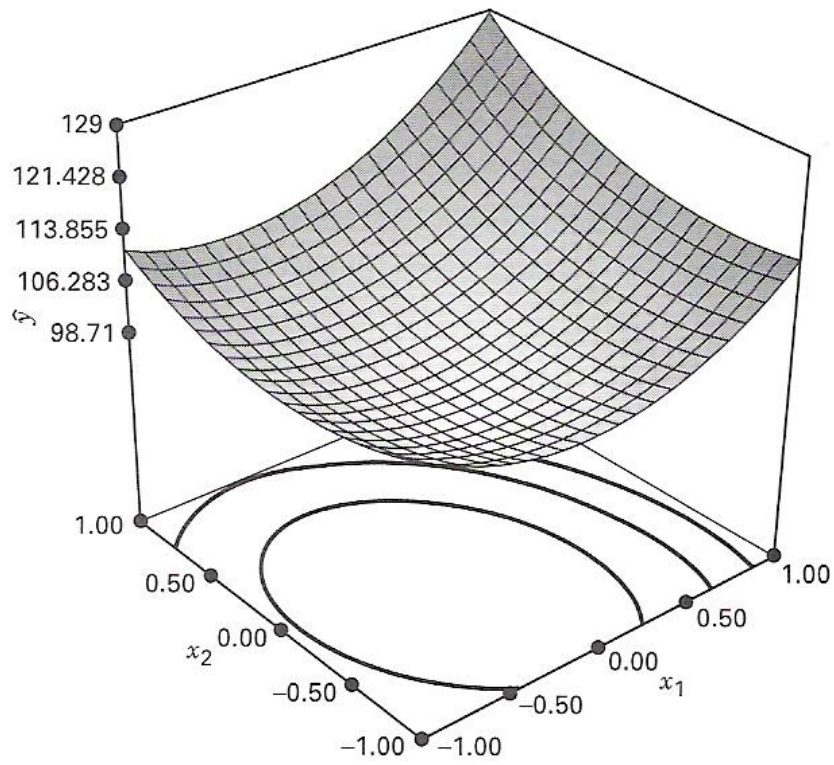
Figure 3.10: Illustration of response surface with a minimum point (Montgomery, 2005).
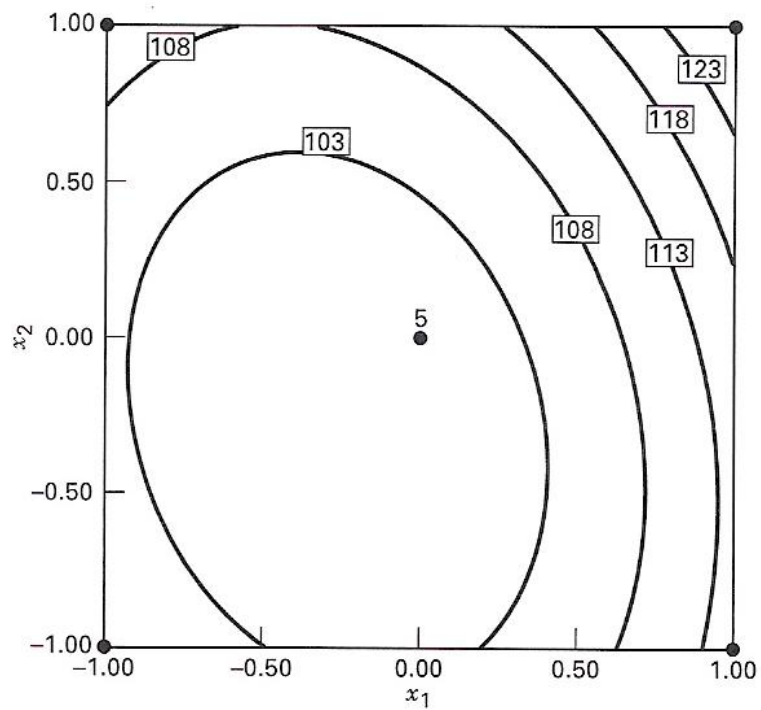
Figure 3.11: Illustration of contouring plot with a minimum point (Montgomery, 2005).
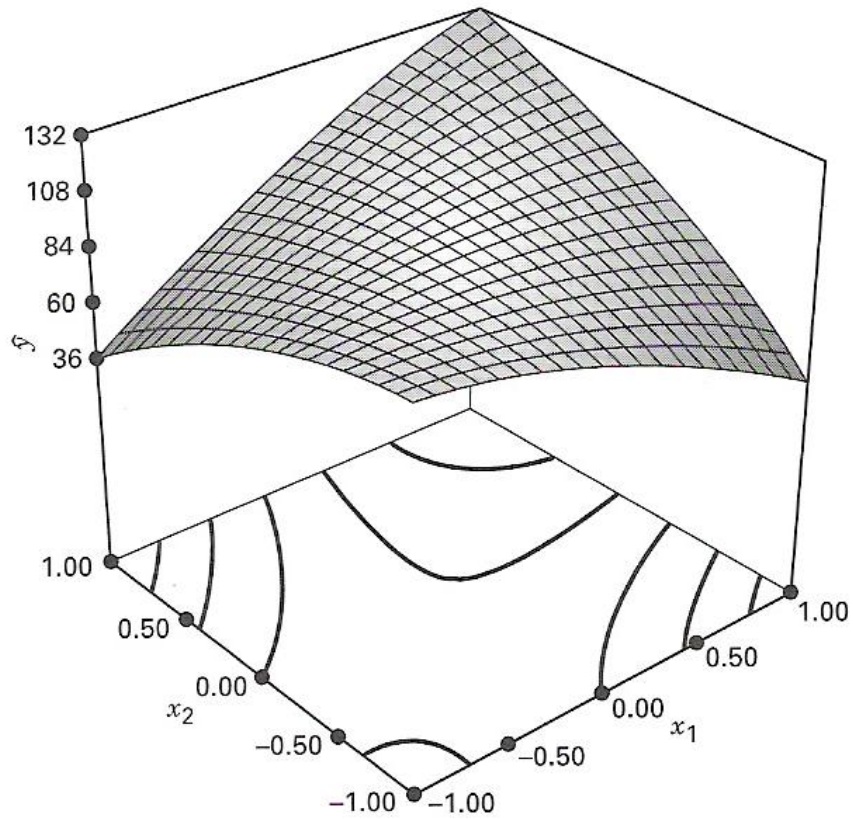
Figure 3.12: Illustration of response surface with a saddle point (Montgomery, 2005).
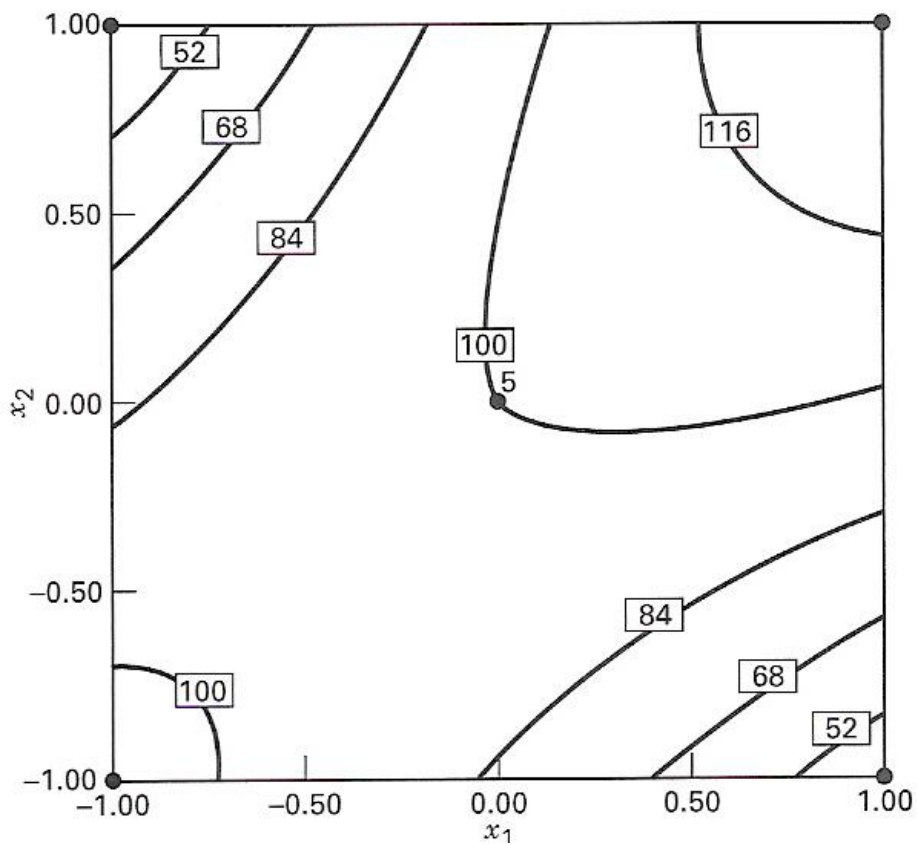
Figure3.13: Illustration of contouring plot with a saddle point (Montgomery, 2005).

3.2.5 Characterizing the Response Surface

After obtaining the stationary point, the response surface can be characterized. This means to determine whether the stationery point is a point of maximum, minimum, or a saddle point. And it also needs to study the relative sensitivity of the response to the variables.

One method is to examine the contour plot of the fitted model. It is easy to construct and interpolate the contour plot of a model if there are two or three variables. If more variables are considered, canonical analysis is recommended (Montgomery, 2005). Figure 3.14 shows an example of canonical form of the second-order model.

First, the model will be transformed into a new coordinate system with the origin at the stationary point. Then, system axes will be rotated until they are parallel to the principal axes of the fitted response surface. This transformation is illustrated in Figure 3.14. It can be shown that this results in the fitted model (Montgomery, 2005):

$$\hat{y} = \hat{y}_s + \lambda_1 \omega_1^2 + \lambda_2 \omega_2^2 + \cdots + \lambda_k \omega_k^2 \qquad (3\text{-}10)$$

where $\{\omega_i\}$ are the transformed independent variables and $\{\lambda_i\}$ are constants. Equation (3-10) is called the canonical form of the model. $\{\lambda_i\}$ are the eigenvalues or characteristic roots of the matrix **B**.

The nature of the response surface can be determined from the stationary point and

the signs and magnitudes of $\{\lambda_i\}$. Assume that the stationary point is within the region of exploration for fitting the second-order model. If $\{\lambda_i\}$ are all positive, then $\mathbf{x}_s$ is a point of minimum response; if $\{\lambda_i\}$ are all negative then $\mathbf{x}_s$ is a point of maximum response; and if $\{\lambda_i\}$ have different signs, $\mathbf{x}_s$ is a saddle point. Furthermore, the surface is steepest in the ω_i direction for which $|\lambda_i|$ is the greatest (Montgomery, 2005; Ryan, 2000).
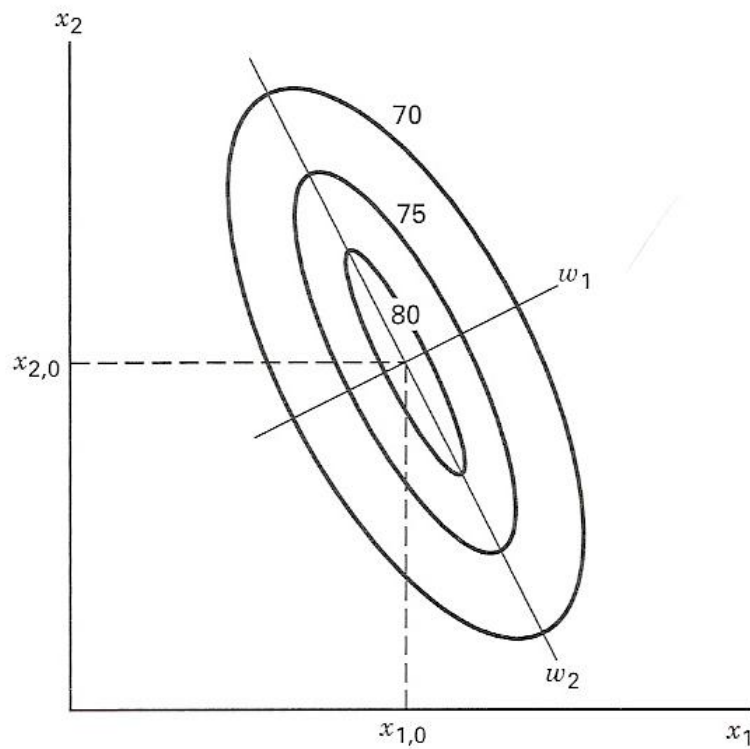
Figure 3.14: Canonical form of the second-order model (Montgomery, 2005).

CHAPTER 4 IMPLEMENTATIONS

In this chapter, the parameters selection of optimization will be summarized in Section 4.1. Section 4.2 outlines the experiment procedures and Section 4.3 describes the substrates for the coating test. Finally, the equipment and apparatus for experiments are given in Section 4.4.

4.1 Parameters Selection for Optimal Coating Process

In this research, cause-and-effect diagram is used to analyze the optimization of the PVD coating process. It provides a systematic way of looking at effects and causes that create or contribute to those effects. This process determines the relationship between the coating conditions and adhesion of coating.

Cause-and-effect diagram is often called Ishikawa diagram or fishbone diagram because of its shape. The diagram is to assist teams in categorizing the many potential causes of problems or issues in an orderly way and in identifying the root causes. The cause-and-effect diagram is also known as the fishbone diagram because it was drawn to resemble the skeleton of a fish, with the main causal categories drawn as "bones" attached to the spine of the fish, as shown in Figure 4.1.
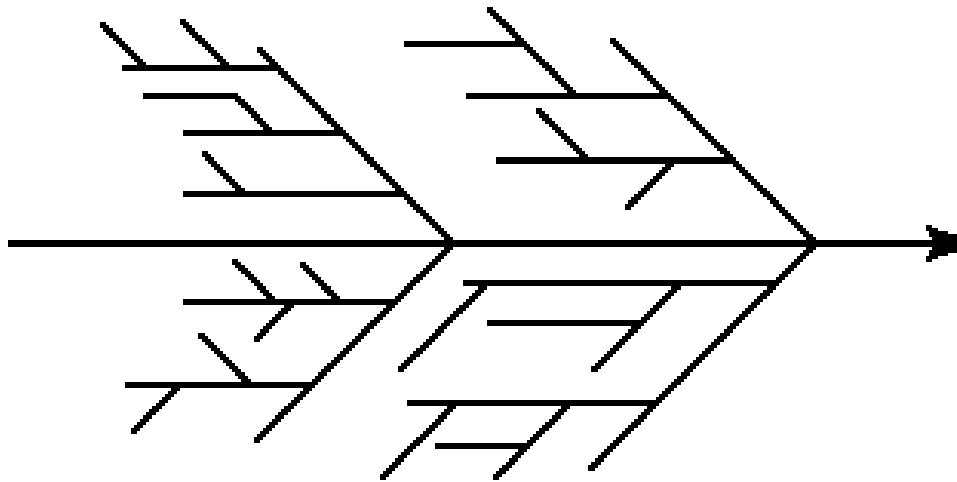
Figure 4.1: Branches in fishbone diagram like the skeletons of a fish.

A cause-and-effect diagram can be categorized into one of three groups (Beckford, 1998; Phillip, 1996, and Montgomery, 2005):

a. Dispersion type

b. Production process classification type

c. Cause enumeration type

Dispersion analysis is helpful for organizing the thought process and for developing the relationships among potential causes. By first developing major categories of potential causes and then breaking these down into subgroups and the subgroups into more specific causes, this type of diagram provides a simple structured technique for generating ideas concerning potential causes of the specific end result that we are concerned with and organizing them in a logical order. However, care must be taken to ensure that all potential causes are included, not just the most obvious ones.

The production process classification diagram can be helpful in giving those not so familiar with the process a better idea of the relationships between each stage and of where the impact of potential factors would be felt. One limitation is the tendency to identify repetitive causes at different process steps, a tendency that, when incorporated into an experiment, can result in an unnecessary potential interactions between factors identified at different process steps (Beckford, 1998; Phillip, 1996 and Montgomery, 2005).

The third type, which has been proven as a particularly effective tool for promoting team brainstorming efforts, is the cause enumeration diagram. Whereas the dispersion analysis diagram begins with major categories and subgroupings to which potential cause are added, cause enumeration begins with brainstorming open to any type of potential cause linked to the effect that the team is investigating. Once all the ideas are listed, they can then be clustered into subgroups, and related subgroups can be combined into major categories. Quite often the ideas can be grouped into five major classifications shows in Figure 4.2 (Beckford, 1998; Phillip, 1996, and Montgomery, 2005). They are:

a. Materials;

b. Machine or equipment;

c. Manpower;

d. Methods, and

e. Measurement.
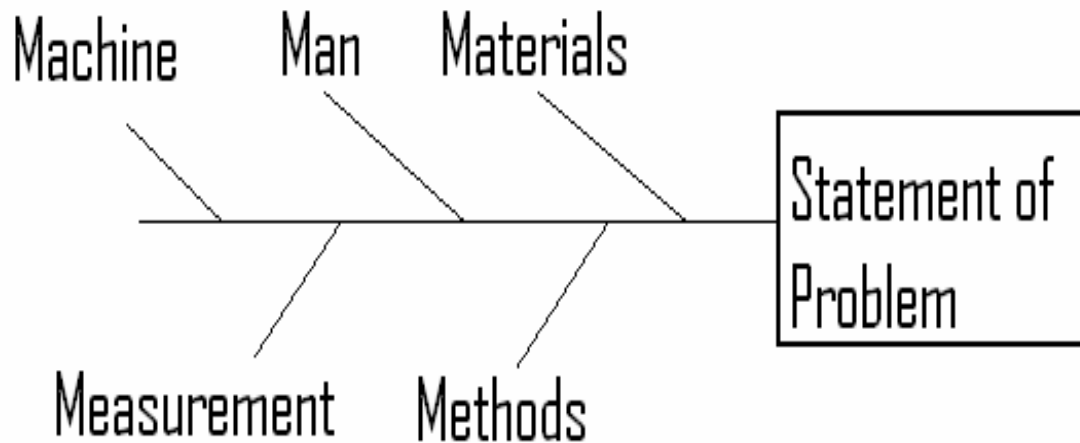
Figure 4.2: Five major classifications of fishbone diagram.

The final result will resemble the dispersion analysis diagram. However, the difference is in the steps to get there. In dispersion analysis, a structure is first built, and then ideas are added to it.

Figure 4.3 shows the cause-and-effect diagram of the factors that influence the adhesion property of coating. Coating time, deposition temperature, surface finishing of substrate material, bias voltage, arc current, coating materials, and nitrogen pressure are factors that will influence the adhesion property of coating.

Although adhesion has great impact on coating, in-depth study cannot be conducted due to limitation of resources in the teaching company. The adhesion would be checked and ensured by using a quick and easy method, Rockwell-C indentation test developed by Mercedes-Benz.

After determination and listing out the possible factors, the most important factors will be selected and be the controlled factors in the experiments. The selection of

these controllable factors depends on the cost and time of the whole process or production.
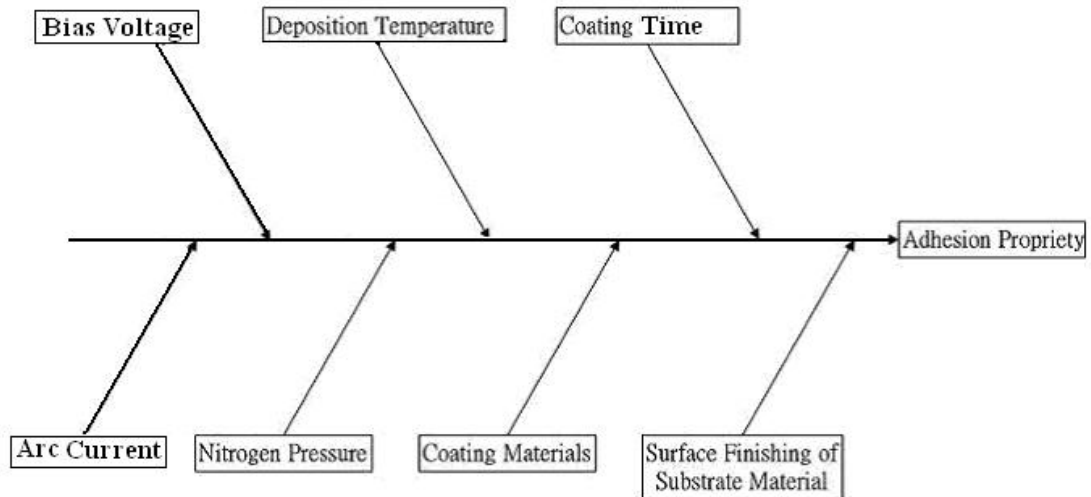
Figure 4.3: Fishbone diagram illustrates the factors that influence the adhesion property of coating.

The coating R_a value is affected by bias voltage of substrates, cathodic arc current, coating time, deposition temperature, substrates surface R_a value, and nitrogen pressure control of chamber during deposition step. Figure 4.4 shows the factors that will affect the surface roughness of coating.
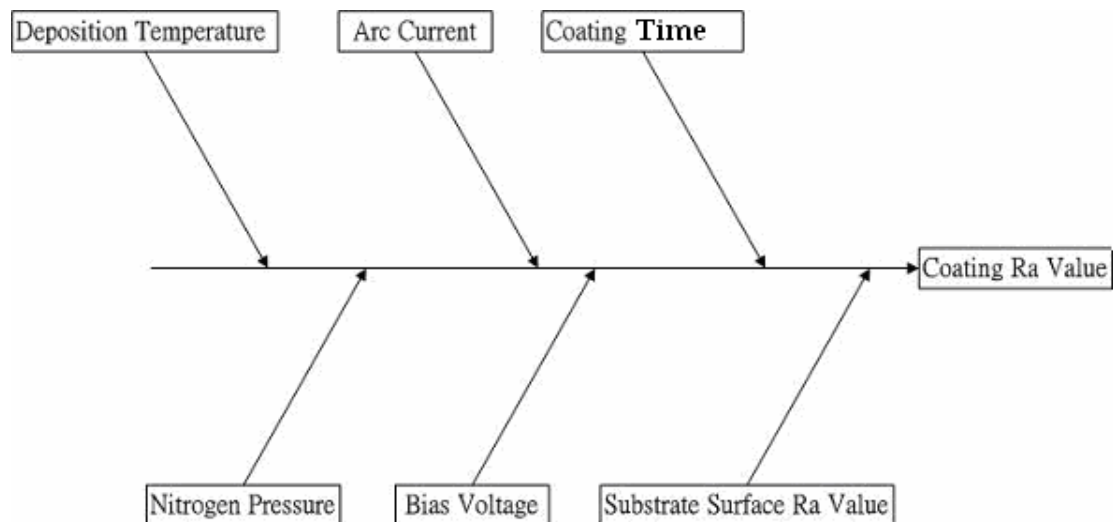
Figure 4.4: Fishbone diagram illustrates the factors that influence the R_a value of coating.

After analyzing the causes with teaching company, the parameters that affect the process most can be identified. For roughness, the most critical factors are bias voltage of substrates, current of cathodic arc and nitrogen pressure control during deposition, and coating time.

It is because, for CAPVD coating process, the best deposition temperature is about 400°C +/- 10°C by the experience of the teaching company. Under this range of coating temperature, the coating adhesion will not be affected. Moreover, the customers of Techmart are mostly required 0.2μm for mould steel application. So, the deposition temperature is assumed to be around 400°C and 0.2μm. Therefore, the factors, the deposition temperature and substrate surface R_a value, are neglected in the Taguchi method.

Therefore, these four factors will be controlled and considered in the experiments for titanium nitride and chromium nitride coatings.

4.2 Experimental Procedures

4.2.1 Coating Process

Figure 4.5 shows the research experiment procedures. First, the substrates are polished to obtain the mean roughness value (R_a) around 0.2μm. Then, the substrates are cleaned by ultrasonic machines with hot alkaline solvent within the temperature range of 65 to 75°C. After that the residual is rinsed by soft water and the substrates are dried out by a dryer.

The coating process is operated at 400°C. It consists of placing the substrates into the chamber. The substrates are pumped down to the desired vacuum pressure and the preheating cycle starts. After the heating cycle is completed, the ion bombardment cycle starts. It cleans the substrates' surfaces before depositing the coating.

After the ion bombardment cycle is completed, the coating cycle begins. Then the target material is evaporated in the CAPVD process. An electrical charge is applied to the substrates so as to draw the ions to the substrates' surfaces. The evaporated material reacts with the gas(es) and emits into the chamber to form the desired coating. The coating cycle continues until the preferred coating time has been deposited. Finally, the substrates are allowed to cool and then took out from the chamber.

Afterward, measurements on R_a value, surface morphology and adhesion test can be carried out.

Preparing substrates

⇩

Cleaning substrates in cleaning line

⇩

Drying substrates by dryer

⇩

Coating substrates

⇩

Measuring adhesion

⇩

Measuring R$_a$ value

⇩

Surface morphology by SEM

(The Hong Kong Polytechnic University Materials Research Centre (MRC))

Figure 4.5: Experiment workflow.

4.2.2 Taguchi Method for Coating Optimization

Taguchi method is one of the most significant methods to undergo optimization of a process or production. In this study, Taguchi method is applied to PLATIT PL50 CAPVD system. Design of experiments, using L_9 (3^4) array, is carried out for optimizing different control factors. These factors affect the adhesion and surface responses in PLATIT CAPVD coating.

The optimization experiments were to optimize the surface roughness after the titanium nitride and chromium nitride coating with a L_9 (3^4) array.

The target materials and control factors for these two types of coating are listed in Table 4.1. The target materials used in the experiments include titanium and chromium. The control factors included bias voltage, arc current, nitrogen pressure and coating time.

Coating	Target Material
Titanium nitride	Titanium
Chromium nitride	Chromium

Table 4.1: Target materials used for TiN and CrN coatings.

The process parameters for each experiment can be setup in the program of the coating machine. The four factors: bias voltage, arc current, nitrogen pressure, and coating time are controlled by the program automatically. There is no need to control or change the settings manually.

4.2.2.1 Calculations on Signal-to-noise Ratio in Taguchi Method

Using the signal-to-noise (S/N) ratio, optimization can be found out. After completing all the experiments, the S/N ratio can be calculated for each level.

A smaller-the-best approach is applied to investigate the optimal condition when considering the roughness.

The smaller-the-best characteristics are defined as follows:

$$\text{S/N ratio} = -10\log_{10}\frac{\sigma}{N} \tag{4-1}$$

$$\sigma = \Sigma(Y_i^2) \tag{4-2}$$

where Y_i is the roughness (R_a) value and N is the number of results of each experiment being carried out.

Equations (4-1) and (4-2) are used to calculate the S/N ratio of roughness values in coating.

4.2.3 Further Optimization by Response Surface Method

After the four factors have been optimized by Taguchi Method, a further optimization using response surface method (RSM) is conducted. The initial points in RSM experiments use results from the Taguchi Method. Firstly, a low-order polynomial was employed to approximate the true function in some region of the independent variables. Secondly, the steepest descent or ascent method was used to move along the path of the maximum decrease or increase in the variables. Lastly, a second-order polynomial was used to finalize the coating roughness performance.

4.3 Substrates for Coating Tests

For TiN coating and CrN coating tests, a common mould steel ASSAB 88 (Composition: C 0.9%, Si 0.9%, Mn 0.5%, Cr 7.8%, Mo 2.5%, and V 0.5%) was used in the experiments. The size of substrates was in dimension $\varnothing$ 20 x 10mm. Before the coating process, the substrates are polished to around $R_a = 0.2$ μm.

Figure 4.6: Substrates used in the experiments.

4.4 Apparatus

In the study, the apparatus being used to carry out the experiments were: (a) Rockwell hardness tester, (b) optical microscope, (c) surface profilometer, and (d) scanning electron microscope.

4.4.1 Rockwell Hardness Tester

For measuring adhesion and hardness of the testpieces, Rockwell hardness tester was used. Then hardness tester was used to measure the hardness of workpieces before coating and after coating. After coating, Rockwell C measurement with loading in 1471N (150kgf) was used to measure the adhesion. To check adhesion, cracking pattern of the indented point was observed.

Figure 4.7: Hardness indenter used for checking goodness of coating adhesion.

4.4.2 Optical Microscope

Optical microscope was used for coating adhesion measurements. The image under the objectives of microscope would be captured and output to the computer. Measurements could then be done with a coating measuring software.
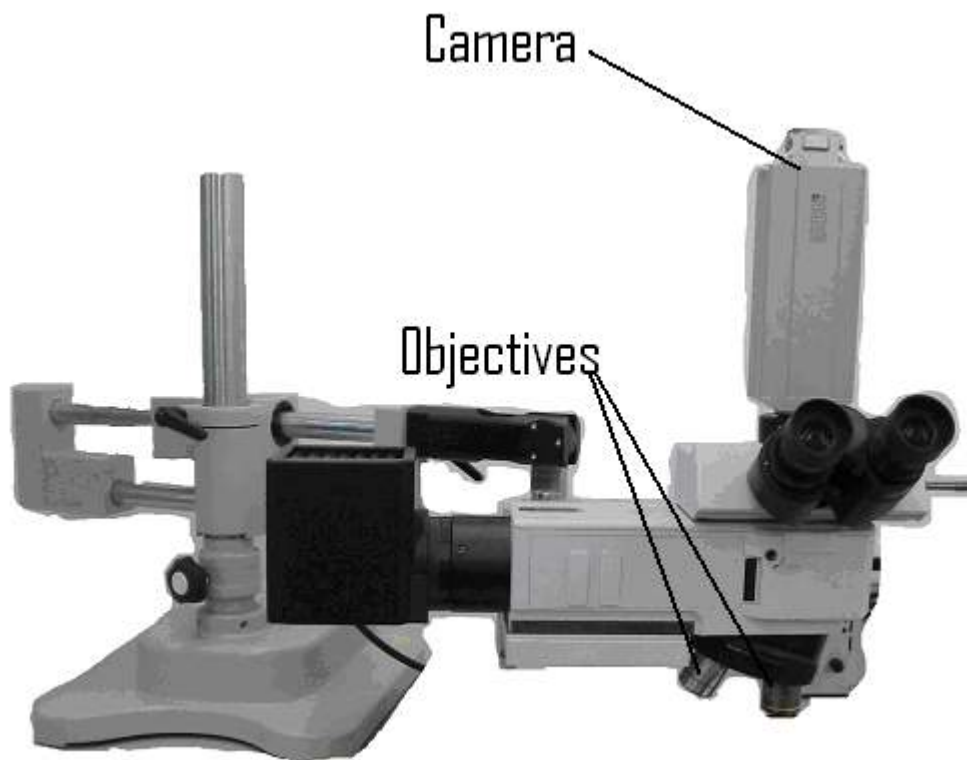
Figure 4.8: Optical microscope for evaluating coating adhesion.
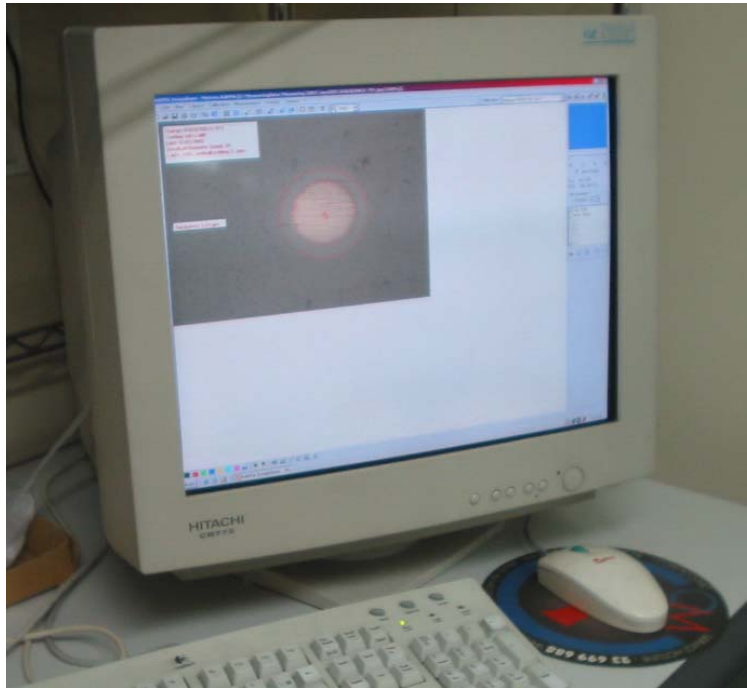
Figure 4.9: Coating measurement by using monitor and software.
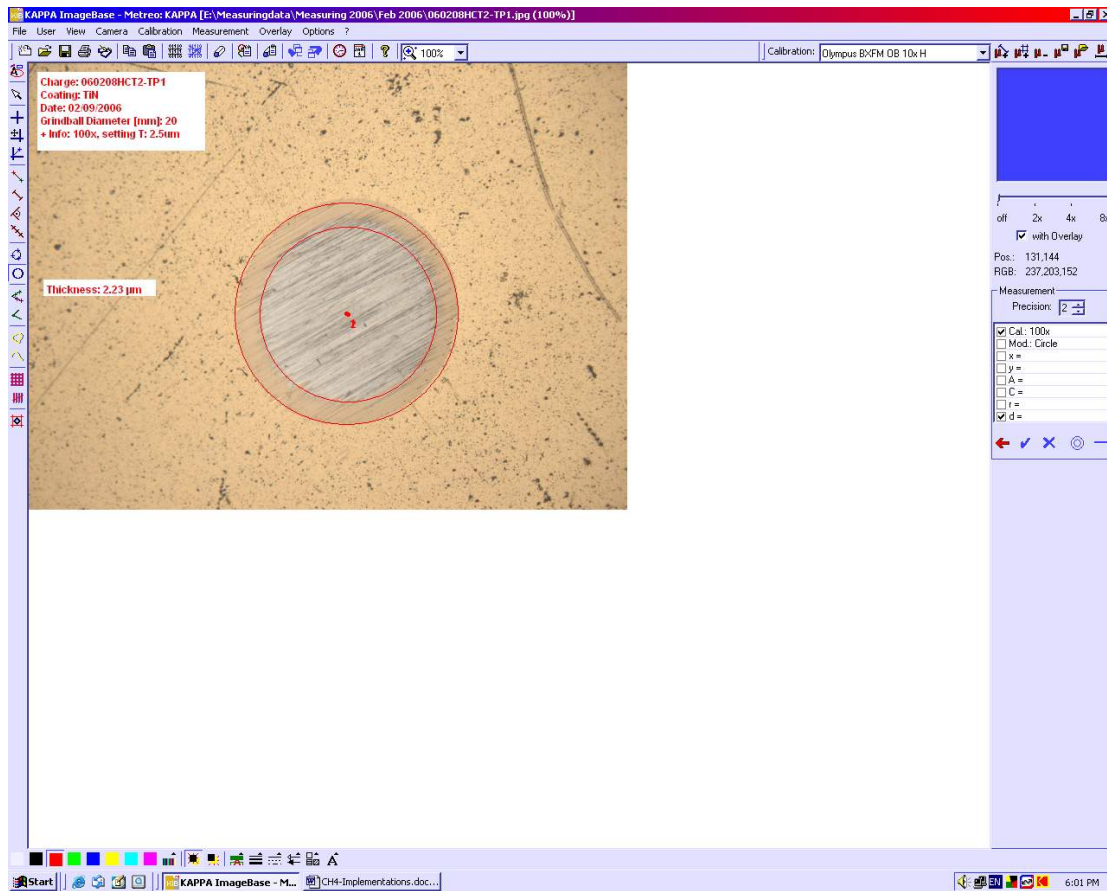
Figure 4.10: Screen display of measuring software.

4.4.3 Surface Profilometer

In the study, surface roughness R_a was measured by using a Mitutoyo surface profilometer. It is an easy, inexpensive and a quick way to measure the surface roughness.

A fine stylus tip is drawn across the surface and is supposed to follow the contours of the measuring surface. The vertical motion of the stylus is converted to an electrical signal that may be processed to present the result in several different ways. A useful form of output of the profilometer is a surface profile graph like Figure 4.14. Magnifications appropriate to the context may be chosen. And the vertical magnifications are many times greater than the horizontal in order to display the relatively fine features of roughness.
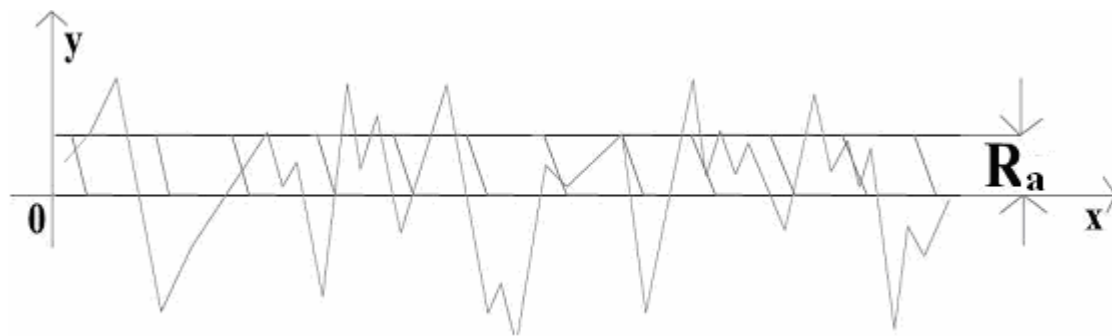
Figure 4.11: Profile graph for R_a measuring (Graham, 2003).

The profile graph is a distorted representation of the shape of the irregularities. A single graph gives an indication of roughness along a single line on the surface. Instruments are available which make a series of transverses over an area and produce a map showing the roughness as contours.

Figure 4.12 Surface profilometer for measuring coating R_a value.

4.4.4 Scanning Electron Microscopy (SEM)

The Scanning Electron Microscopy (SEM) is designed for direct studying the surfaces of solid objects. SEM is used to investigate the surface morphology of coating in this experiment. The operation of the microscope is based on scanning with an electron beam. A beam is generated and focused on the electronic microscope. Then, an image is formed in the computer monitor.   Some of metal grains and grain boundaries can be observed. The magnifying power of SEM can reach 200, 000x.

Figure 4.13: SEM for surface morphology (The Hong Kong Polytechnic University Materials Research Centre (MRC)).

CHAPTER 5 RESULTS & ANALYSES

5.1 Experiments on TiN Coatings

A L_9 orthogonal array design of experiment is used to optimize the coating process. The four controllable factors for the experiment are listed in Table 5.1. The three levels of each factor are represented by a '0',' 1' or '2' in the matrix.

The control factors for TiN coating are bias voltage (V), arc current (A), nitrogen pressure (mbar) and the coating time (mins.). The R_a measurement would be measured twice to increase the accuracy of the experiments. Factor A was assigned to row 1, factor B was assigned to row 2, factor 3 was assigned to row 3, and factor D was assigned to row 4.

Factors	Levels		
	0	1	2
A. Bias voltage (V)	-50	-80	-110
B. Arc current (A)	100	120	140
C. Nitrogen pressure (x10E-03 mbar)	6	8	10
D. Coating time (mins.)	35	50	70

Table 5.1: Factors and levels used in the experiment.

Totally, 9 experiments were conducted by using the Taguchi method instead of doing 81 experiments in traditional full factorial experiment method. The differences are shown in Appendix A.

Before measuring the R_a value of the experiments, adhesion test based on Mercedes Benz method have been conducted to make sure that there is no adhesion problem in the coating. Table 5.2 indicates the adhesion test of TiN coating. The tests show that all combination provides good adhesion. No experiment is in bad adhesion and all experiments are accepted.

Trial no.	L9					
	Coating Parameters or factors				Adhesion Classification	
					1st sample	2nd sample
	A	B	C	D		
1	0	0	0	0	HF2	HF1
2	0	1	1	1	HF1	HF1
3	0	2	2	2	HF1	HF2
4	1	0	1	2	HF1	HF1
5	1	1	2	0	HF1	HF1
6	1	2	0	1	HF2	HF2
7	2	0	2	1	HF1	HF1
8	2	1	0	2	HF1	HF1
9	2	2	1	0	HF2	HF1

Table 5.2: Adhesion checking before R_a measuring test of TiN coating.

Table 5.3 shows the L9 orthogonal array for the experiments, R_a values and the S/N ratio for each run. Two samples will be taken in R_a value of each run. After the roughness measurements, S/N ratio in smaller-the-best characteristic can be calculated.

| Trial no. | Coating parameters or factors | | | | R_a value (μm) | | S/N ratio |
	A	B	C	D	1st sample	2nd sample	
1	0	0	0	0	0.366	0.310	9.39
2	0	1	1	1	0.243	0.260	11.98
3	0	2	2	2	0.346	0.216	10.80
4	1	0	1	2	0.263	0.246	11.88
5	1	1	2	0	0.253	0.190	13.01
6	1	2	0	1	0.220	0.260	12.37
7	2	0	2	1	0.183	0.206	14.21
8	2	1	0	2	0.243	0.235	12.43
9	2	2	1	0	0.233	0.210	13.08

(L9 header spans the full table)

Table 5.3: The L9 Orthogonal array for the experiments, R_a value and S/N ratio for each run

of TiN coating.

5.1.1 Normal Probability Plot of S/N Response Ratio in TiN Coating

The normal probability plot is for evaluating whether the data follows normal distribution. Figure 5.1 shows that the R_a response in TiN coating does follow the normal distribution within 95% confidence level.
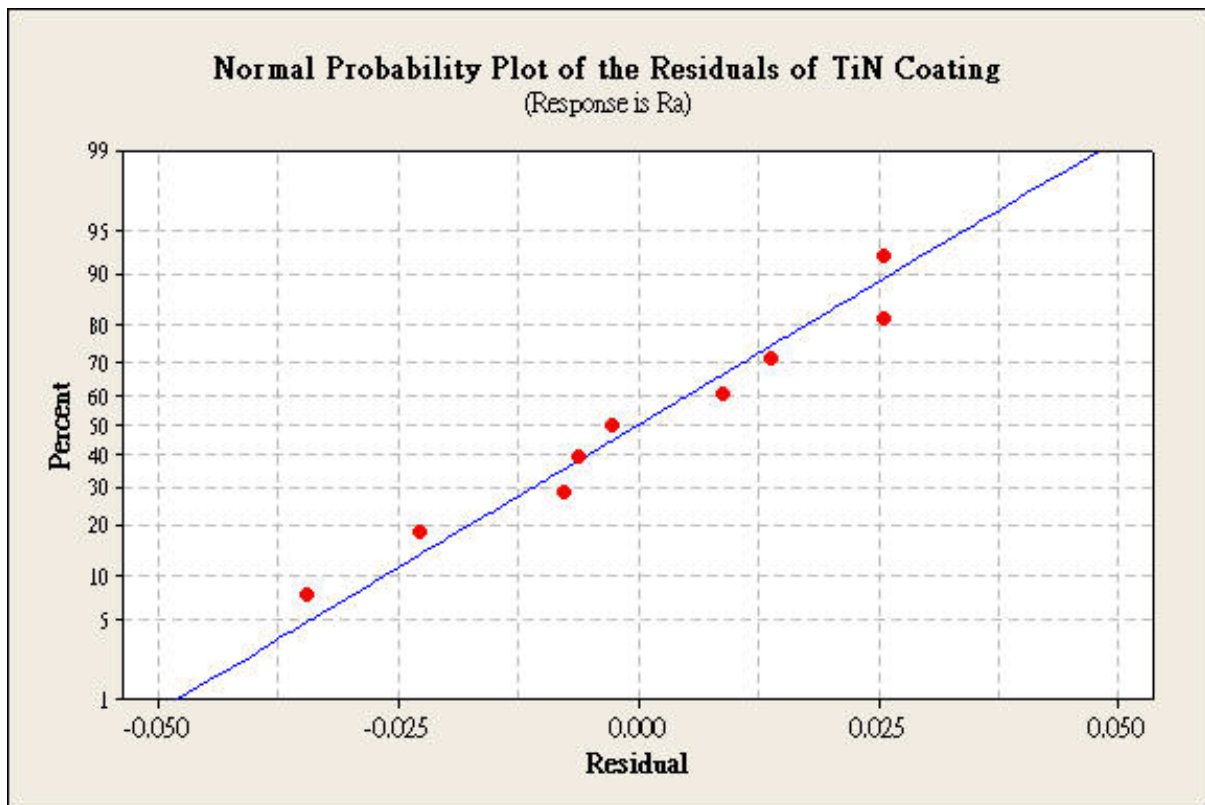
Figure 5.1: Normal probability plot graph of residual for the TiN roughness test.

5.1.2 S/N Response Ratio of TiN coating

Table 5.4 indicates the mean S/N response ratio of TiN coating under different coating parameters. It shows that the nitrogen pressure is the most critical factor to roughness value whereas the arc current shows less interaction with the roughness in TiN coating.

Levels	Mean S/N response ratios			
	A	B	C	D
0	10.73	11.83	11.40	11.83
1	12.42	*12.47*	12.32	*12.85*
2	*13.24*	12.17	*12.67*	11.70
Maximum-Minimum	*2.51*	0.65	1.27	1.15
Rank	*1*	4	2	3

Table 5.4: Mean S/N response ratios of TiN coating.

The effects of S/N ratios can be represented by diagram or plot. Figure 5.2 shows the main effects plot of S/N ratio of TiN coating R_a value. It demonstrates which factor provides great effect and influence on the coating process.

Table 5.4 shows more clearly that the main effect is factor A, the bias voltage. Then it is factor C the nitrogen pressure. The next one is the factor B, the arc current and the final one is factor D, the coating time. It shows that the best condition or parameter is in A2B1C2D1. When bias voltage = –110V, arc current = 120, nitrogen pressure = 8.0 x 10E-03, and coating time = 50mins., the optimal condition can be obtained.
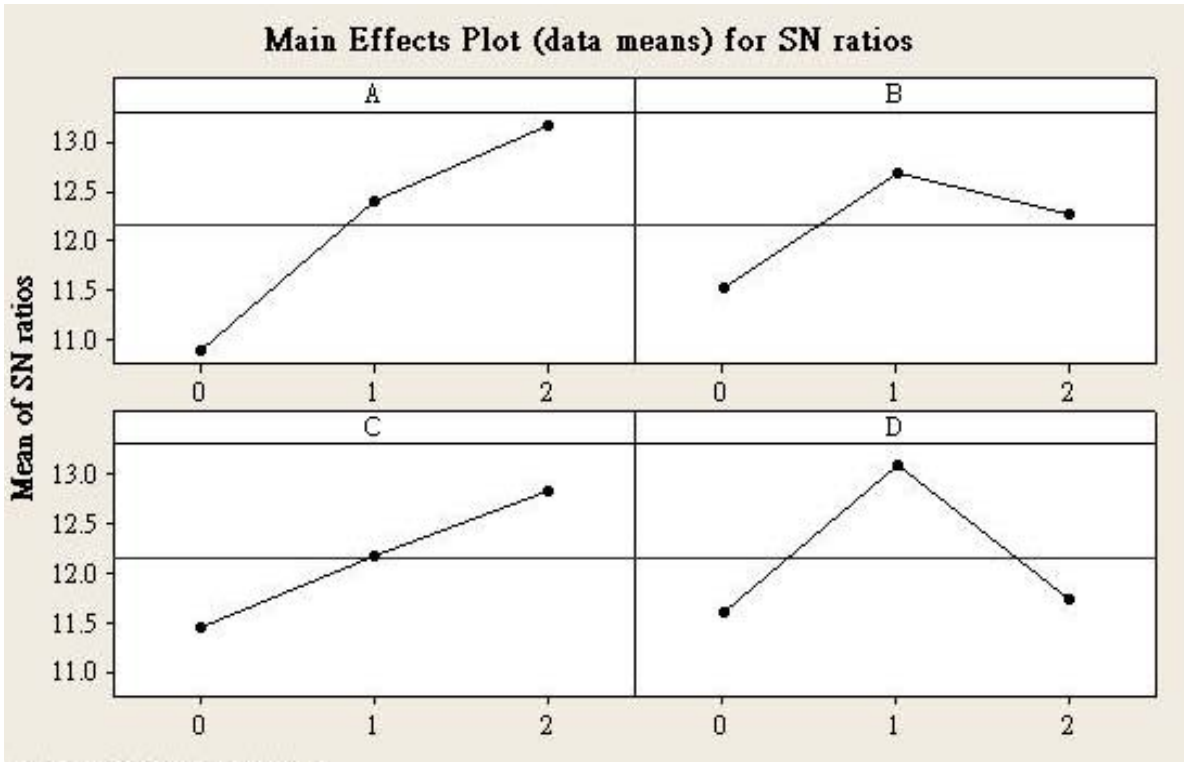
Figure 5.2: S/N ratios response graph for TiN coating.

5.1.3 ANOVA for S/N Ratio in TiN Coating

Analysis of Variance (ANOVA) method was developed by Sir Ronald Fisher in the 1930s as a method to interpret the results from agricultural experiments (Montgomery, 1997). ANOVA is a mathematical tool to detect differences in average performance of groups of items tested.

Source	Degrees of freedom	Sum of square	Mean variance	Percentage Contribution
Bias Voltage	2	9.86	4.93	63.7
Arc Current	2	0.64	0.32	4.1
Nitrogen Pressure	2	2.60	1.30	16.8
Coating Time	2	2.39	1.12	15.4
Residual Error	0	*	*	*
Total	8	15.48	*	100

Table 5.5: ANOVA table for TiN coating R_a test.

Percentage contribution is to determine the amount of influence each factor has on the final outcome. Table 5.5 shows that the bias voltage has the highest percentage contribution in TiN coating test. It explains that the most important factor needed to be controlled is the bias voltage and then the nitrogen pressure, the coating time, and finally is the arc current. The result matches with that of Taguchi method.

5.2 Experiments on CrN Coatings

The control factors for CrN coating are the bias voltage (V), the arc current (A), the nitrogen pressure (mbar), and the coating time (mins.). The levels for each factor are shown in Table 5.6.

Control factors	Levels		
	0	1	2
A. Bias voltage (V)	-60	-80	-110
B. Arc current (A)	110	130	150
C. Nitrogen pressure (x 10E-03 mbar)	7	9	10
D. Coating time (mins.)	38	57	76

Table 5.6: Factors and levels used in the experiment for CrN coating.

Like TiN coating test, factor A is assigned to row 1, factor B is assigned to row 2, factor 3 is assigned to row 3 and factor D is assigned to row 4. Table 5.7 shows the adhesion checking test result before the R_a measuring test of CrN coating.

Trial no.	L₉					
	Coating Parameters or factors				Adhesion Classification	
					1st sample	2nd sample
	A	B	C	D		
1	0	0	0	0	HF1	HF2
2	0	1	1	1	HF1	HF1
3	0	2	2	2	HF1	HF1
4	1	0	1	2	HF2	HF1
5	1	1	2	0	HF1	HF1
6	1	2	0	1	HF2	HF2
7	2	0	2	1	HF1	HF1
8	2	1	0	2	HF1	HF1
9	2	2	1	0	HF2	HF1

Table 5.7: Adhesion checking before R_a measuring test of CrN coating.

By using S/N ratio Equations (4-1) and (4-2), the S/N response ratios with smaller-the-best characteristic for CrN coating surface roughness are listed in Table 5.8.

Two R_a measurements would be taken on each run to increase the accuracy of the experiments.

Trial no.	Coating Parameters or factors				R_a value (μm)		S/N ratio
					1st sample	2nd sample	
	A	B	C	D			
1	0	0	0	0	0.33	0.31	9.89
2	0	1	1	1	0.29	0.26	11.20
3	0	2	2	2	0.24	0.22	12.83
4	1	0	1	2	0.33	0.31	9.89
5	1	1	2	0	0.22	0.21	13.27
6	1	2	0	1	0.27	0.26	11.53
7	2	0	2	1	0.26	0.28	11.37
8	2	1	0	2	0.36	0.37	8.75
9	2	2	1	0	0.31	0.29	10.45

(Table header spanning label: L_9)

Table 5.8: L_9 orthogonal array, R_a value, and S/N ratio for the CrN coating experiment.

5.2.1 Normal Probability Plot of S/N Response Ratio in CrN Coating

Figure 5.3 shows that the S/N response in CrN coating does follow the normal distribution with the 95% confidence level. Nearly all points fall on the line of normal distribution.
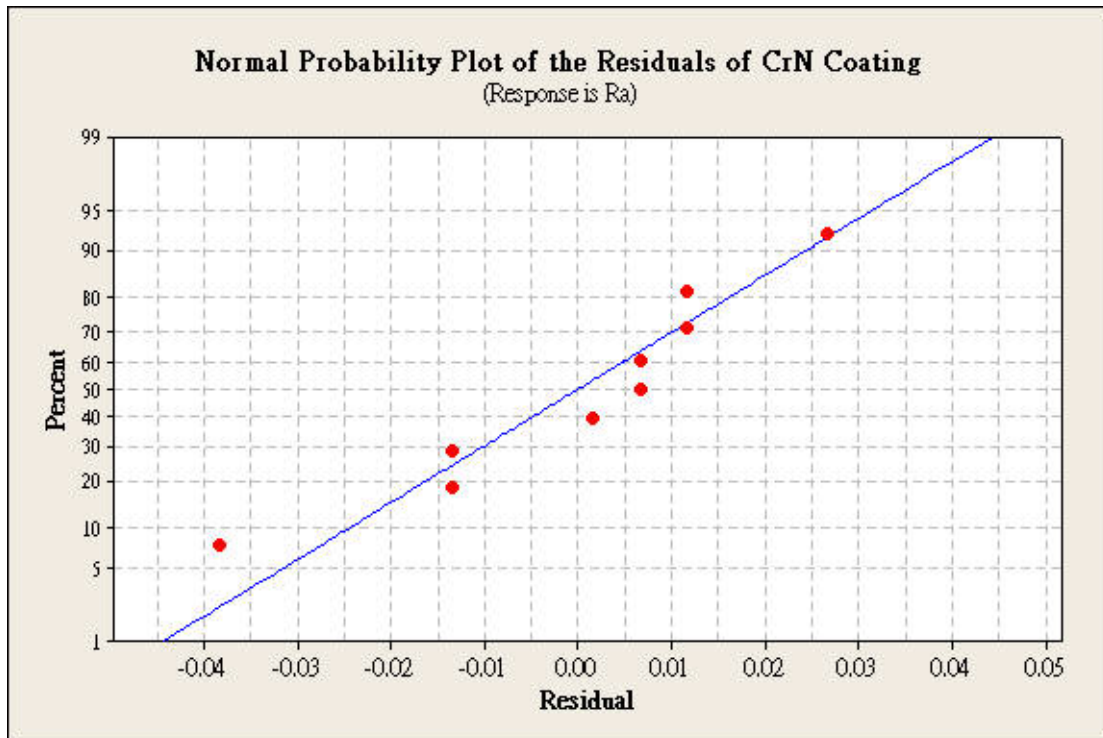
Figure 5.3: Normal probability plot of the S/N ratios in CrN coating.

5.2.2 S/N Response Ratio of CrN Coating

Table 5.9 indicates the mean S/N response ratio of CrN coating under different coating parameters. By calculating the mean S/N response, the ranking of the four factors can be found.

Levels	Mean S/N response ratios			
	A	B	C	D
0	11.31	10.38	10.06	11.20
1	*11.56*	11.07	10.52	*11.37*
2	10.19	*11.61*	*12.49*	10.49
Maximum-Minimum	1.37	1.22	2.43	0.88
Rank	2	3	*1*	4

Table 5.9: Mean S/N response ratios of CrN coating.
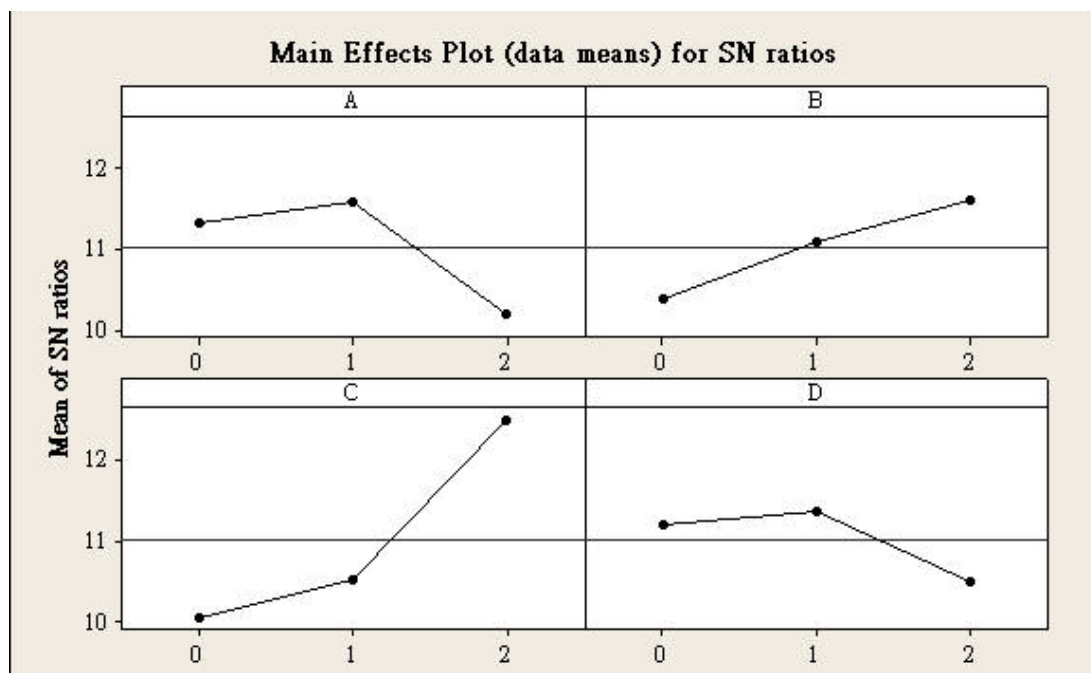
Figure 5.4: S/N ratios response graph for CrN coating.

Figure 5.4 shows the S/N ratios response graph for CrN coating. The response is less than that of TiN coating. It can be seen that the main effect is factor C, the nitrogen pressure. Then it is factor A, the bias voltage. The next one is factor B, the arc current, and the final one is factor D, the coating time. It shows that the best condition or parameter is in A1B2C2D1. When bias voltage = –80V, arc current = 150A, nitrogen pressure = 10 x 10E-03mbar, and coating time = 57mins., the optimal condition can be obtained. In CrN coating, difference in nitrogen pressure response does influence the coating roughness in CrN coating.

5.2.3 ANOVA for CrN Coating S/N Ratios in Roughness Test

Source	Degrees of freedom	Sum of Square	Mean Variance	% Contribution
Bias Voltage	2	3.20	1.60	19.1
Arc Current	2	2.24	1.12	13.4
Nitrogen Pressure	2	10.00	5.00	59.7
Coating Time	2	1.30	0.65	7.8
Residual Error	0	*	*	0
Total	8	16.74	*	100

Table 5.10: ANOVA table for S/N ratio of CrN coating in R_a test.

Table 5.10 shows that nitrogen pressure has the highest percentage contribution in CrN coating test. The most important factors in CrN coating for R_a value needed to be controlled is nitrogen pressure, then bias voltage, arc current, and finally is the coating time.

5.3 Response Surface Method for TiN Coating

After using the Taguchi Method's screening experiment, it is found that factors A and C have significant influence on the variability of roughness of TiN coating. A second batch of experiments is then used to find the best settings of the four corners of the optimal window. The response surface method can be categorized into four steps:

    a   Finding first-order model

    b   Finding steepest ascent/ descent step size

    c   Finding new first-order model

    d   Finding second-order model

The first-order model started with 4 runs and 2 replications. In each run, 2 samples are taken. Coded variable will be used to represent the natural variable, the bias voltage (factor A), and the nitrogen pressure (factor C). Table 5.11 shows the results of adhesion test of the substrate. All testpieces are accepted in adhesion. Table 5.12 and Table 5.13 show the relationship between natural variables and coded variable and the results of TiN coating R_a measurements.

From Taguchi method results and figures, the optimum region in TiN coating is from -110 to -80V and nitrogen pressure is around 8 x 10E-03mbar to 10 x 10E-03mbar.

Therefore, the centre points used for finding the first-order-degree regression model are:

$$x_1 = \frac{2\,(\text{Bias voltage}) - [-110 + (-80)]}{-110 - (80)} = \frac{\text{Bias voltage} + 95}{-15}$$

and

$$x_2 = \frac{2 \, (N_2 \text{ pressure}) - (8 \times 10\,E\text{-}03 + 10 \times 10\,E\text{-}03)}{(10 - 8) \times 10E\text{-}3} = \frac{N_2 \text{ pressure} - (9 \times 10\,E\text{-}03)}{1 \times 10\,E\text{-}3}.$$

Factors		Coded variable		Adhesion Classification	
A. Bias voltage (V)	C. N_2 pressure (mbar)	x_1	x_2	1st sample	2nd sample
-80	8 x 10 E-03	-1	-1	HF1	HF1
-110	8 x 10 E-03	1	-1	HF1	HF1
-80	10 x 10 E-03	-1	1	HF2	HF1
-110	10 x 10 E-03	1	1	HF1	HF1

Table 5.11: Adhesion test for TiN coating test.

Factors		Coded variable		R_a Value (μm)		
A. Bias voltage (V)	C. N_2 pressure (mbar)	x_1	x_2	1st sample	2nd sample	Mean
-80	8 x 10 E-03	-1	-1	0.30	0.29	0.30
-110	8 x 10 E-03	1	-1	0.24	0.26	0.26
-80	10 x 10 E-03	-1	1	0.29	0.28	0.29
-110	10 x 10 E-03	1	1	0.23	0.24	0.24

Table 5.12: Relationship between natural variables and coded variables, and the result of TiN

coating R_a measurements for the first replicate.

Factors		Coded variable		R_a Value (μ m)		
A. Bias voltage (V)	C. N$_2$ pressure (mbar)	x_1	x_2	1st sample	2nd sample	Mean
-80	8 x 10 E-03	-1	-1	0.29	0.28	0.29
-110	8 x 10 E-03	1	-1	0.27	0.28	0.28
-80	10 x 10 E-03	-1	1	0.28	0.29	0.29
-110	10 x 10 E-03	1	1	0.22	0.23	0.23

Table 5.13: Relationship between natural variables, and coded variables, and the result of TiN coating R_a measurements for the second replicate.

Source	Degrees of freedom	Sum of Square	Mean Variance	F	R^2	R^2_{adj}
Regression	2	0.0040	0.0020	13.33	0.842	0.779
Residual Error	5	0.0075	0.0002	*	*	*
Lack of Fit	1	0.0045	0.0045	6.00	*	*
Pure Error	4	0.0003	0.0001	*	*	*
Total	7	0.0047	*	*	*	*

Table 5.14: ANOVA of the first-order model of TiN coating.

From ANOVA Table 5.14, the variation is great in the regression model since $R^2 = 0.842$. The model does not fit. Using coded variables, a first-degree-regression model can be represented as follows:

$$\hat{y} = 0.273 - 0.020x_1 + 0.010 \, x_2 \tag{5-1}$$

where $\hat{y}$ is the mean R_a value.

Since the regression $F = 13.33 > F_{(0.05,2,5)} = 5.79$, the factor is significant. The F value of lack of fit is 6.00 which does not exceed the $F_{(0.05,1,4)} = 7.71$. The model does not indicate lack of fit. $R^2 = 0.842$ and $R^2_{adj} = 0.779$ indicates that most of the variations can be explained by the regression model.

5.3.1 Steepest Ascent/Descent Experiments of TiN coating

After finding out the first-order model, slope of Equation (5-1) can be found for the steepest ascent/descent experiments.

For every 0.02 movement in the x_1 direction, it will cause 0.01 movements in the x_2 direction. Thus, the path of steepest ascent passes through the point ($x_1 = 0$, $x_2 = 0$). The slope of the first order regression is equal to:

$$\frac{\text{Coefficient of } x_2}{\text{Coefficient of } x_1} = \frac{0.01}{0.02} = 0.5 .$$

For the original region of experiment, the bias voltage is between –80V to –110V and the nitrogen pressure is between 8 x 10 E-03mbar to 10x 10 E-03mbar. After consulting with engineers in the company, it was decided to select 0.5 x 10E-03mbar as the steepest ascent/descent step in the coded variable x_2 of $\Delta x_2 = 1$. Therefore, the steps along the path of steepest ascent/descent are $\Delta x_2 = 1$ and $\Delta x_1 = \Delta x_2 / 0.5 = 2$.

For bias voltage, only integer can be changed in the coating machine. And for nitrogen pressure control, only two decimal places can be accepted.

From Equation (5-1), the slope is:

$$x_1 = (0.02/0.01) = 2x_2$$

The experiment started from (-1, -0.5). The second point was (0,0), then ascent to (1,0.5) and finally was point (2,1). Table 5.15 and Table 5.16 show the adhesion test and the result of TiN coating R_a test for steepest ascent/descent test respectively. From Figure 5.5, it implies that the path is steepest descent.

Natural variable		Coded variable		R_a Value (μ m)	
A. Bias voltage (V)	C. N_2 pressure (mbar)	x_1	x_2	1st sample	2nd sample
-80	8.5 x 10 E-03	-1	-0.5	HF1	HF2
-95	9 x 10 E-03	0	0	HF1	HF1
-110	9.5 x 10 E-03	1	0.5	HF1	HF1
-125	10 x 10 E-03	2	1	HF2	HF1

Table 5.15: Adhesion test for steepest ascent/descent test of TiN coating.

Natural variable		Coded variable		R_a Value (μ m)		
A. Bias voltage (V)	C. N_2 pressure (mbar)	x_1	x_2	1st sample	2nd sample	Mean
-80	8.5 x 10 E-03	-1	-0.5	0.27	0.26	0.27
-95	9 x 10 E-03	0	0	0.25	0.25	0.25
-110	*9.5 x 10 E-03*	*1*	*0.5*	0.22	*0.22*	*0.22*
-125	10 x 10 E-03	2	1	0.30	0.29	0.30

Table 5.16: Experiment results of the steepest ascent/descent of TiN coating.
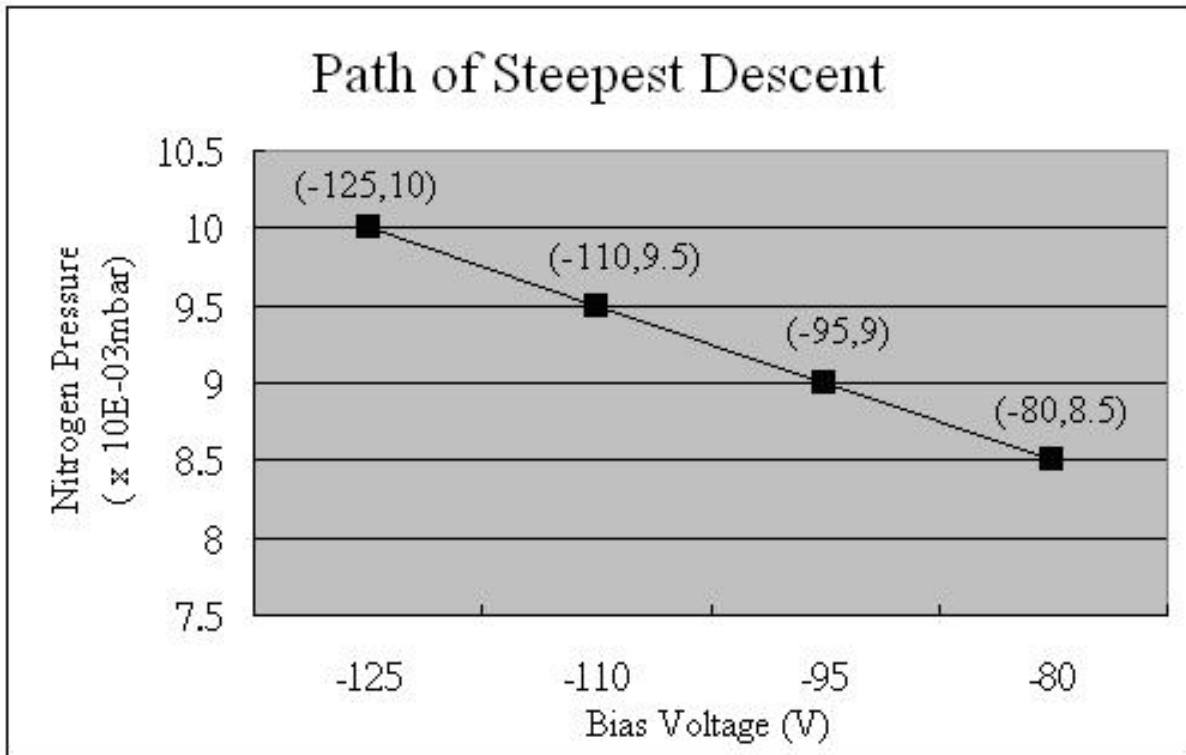
Figure 5.5: Diagram for steepest test of TiN coating.

5.3.2 New First-order Model for TiN Coating Test

Based on the steepest descent experiment results in Table 5.16 and Figure 5.5, another set of experiment with centre point (1, 0.5) was constructed to fit the first-order model. Five replications of centre points were used to smooth out the experimental error and check the adequacy of the first model. Totally nine runs were conducted in this new set of experiment. Table 5.17 and Table 5.18 show the adhesion measurement results and R_a result respectively.

$$x_1 = \frac{\text{Bias voltage} + 90}{-15}$$

$$x_2 = \frac{\text{N}_2 \text{ pressure} - (9 \times 10\,\text{E} - 03)}{0.5 \times 10\text{E} - 03}$$

Factors		Coded variable		R_a Value (μ m)	
A. Bias voltage (V)	C. N_2 pressure (mbar)	x_1	x_2	1st sample	2nd sample
-95	9 x 10 E-03	-1	-1	HF1	HF1
-125	9 x 10 E-03	1	-1	HF1	HF2
-95	10 x 10 E-03	-1	1	HF1	HF1
-125	10 x 10 E-03	1	1	HF1	HF1
-110	9.5 x 10 E-03	0	0	HF2	HF1
-110	9.5 x 10 E-03	0	0	HF1	HF1
-110	9.5 x 10 E-03	0	0	HF2	HF2
-110	9.5 x 10 E-03	0	0	HF1	HF1
-110	9.5 x 10 E-03	0	0	HF1	HF2

Table 5.17: Adhesion test for new first-order model of TiN coating.

Factors		Coded variable		R_a Value (μ m)		
A. Bias voltage (V)	C. N_2 pressure (mbar)	x_1	x_2	1st sample	2nd sample	Mean
-95	9 x 10 E-03	-1	-1	0.29	0.28	0.29
-125	9 x 10 E-03	1	-1	0.28	0.27	0.26
-95	10 x 10 E-03	-1	1	0.29	0.28	0.29
-125	10 x 10 E-03	1	1	0.24	0.25	0.21
-110	9.5 x 10 E-03	0	0	0.22	0.22	0.22
-110	9.5 x 10 E-03	0	0	0.23	0.21	0.22
-110	9.5 x 10 E-03	0	0	0.22	0.24	0.23
-110	9.5 x 10 E-03	0	0	0.23	0.24	0.26
-110	9.5 x 10 E-03	0	0	0.24	0.25	0.25

Table 5.18: Factors and results for new first-order model of TiN coating.

The new first-order model regression equation in coded variable was:

$$\hat{y} = 0.247 - 0.0275x_1 - 0.0125x_2 \qquad (5\text{-}2)$$

where $\hat{y}$ is the mean R_a value.

The new first-order model ANOVA is shown in Table 5.19. For the new first-order model, the F value of regression = 8.11 is slightly more than $F_{(0.05,2,6)} = 5.14$. The regression of null hypothesis should therefore be rejected. The F value of lack of fit = 0.5 is less than $F_{(0.05,2,4)} = 6.94$. This indicated that the new first-order model is not lack of fit. $R^2 = 0.73$ and $R^2_{adj} = 0.64$ indicate that most of the variations can be explained by the new first-order regression model.

Source	Degrees of freedom	Sum of Square	Mean Variance	F	R^2	R^2_{adj}
Regression	2	0.00365	0.0018	8.11	0.730	0.640
Residual Error	6	0.00135	0.0002			
Lack of Fit	2	0.00027	0.00014	0.50		
Pure Error	4	0.00108	0.00027			
Total	8	0.00500				

Table 5.19: ANOVA of the new first-order model of TiN coating.

5.3.3 Second-order Model for TiN Coating

After found out the optimal region by using the new first-order model, a further optimization can be located by using the second-order model, and quadratic equation. Centre composite design (CCD) is adopted to regress this second-order model. For two factors, four additional points is added on the two axes. The four axial points are shown graphically in Figure 5.6. They are (1.414,0), (0,1.414), (-1.414,0) and (0,-1.414). The result of the centre composite design is in Table 5.20.
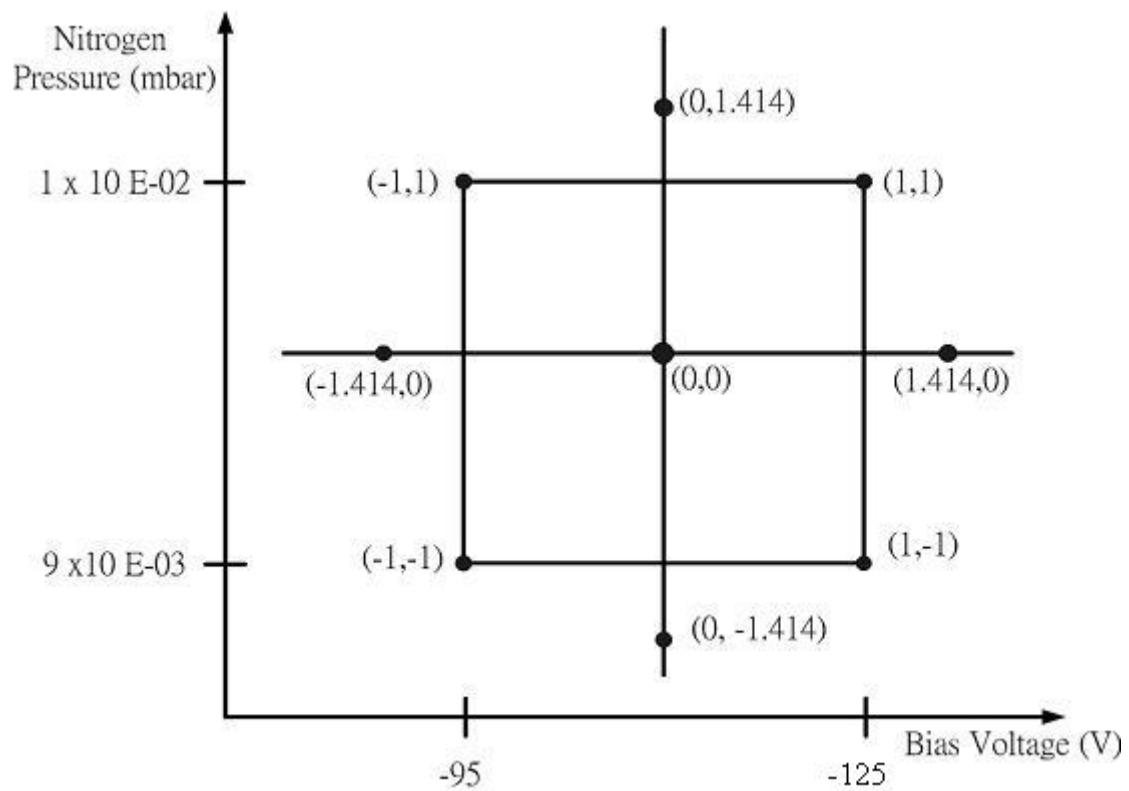
Figure 5.6: Centre Composite Design for second-order model of TiN coating.

Factors		Coded variable		R_a Value (μm)		
A. Bias voltage (V)	C. N$_2$ pressure (mbar)	x_1	x_2	1st sample	2nd sample	Mean
-95	9 x 10 E-03	-1	-1	0.29	0.28	0.29
-125	9 x 10 E-03	1	-1	0.28	0.27	0.26
-95	10 x 10 E-03	-1	1	0.29	0.28	0.29
-125	10 x 10 E-03	1	1	0.24	0.25	0.21
-110	9.5 x 10 E-03	0	0	0.22	0.22	0.22
-110	9.5 x 10 E-03	0	0	0.23	0.21	0.22
-110	9.5 x 10 E-03	0	0	0.22	0.24	0.23
-110	9.5 x 10 E-03	0	0	0.23	0.24	0.26
-110	9.5 x 10 E-03	0	0	0.24	0.25	0.25
-103	9.5 x 10 E-03	$-\sqrt{2}$	0	0.33	0.34	0.34
-116	9.5 x 10 E-03	$\sqrt{2}$	0	0.31	0.29	0.30
-103	9.5 x 10 E-03	0	$-\sqrt{2}$	0.29	0.29	0.29
-116	9.5 x 10 E-03	0	$\sqrt{2}$	0.33	0.32	0.33

Table 5.20: Results of the Centre Composite Design of TiN coating.

Figure 5.7 shows the normal plot of R_a residuals. It implies that the R_a value of the second-order model does follow the normal distribution within 95% of confidence level.
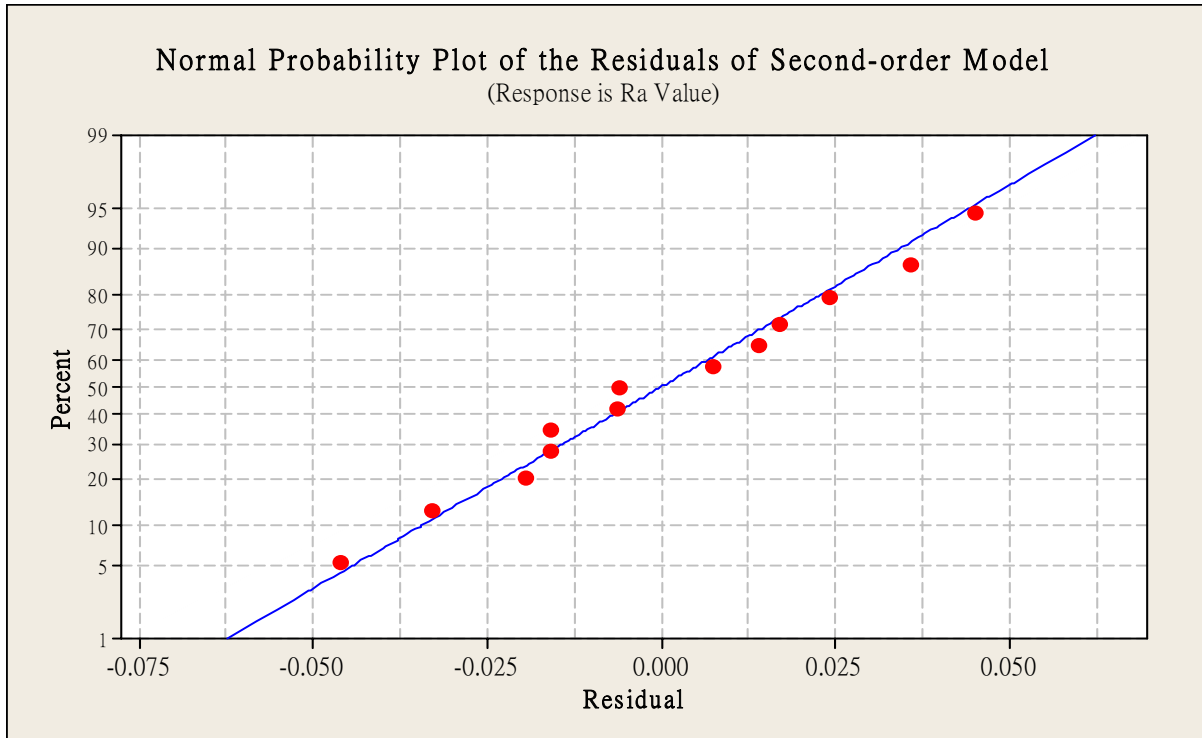
Figure 5.7: Second-order model normal probability plot of residuals of TiN coating.

The second-order model regression equation based on using CCD was:

$$\hat{y} = 0.236 - 0.021x_1 + 0.001\ x_2 + 0.029\ x_1^2 + 0.024\ x_2^2 - 0.013\ x_1x_2 \tag{5-3}$$

where $\hat{y}$ is the mean R_a value.

From Table 5.21, the CCD ANOVA table, F = 2.08 is less than $F_{(0.10,5,7)}$ = 2.88. This implies that regression is not significant at the 0.10 level of significance. R^2 = 0.6 and R^2_{adj} = 0.031 shows that a very small proportion of variation is explained by this regression model. Therefore, this model fits.

Source	Degrees of freedom	Sum of Square	Mean Variance	F	R^2	R^2_{adj}
Regression	5	0.013	0.003	2.08	0.60	0.031
Linear	2	0.003	0.002	1.41		
Square	2	0.009	0.004	3.52		
Interaction	1	0.001	0.001	0.51		
Residual Error	7	0.009	0.001			
Lack of Fit	3	0.007	0.002	7.36		
Pure Error	4	0.001	0.000			
Total	12	0.021				

Table 5.21: ANOVA of second-order model for TiN coating.

After fitting the second-order model to determine the optimum region, stationary points should be found out and identified by using partial differentiation of the regressed second-order model.

From Equation (3-6),

$$\hat{y} = \hat{\beta}_0 + \mathbf{x}^T\mathbf{b} + \mathbf{x}^T\mathbf{B}\mathbf{x}$$

where $\mathbf{x} = \begin{bmatrix} x_1 \\ x_2 \\ \vdots \\ x_k \end{bmatrix}$, $\mathbf{b} = \begin{bmatrix} \hat{\beta}_1 \\ \hat{\beta}_2 \\ \vdots \\ \hat{\beta}_k \end{bmatrix}$ and $\mathbf{B} = \begin{bmatrix} \hat{\beta}_{11} & \hat{\beta}_{12}/2 & \cdots & \hat{\beta}_{1k}/2 \\ & \hat{\beta}_{22} & \cdots & \hat{\beta}_{2k}/2 \\ & & \ddots & \\ symmetrical & & & \hat{\beta}_{kk} \end{bmatrix}$.

The second-order fitting regression model could be written as:

$$\hat{y} = 0.236 - [x_1 x_2]\begin{bmatrix} -0.021 \\ 0.001 \end{bmatrix} + \begin{bmatrix} 0.029 & -0.007 \\ -0.007 & 0.024 \end{bmatrix}\begin{bmatrix} x_1 \\ x_2 \end{bmatrix} \qquad (5\text{-}4)$$

To examine the surface further, the stationary point $\mathbf{x_s}$ and the yield y_0 should be found.

From Equation (3-8),

$$\mathbf{x}_s = -\tfrac{1}{2}\,\mathbf{B}^{-1}\mathbf{b}.$$

where $\mathbf{B} = \begin{bmatrix} 0.029 & -0.007 \\ -0.007 & 0.024 \end{bmatrix}$

Now,

$$\mathbf{B^{-1}} = \frac{1}{|0.00067|} \begin{bmatrix} 0.024 & 0.007 \\ 0.007 & 0.029 \end{bmatrix} = \begin{bmatrix} 37.1 & 10.82 \\ 10.82 & 44.82 \end{bmatrix}$$

Therefore,

$$\mathbf{x_s} = -\frac{1}{2} \begin{bmatrix} 37.1 & 10.82 \\ 10.82 & 44.82 \end{bmatrix} \begin{bmatrix} -0.021 \\ 0.001 \end{bmatrix} = \begin{bmatrix} 0.384 \\ 0.091 \end{bmatrix}$$

Or, the stationary point is at (0.384, 0.091). In terms of the natural variable, the stationary point is at:

$$0.384 = \frac{\xi_1 + 110}{-15}, 0.091 = \frac{\xi_2 - (9.5 \times 10 \text{ E - 03})}{0.5 \times 10 \text{E - 03}}$$

As a result, $\xi_1 = -115$ V of bias voltage and $\xi_2 = 9.54 \times 10$ E-03 mbar of N_2 pressure.

From Equation (3-9),

$$\hat{y}_s = 0.236 + \frac{1}{2}\begin{bmatrix} 0.384 & 0.091 \end{bmatrix}\begin{bmatrix} -0.021 \\ 0.001 \end{bmatrix} = 0.236 - 0.004 = 0.23$$

Finally, canonical analysis is carried out to determine whether the stationary point being found is a local maximum, minimum, or saddle pint. An equation could be set up as follows:

$$| \mathbf{B} - \lambda \mathbf{I} | = 0$$

$$\begin{vmatrix} 0.029 - \lambda & -0.007 \\ -0.007 & 0.024 - \lambda \end{vmatrix} = 0$$

which can be reduced to $\lambda^2 - 0.053\lambda + 0.000647 = 0$

The roots of this quadratic equation were $\lambda_1 = 0.019$ and $\lambda_2 = 0.034$. Since the two roots are all positive, the stationary point (0.384, 0.091) is a minimum. Figure 5.8 and Figure 5.9 show respectively the 3D surface plot and the contour plot of the response yield mean R_a value of TiN coating.
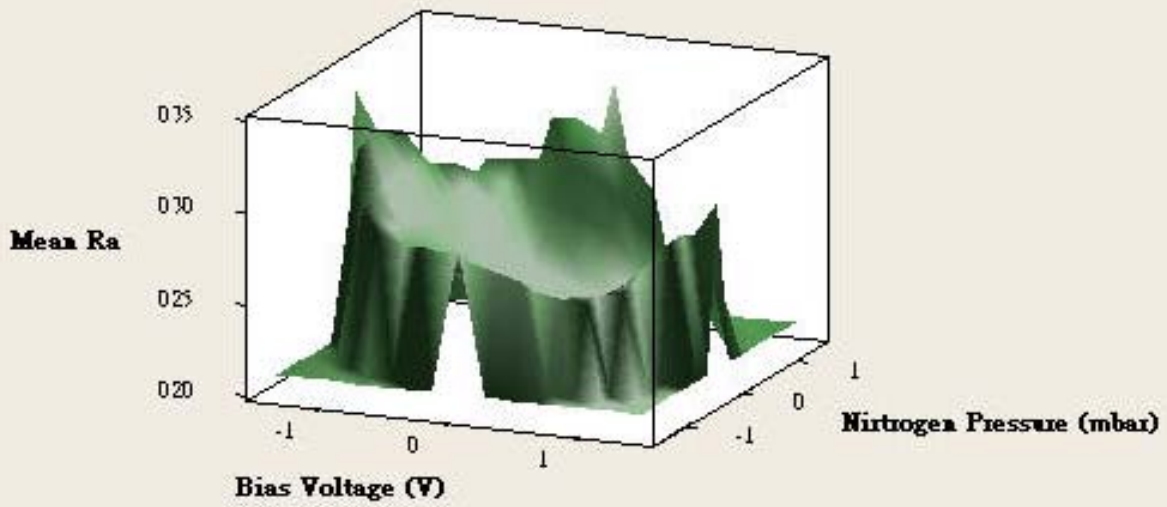
Figure 5.8: 3D surface plot for TiNcoating R_a value.
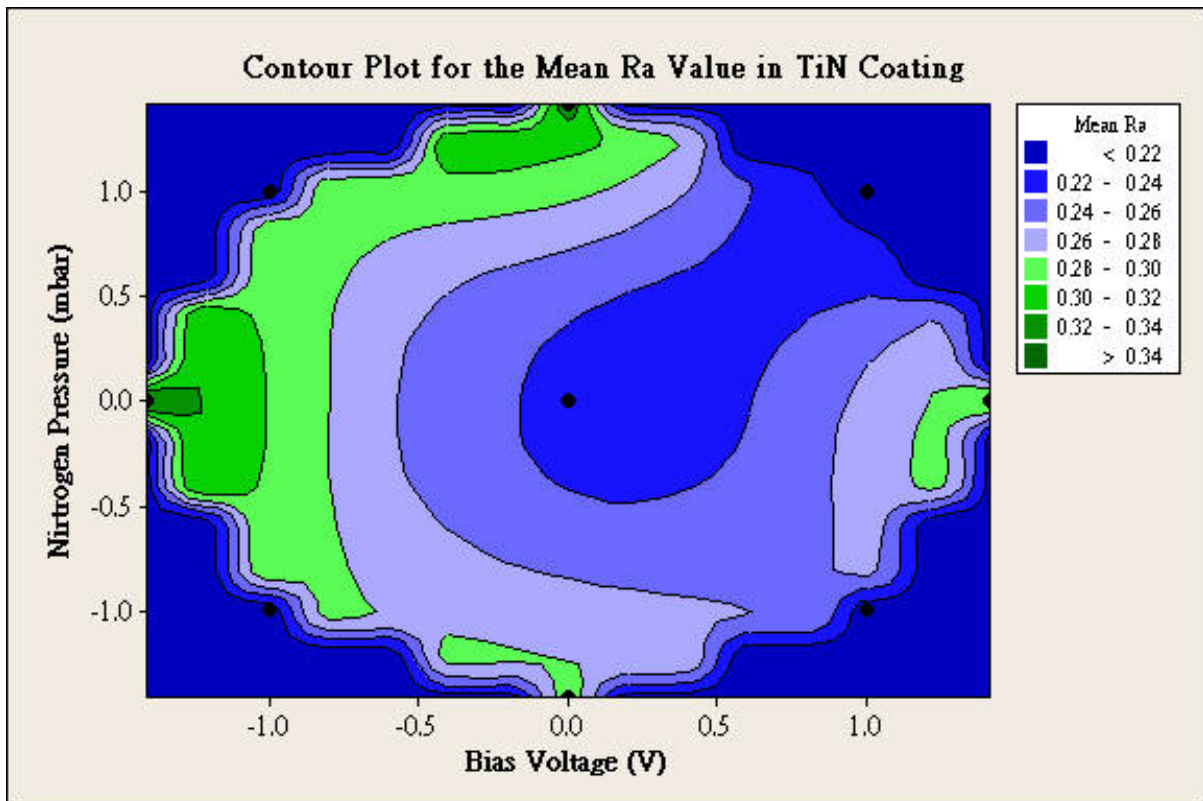
Figure 5.9: Contour plot for TiN coating R_a value.

5.4 Response Surface Method for CrN Coating

After using Taguchi Method's screening experiments, it is found that factor A, the bias voltage, and factor C, the nitrogen pressure have significant influence on the variability of roughness of CrN coating. As second batch of experiments, including finding first-order model and steepest ascent/descent step size, new first-order model and second-order model are used to find the best settings of the four corners of the optimal window for CrN coating.

Again, the first-order model is using 2^2 full factorial design and started with 4 runs, 2 samples in each run and 2 replications. Coded variable x_1 and x_2 will be used to represent the natural variable, the bias voltage (factor A) and the nitrogen pressure (factor C) respectively. Table 5.22 shows the results of adhesion test of the substrate. All testpieces are accepted in adhesion. Table 5.23 and Table 5.24 show the relationship between natural variables and coded variable, and the result of CrN coating R_a measurements.

From the Taguchi method results and figures, the optimum regions is from bias voltage - 110V to -60V and nitrogen pressure is from 9 x 10E-03mbar to 10x 10E-03mbar.

Therefore, the centre points used for finding the first-order-degree regression model is:

$$x_1 = \frac{2\,(\text{Bias voltage}) - [-110 + (-60)]}{-110 - (60)} = \frac{\text{Bias voltage} + 85}{-25}$$

and

$$x_2 = \frac{2\,(\text{N}_2\ \text{pressure}) - (9 \times 10\,\text{E} - 03 + 10 \times 10\,\text{E} - 03)}{(10 - 9) \times 10\text{E} - 03} = \frac{\text{N}_2\ \text{pressure} - (9.5 \times 10\,\text{E} - 03)}{0.5 \times 10\,\text{E} - 03}.$$

Factors		Coded variable		Adhesion Classification	
A. Bias voltage (V)	C. N_2 pressure (mbar)	x_1	x_2	1st sample	2nd sample
-60	9 x 10 E-03	-1	-1	HF1	HF1
-110	9 x 10 E-03	1	-1	HF1	HF1
-60	10 x 10 E-03	-1	1	HF1	HF1
-110	10 x 10 E-03	1	1	HF1	HF1

Table 5.22: Adhesion test for CrN coating test.

Factors		Coded variable		R_a Value (μm)		
A. Bias voltage (V)	C. N_2 pressure (mbar)	x_1	x_2	1st sample	2nd sample	Mean
-60	9 x 10 E-03	-1	-1	0.33	0.34	0.32
-110	9 x 10 E-03	1	-1	0.29	0.27	0.28
-60	10 x 10 E-03	-1	1	0.29	0.28	0.29
-110	10 x 10 E-03	1	1	0.25	0.26	0.26

Table 5.23: Relationship between natural variables, coded variables, and the result of CrN coating R_a measurements for the first replicate.

Factors		Coded variable		R_a Value (μm)		
A. Bias voltage (V)	C. N_2 pressure (mbar)	x_1	x_2	1st sample	2nd sample	Mean
-60	9 x 10 E-03	-1	-1	0.32	0.34	0.33
-110	9 x 10 E-03	1	-1	0.30	0.29	0.30
-60	10 x 10 E-03	-1	1	0.29	0.28	0.29
-110	10 x 10 E-03	1	1	0.25	0.26	0.26

Table 5.24: Relationship between natural variable, coded variables, and the result of CrN coating R_a measurements for the second replicate.

Source	Degrees of freedom	Sum of Square	Mean Variance	F	R^2	R^2_{adj}
Regression	2	0.0042	0.0021	40.24	0.942	0.918
Residual Error	5	0.0002	0.0001	*	*	*
Lack of Fit	1	0.0000	0.0000	0.2	*	*
Pure Error	4	0.0002	0.0001	*	*	*
Total	7	0.0046	*	*	*	*

Table 5.25: ANOVA of the first-order model of CrN coating.

From Table 5.25, the variation is great in the first-order model since $R^2 = 0.942$. The model does not fit at this stage. Further experiments will be carried out to fit the model. Using coded variables, the first degree of regression model of CrN coating can be represented as:

$$\hat{y} = 0.291 - 0.016x_1 + 0.016\,x_2 \tag{5-5}$$

where $\hat{y}$ is the mean R_a value.

Since the regression $F = 40.24 > F_{(0.05,2,5)} = 5.79$, the factor is significant. The F value of lack of fit is 0.20 which does not exceeds $F_{(0.05,1,4)} = 7.71$. The model does not indicate lack of fit. $R^2 = 0.942$ and $R^2_{adj} = 0.918$ indicates that most of the variations can be explained by the regression model.

5.4.1 Steepest Ascent/Descent Experiments of CrN coating

The slope of Equation (5-5) can be found for steepest ascent/descent experiments.

$$x_1 = (0.016/0.016)x_2$$

$$x_1 = x_2$$

It was decided to select x_2 as the steepest ascent/descent step. For bias voltage, only integer can be changed in the coating machine. And for nitrogen pressure control, only two decimal places can be accepted.

The experiment started with (-1, -1). The second point was (0, 0), then ascent to (1, 1) and finally was point (2, 2). Table 5.26 and Table 5.27 show the adhesion test and the result of CrN coating R_a test for steepest descent test respectively. From Figure 5.10, it implies that the path is steepest descent.

Natural variable		Coded variable		R_a Value (μ m)	
A. Bias voltage (V)	C. N_2 pressure (mbar)	x_1	x_2	1st sample	2nd sample
-60	8.5 x 10 E-03	-1	-1	HF1	HF2
-85	9.0 x 10 E-03	0	0	HF2	HF1
-110	9.5 x 10 E-03	1	1	HF2	HF2
-152	10 x 10 E-03	2	2	HF1	HF1

Table 5.26: Adhesion test for steepest ascent/descent test of CrN coating.

Natural variable		Coded variable		R_a Value (μ m)		
A. Bias voltage (V)	C. N$_2$ pressure (mbar)	x_1	x_2	1st sample	2nd sample	Mean
-60	8.5 x 10 E-03	-1	-1	0.33	0.32	0.33
-85	9.0 x 10 E-03	0	0	0.27	0.28	0.28
-110	9.5 x 10 E-03	1	1	0.25	0.25	0.25
-152	10 x 10 E-03	2	2	0.31	0.29	0.30

Table 5.27: Experiment results of the steepest ascent.
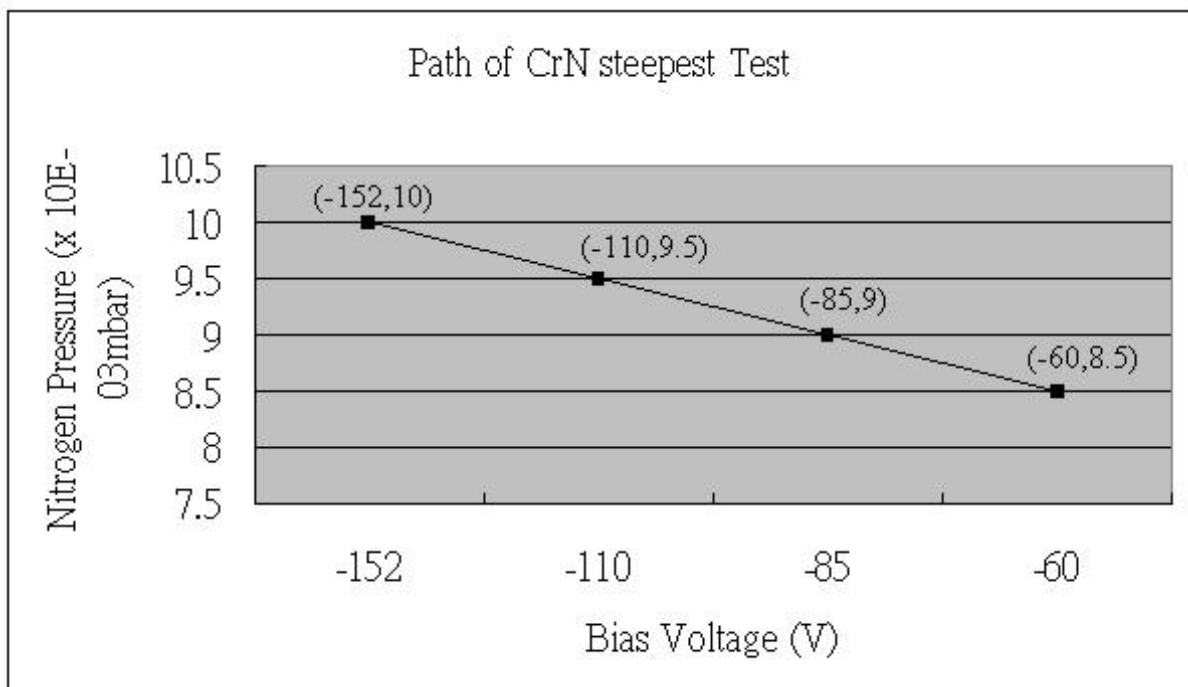
Figure 5.10: Diagram for steepest test.

5.4.2 New First-order Model for CrN Coating Test

Based on the steepest ascent experiment results in Table 5.27 and Figure 5.10, another set of experiment with centre point (1, 1) was constructed to fit the first-order model. Five replications of centre points are used to approximate the experiment error and check the adequacy of the first model. Therefore, 9 runs were used to conduct the new set of experiment. Table 5.28 and Table 5.29 show the adhesion measurement results and R_a result respectively.

$$x_1 = \frac{\text{Bias voltage} + 118.5}{33.5}, x_2 = \frac{N_2 \text{ pressure} - (9.5 \times 10 \, E - 03)}{0.5 \times 10E - 03}$$

Factors		Coded variable		R_a Value (μ m)	
A. Bias voltage (V)	C. N_2 pressure (mbar)	x_1	x_2	1st sample	2nd sample
-85	9.0 x 10 E-03	-1	-1	HF1	HF1
-152	9.0 x 10 E-03	1	-1	HF1	HF1
-85	10 x 10 E-03	-1	1	HF1	HF1
-152	10 x 10 E-03	1	1	HF1	HF2
-110	9.5 x 10 E-03	0	0	HF2	HF1
-110	9.5 x 10 E-03	0	0	HF2	HF1
-110	9.5 x 10 E-03	0	0	HF1	HF2
-110	9.5 x 10 E-03	0	0	HF2	HF1
-110	9.5 x 10 E-03	0	0	HF1	HF1

Table 5.28: Adhesion test for new first-order model in CrN coating.

Factors		Coded variable		R_a Value (μ m)		
A. Bias voltage (V)	C. N_2 pressure (mbar)	x_1	x_2	1st sample	2nd sample	Mean
-85	9.0 x 10 E-03	-1	-1	0.30	0.29	0.30
-152	9.0 x 10 E-03	1	-1	0.26	0.27	0.27
-85	10 x 10 E-03	-1	1	0.29	0.28	0.29
-152	10 x 10 E-03	1	1	0.25	0.26	0.26
-110	9.5 x 10 E-03	0	0	0.26	0.25	0.26
-110	9.5 x 10 E-03	0	0	0.26	0.25	0.26
-110	9.5 x 10 E-03	0	0	0.24	0.25	0.25
-110	9.5 x 10 E-03	0	0	0.24	0.24	0.24
-110	9.5 x 10 E-03	0	0	0.25	0.26	0.26

Table 5.29: Factors and results for new first-order model for CrN coating.

The new first-order model regression equation in coded variable was:

$$\hat{y} = 0.266 - 0.015x_1 - 0.005x_2 \qquad (5\text{-}6)$$

where $\hat{y}$ is the mean R_a value.

The new first-order model ANOVA table is shown in Table 5.30. For this new first-order model, the F value of regression = 1.65 is less than $F_{(0.05,2,6)}$ = 5.14. The hypothesis should therefore be accepted. The F value of lack of fit = 9.39 is more than $F_{(0.05,2,4)}$ =6.94. This indicated that new first-order model is lack of fit. On the other hand, R^2 = 0.354 and R^2_{adj} = 0.139 indicated that only a very small proportion of the variation is explained by the regression model.

Source	Degrees of freedom	Sum of Square	Mean Variance	F	R^2	R^2_{adj}
Regression	2	0.0010	0.0005	1.65	0.354	0.139
Residual Error	6	0.0018	0.0003	*	*	*
Lack of Fit	2	0.0002	0.0010	9.39	*	*
Pure Error	4	0.0003	0.0001	*	*	*
Total	8	0.0028	*	*	*	*

Table 5.30: ANOVA table for new first-order model for CrN coating.

5.4.3 Second-order Model for CrN Coating

After found out the optimal region by using the new first-order model, a further optimization can be located by using the second-order model. Centre composite design (CCD) with two factors was adopted to regress this second-order model. The four axial points (1.414,0), (0,1.414), (-1.414,0) and (0,-1.414) and the CCD diagram are shown graphically in Figure 5.11. The result of the centre composite design is in Table 5.31.
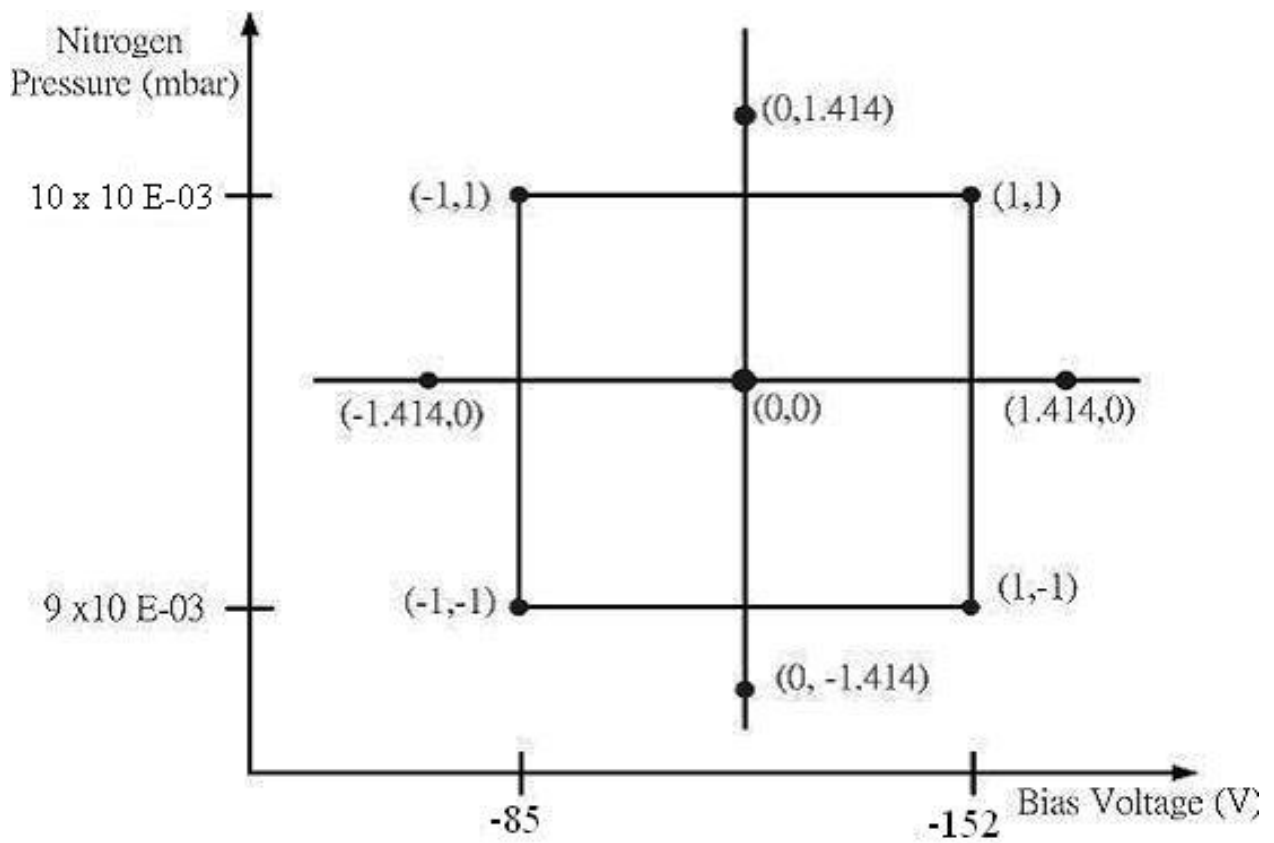
Figure 5.11: CCD of CrN coating for second-order model.

Factors		Coded variable		R_a Value (μm)		
A. Bias voltage (V)	C. N_2 pressure (mbar)	x_1	x_2	1st sample	2nd sample	Mean
-85	9 x 10 E-03	-1	-1	0.30	0.29	0.30
-152	9 x 10 E-03	1	-1	0.26	0.27	0.27
-85	10 x 10 E-03	-1	1	0.29	0.28	0.29
-152	10 x 10 E-03	1	1	0.25	0.26	0.26
-110	9.5 x 10 E-03	0	0	0.26	0.25	0.26
-110	9.5 x 10 E-03	0	0	0.26	0.25	0.26
-110	9.5 x 10 E-03	0	0	0.24	0.25	0.25
-110	9.5 x 10 E-03	0	0	0.24	0.24	0.24
-110	9.5 x 10 E-03	0	0	0.25	0.26	0.26
-93	9.5 x 10 E-03	$-\sqrt{2}$	0	0.34	0.33	0.34
-127	9.5 x 10 E-03	$\sqrt{2}$	0	0.31	0.30	0.31
-110	9.29 x 10 E-03	0	$-\sqrt{2}$	0.27	0.28	0.28
-110	9.71 x 10 E-03	0	$\sqrt{2}$	0.27	0.26	0.27

Table 5.31: Results of the CCD of CrN coating.

Figure 5.12 shows the normal plot of R_a residuals. It implies that the R_a value of the second-order model does follow the normal distribution within 95% confidence level.
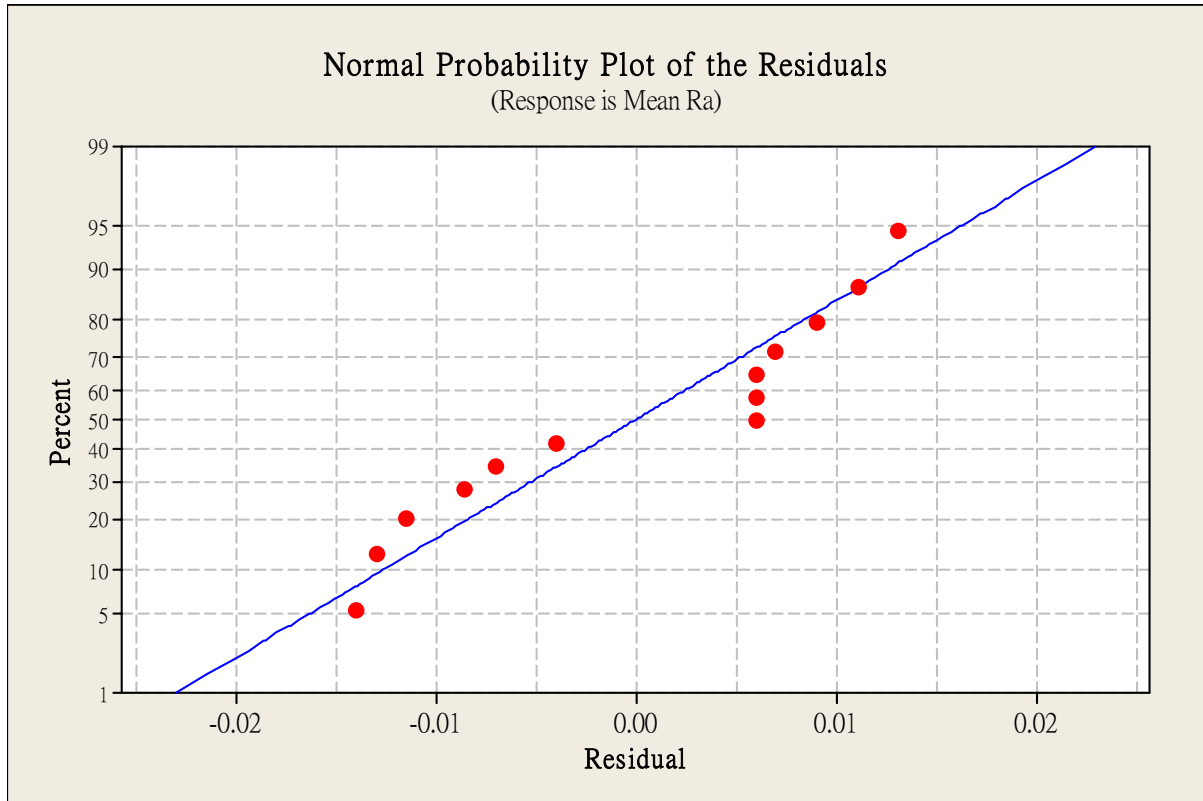
Figure 5.12: Second-order model normal probability plots of residuals for CrN coating.

The second-order model regression equation based on using CCD design was:

$$\hat{y} = 0.254 - 0.013x_1 - 0.004\,x_2 + 0.031\,x_1^2 + 0.006\,x_2^2 - 0\,x_1x_2 \qquad (5\text{-}7)$$

where $\hat{y}$ is the mean R_a value.

From Table 5.32, ANOVA table of the CCD for CrN coating, F = 9.56 is greater than $F_{(0.10,5,7)}$ = 2.88. This implies that regression is significant at the 0.10 level of significance. R^2 = 0.872 and R^2_{adj} = 0.781 shows that most of the variation can be explained by this regression model. Therefore, this model fits.

Source	Degrees of Freedom	Sum of Square	Mean Variance	F	R^2	R^2_{adj}
Regression	5	0.008	0.002	9.56	0.872	0.781
Linear	2	0.002	0.001	1.41		
Square	2	0.009	0.004	3.52		
Interaction	1	0.000	0.000	0.00		
Residual Error	7	0.001	0.000			
Lack of Fit	3	0.001	0.000	3.51		
Pure Error	4	0.000	0.000			
Total	12	0.009				

Table 5.32: ANOVA of second-order model for CrN coating.

After fitting the second-order model to determine the optimum region, stationary points should be found and identified by using partial differentiation of the regressed second-order model.

From Equation (3-6),

$$\hat{y} = \hat{\beta}_0 + \mathbf{x}^T \mathbf{b} + \mathbf{x}^T \mathbf{B} \mathbf{x}$$

where $\mathbf{x} = \begin{bmatrix} x_1 \\ x_2 \\ \vdots \\ x_k \end{bmatrix}$, $\mathbf{b} = \begin{bmatrix} \hat{\beta}_1 \\ \hat{\beta}_2 \\ \vdots \\ \hat{\beta}_k \end{bmatrix}$ and $\mathbf{B} = \begin{bmatrix} \hat{\beta}_{11} & \hat{\beta}_{12}/2 & \cdots & \hat{\beta}_{1k}/2 \\ & \hat{\beta}_{22} & \cdots & \hat{\beta}_{2k}/2 \\ & & \ddots & \\ symmetrical & & & \hat{\beta}_{kk} \end{bmatrix}$.

the second-order fitting regression model could be written as:

$$\hat{y} = 0.254 - [x_1 x_2] \begin{bmatrix} -0.013 \\ -0.004 \end{bmatrix} + \begin{bmatrix} 0.031 & 0 \\ 0 & 0.006 \end{bmatrix} \begin{bmatrix} x_1 \\ x_2 \end{bmatrix} \qquad (5\text{-}4)$$

To examine the surface further, the stationary point $\mathbf{x_s}$ and the yield y_0 should be found.

From Equation (3-8),

$$\mathbf{x}_s = -\tfrac{1}{2}\, \mathbf{B}^{-1} \mathbf{b}.$$

Now,

$$\text{where } \mathbf{B} = \begin{bmatrix} 0.031 & 0 \\ 0 & 0.006 \end{bmatrix}$$

$$\mathbf{B^{-1}} = \frac{1}{|0.00019|}\begin{bmatrix} 0.031 & 0 \\ 0 & 0.006 \end{bmatrix} = \begin{bmatrix} 163.2 & 0 \\ 0 & 31.6 \end{bmatrix}$$

Therefore,

$$\mathbf{x_s} = -\frac{1}{2}\begin{bmatrix} 163.2 & 0 \\ 0 & 31.6 \end{bmatrix}\begin{bmatrix} -0.013 \\ -0.004 \end{bmatrix} = \begin{bmatrix} 1.061 \\ -0.063 \end{bmatrix}$$

Or, the stationary point is at (1.061, -0.063). In terms of the natural variable, the stationary point is at:

$$1.061 = \frac{\xi_1 + 85}{-33.5}, -0.063 = \frac{\xi_2 - (9.5 \text{ x } 10 \text{ E - 03})}{0.5 \text{ x } 10\text{E - 03}}$$

As a result, $\xi_1 = -121\,\text{V}$ of bias voltage and $\xi_2 = 9.46 \text{ x } 10\,\text{E-03mbar}$ of N_2 pressure.

From Equation (3-9),

$$\hat{y}_s = 0.254 + \frac{1}{2}\begin{bmatrix}1.061 & -0.063\end{bmatrix}\begin{bmatrix}-0.013 \\ -0.004\end{bmatrix} = 0.254 - 0.007 = 0.25$$

Finally, canonical analysis is carried out to determine whether the stationary point being found is a local maximum, minimum, or saddle pint. An equation could be set up as follows:

$$|\mathbf{B} - \lambda \mathbf{I}| = 0$$

$$\begin{vmatrix} 0.031 - \lambda & 0 \\ 0 & 0.006 - \lambda \end{vmatrix} = 0$$

which can be reduced to $\lambda^2 - 0.037\lambda + 0.000186 = 0$

The roots of this quadratic equation were $\lambda_1 = 0.025$ and $\lambda_2 = 0.050$. Since the two roots are all positive, the stationary point (1.061, -0.063) is a minimum. Figure 5.13 and Figure 5.14 shows respectively the 3D surface plot and the contour plot of the response yield mean R_a value of CrN coating.

3D Surface Plot for Mean Ra Value in CrN Coating
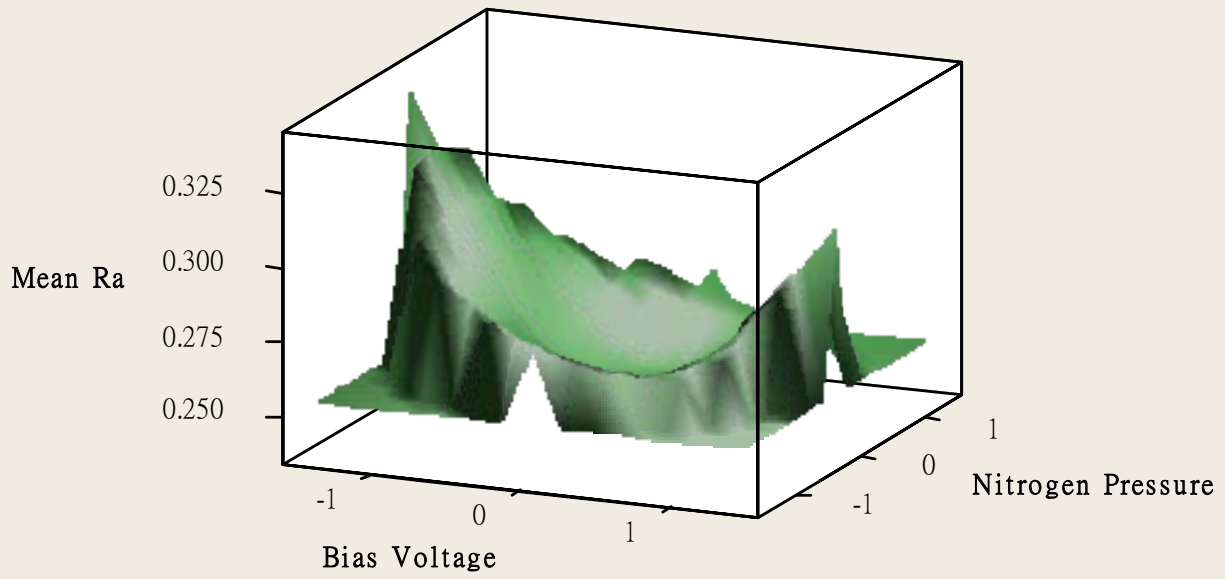
Figure 5.13: 3D surface plot for CrN coating R_a value.

Contour Plot for Mean Ra Value in CrN Coating
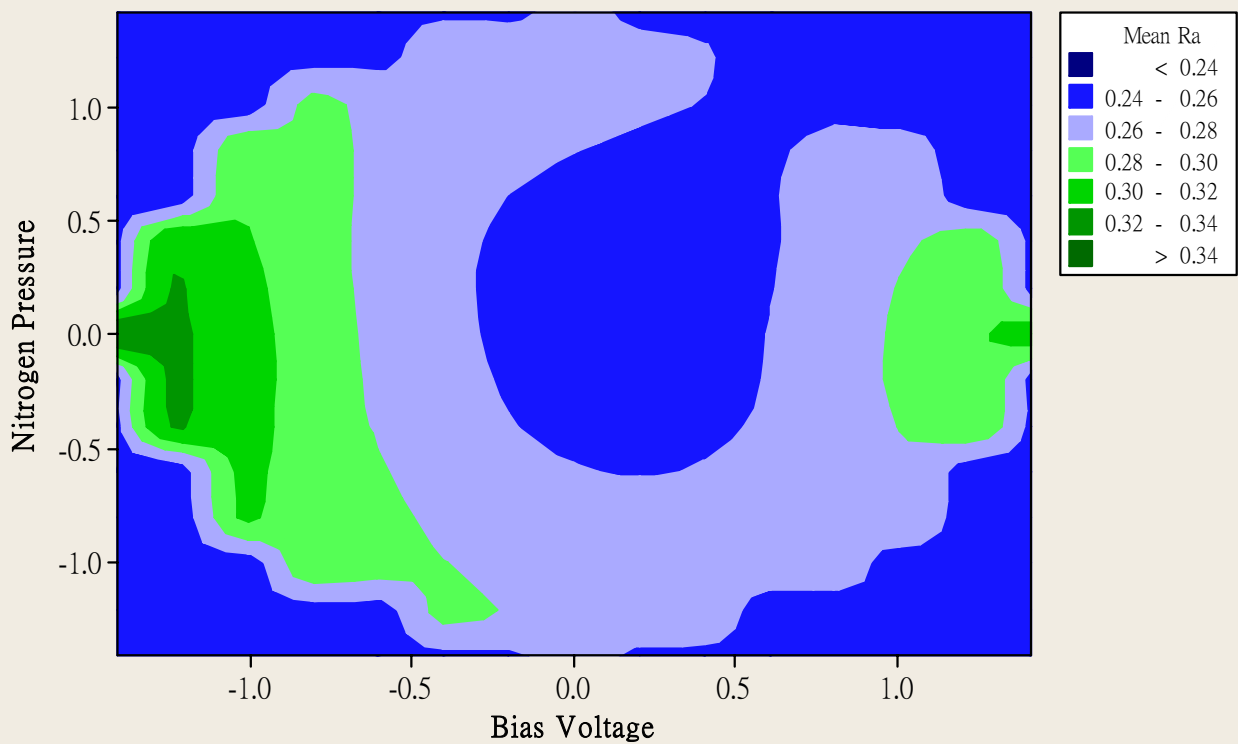
Figure 5.14: Contour plot for CrN coating R_a value.

5.5 Surface Morphology of Different Coatings

Figure 5.15 and Figure 5.16 show the surface morphologies of TiN and CrN coatings by using SEM respectively. During coating process, un-reacted target material and residuals from the chamber could produce droplets. It can be seen that the surface of CrN coating is rougher than TiN coating. The droplets (white spots) number and size was bigger and more in CrN coating. Figure 5.15 and 5.16 shows that Ti and Cr are in white spots and carbon (C) is in gray spots.
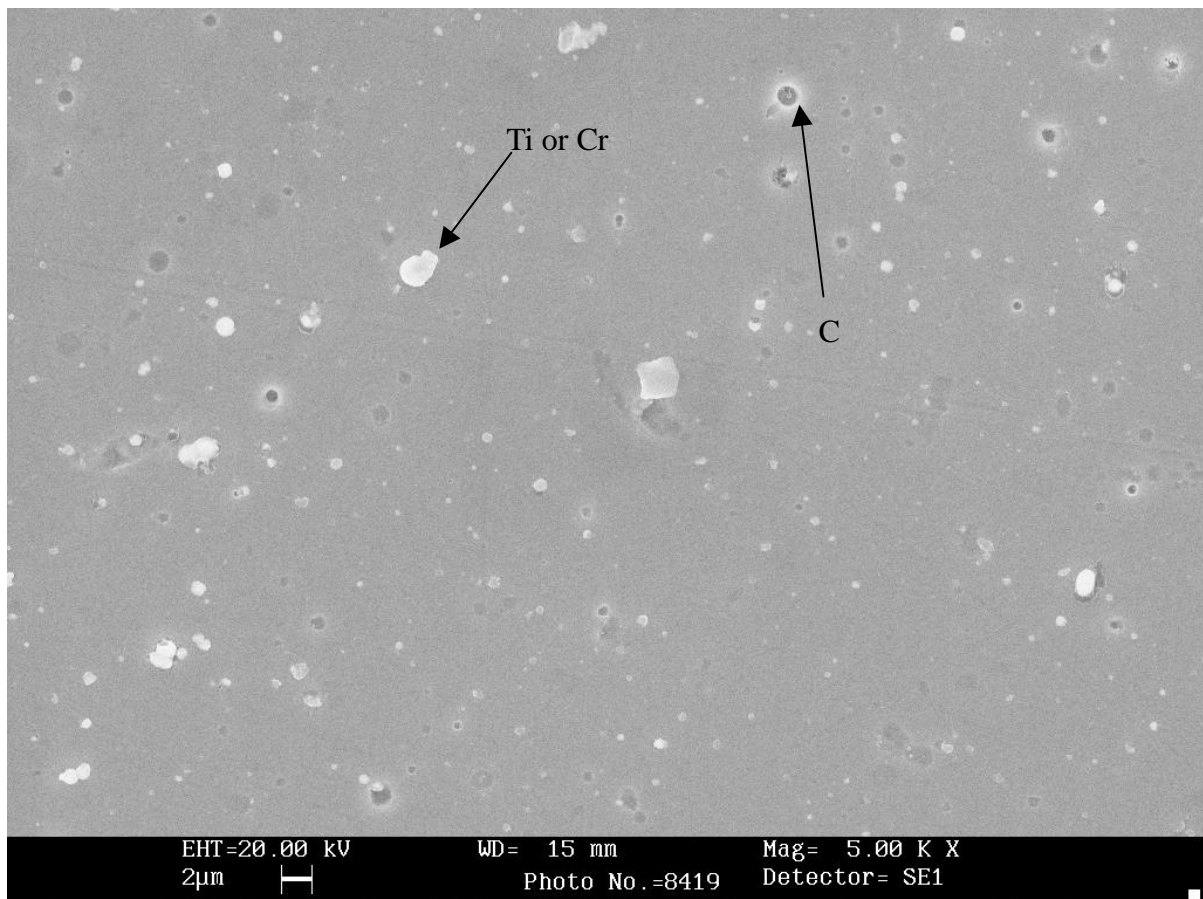
Figure 5.15: SEM photography of TiN coating
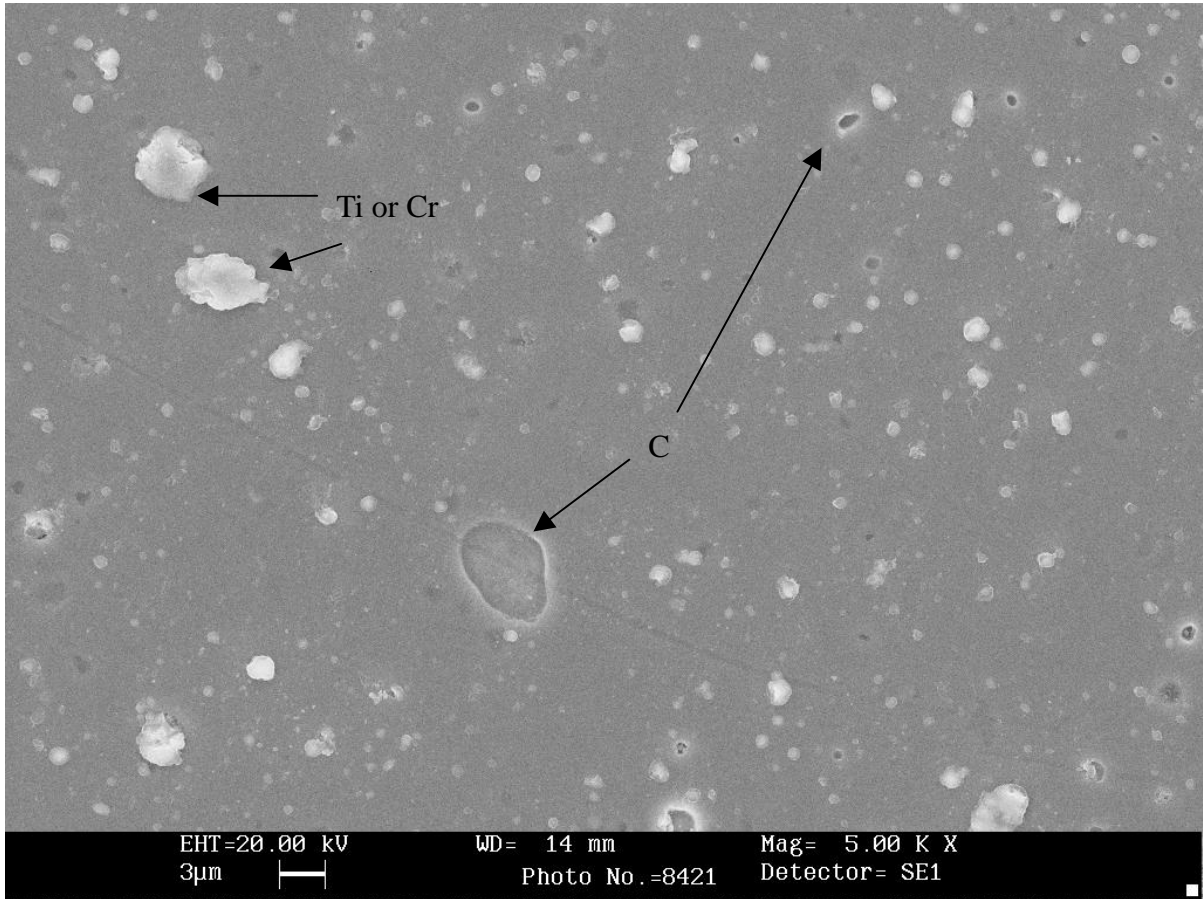
Figure 5.16: SEM photography of CrN coating

5.6 Summary of Results

For TiN coating, roughness test have been conducted for optimization. It is found that the bias voltage was the most critical factor to roughness value whereas the arc current shows less interaction with the roughness in TiN coating.

For CrN coating, the nitrogen pressure was the most critical factor to roughness value whereas the coating time shows less interaction with the roughness.

For further optimization, the Response Surface Method was used to help finding out the optimal region. First, first-order models were found out. Then, steepest ascent experiments were used to obtain the middle point of the first-order fitting model. After that new first-order models were found. And finally, the second-order models were obtained.

For TiN coating, the optimal point is at (0.384, 0.091), where bias voltage = -115V and N_2 pressure = 9.54 x 10E-03 mbar. And this point is a minimum point. For CrN coating, the optimal point is at (1.061, -0.063), where bias voltage = -121V and N_2 pressure = 9.46 x 10E-03 mbar. And this is a minimum point.

CHAPTER 6 DISCUSSION AND FUTURE WORK

6.1 Discussion on Result

Both the Taguchi Method and Response Surface Method (RSM) can help to find out the optimization region and response. In the research, the Taguchi Method is used for screening experiments. Further optimizations are found out by using response surface methods. By combing these two methods, the optimal condition in cathodic arc physical vapor deposition (CAPVD) can be found out and under control.

However, further confirmation experiments on the result of RSM need to be conducted. The actual results may have deviation from the predicted result. This may be due to the errors in the experiments such as the measurement error of R_a value and the chamber condition. Therefore, more experiments should be conducted before bringing the result to production.

On the other hand, in first-order model of TiN, it shows than $R^2_{adj} = 0.779$ which implies the model is better than that of the new first-order model with $R^2_{adj} = 0.64$ and that of the second-order model $R^2_{adj} = 0.031$. In this case, the stationary point, obtained from the second-order model, might not be appropriate. It implies that 3.1% of the variation in R_a value is explained by the second-order model. And 96.9% of sample variability in R_a value is due to other factors.

For CrN coating, the $R^2_{adj} = 0.918$ for first-order model is better than the second-order model, $R^2_{adj} = 0.781$. In the case, minimum stationary point found from second-order model might not be appropriate. For second-order model, it implies that 78.1% of the variation in R_a value is explained by the second-order model. And 21.9% of sample variability in R_a value is due to other factors.

Hypothesis testing can be used to supplement the research methods being adopted. After predicting the R_a value by Taguchi method and RSM, the sample information can be used to assess the validity of some hypothesis.

6.2 Discussion on Method

Other factors will also influence the quality of the characteristic, which can be investigated further. For example, the temperature changing effect on coating process has not been considered in the parameters and it is assumed to be under control. The optimization experiments were also assumed to be conducted under homogeneous conditions. Moreover, the blocking effect on each run has not been investigated. These should be further investigated.

6.3 Limitation

In this research, many different difficulties have to be overcome.

6.3.1 Limitation of Time

The coating experiments are mainly conducted in the teaching company. For CAPVD coating process, it needed about three to five hours for a batch including pumping time for vacuum. If the number of newly experiments was high, the finished time to determine the optimal solution in process would take a long time.

If a twenty-four hours working times was used for the coating centers, five to six batches could be processed in a day. Therefore, the quickest time to finish the experiments is 30 / 5 = 6 days. However, in real production, it is not possible to conduct experiments occupying a whole day due to the high production cost. 1 to 2 batches is already too much for the experiments. Sometimes, only one batch can be run within 2 weeks.

Due to the tight schedule, only the main effect can be considered. If the time schedule is less tight, more experiments can be carried out and more factors can be considered in the screening experiments.

6.3.2 Limitation of Hardware

Being a Teaching Company Scheme (TCS) project, lot of equipment and machine of the company were used. The measuring method should be simple and inexpensive. Otherwise, it will affect the production and planning of the company. If the cost is too high, it is not economic to do so. Therefore, it is a difficult decision to select the suitable methods and apparatus.

Although checking adhesion by using the Mercedes-Benz adhesion method is quick and well developed, the result cannot show the numerical data between the same and difference classes. No numerical compression can be made by using this adhesion method. Moreover, sometimes it was difficult to distinguish the class of the adhesion checked. Especially, it is hard to distinguish the marginal case, the HF3 and HF4 class. It is a difficult decision to accept the quality than to reject in production.

The substrate surface roughness sometimes is relatively higher when comparing with that of the coating in both two coatings. It may be due to the measuring method. For surface profilometer, the measuring tip is drawing a line on the surface in each measurement. The actually R_a value of the substrate surface may not be represented. If there is enough time and resources, atomic force microscope (AFM) can be used to study the surface profile in three dimensions.

6.4 Future Work

6.4.1 Evolutionary

Response surface method is often applied to real production by research and development purpose. However, it is rarely done or very infrequent because the experimental procedure is relatively complex.

One problem for the RSM is that optimum condition for experimental size may not be equal to that of the full-scale process in production. This "scale-up" action for production process usually results in distortion of the optimum conditions. Even if the full-scale plant begins operation at the optimum, it will eventually have variation from that point because of variations in raw materials, environmental changes and operating personnel.

A method is needed for the continuous monitoring and improvement of a full-scale process with the goal of moving the operating conditions toward the optimum or following a "shift". At the same time, this method shall not bring large or sudden changes in operating conditions that might disrupt the production.

Evolutionary operation (EVOP) was proposed by Box (1957) as such an operating procedure. It is designed as a method for routine plant and production operation that is carried out by manufacturing personnel with minimum assistance from the research and development staff.

The operation consists of introducing small changes in the levels of the operating variables under consideration. Usually, a 2^k design is employed to do so. The changes in the variables are assumed to be small enough that serious disturbances in quality and quantity will not happen. Large enough potential improvements in process performance will finally be discovered. Data are collected on the response variables of interest at each point of the 2^k design. When one observation has been taken at each design point, a cycle is completed. Then, the effects and interactions of the process variables may be computed.

After several cycles, the effect of one or more process variables or their interactions may show to have a significant effect on the response. At this point, decisions may be made to change the basic operating conditions to improve the response. A phase is completed when improved conditions have been decided (Montgomery, 2005 and Box, 1957).

When testing the significance of process variables and interactions, an approximation of experimental error is required. This is calculated from the cycle data. Again, the 2^k design is usually centered about the current best operating conditions. By comparing the response at this point with the 2^k points in the factorial portion, it may check on curvature or change in mean. It means that if the process is really centered at the maximum, the response at the center should be significantly greater than the responses at the 2^k-peripheral points. In theory, EVOP can be applied to k process variables. In practice, not more than two or three variables are usually considered (Montgomery, 2005 and Box, 1957).

6.4.2 Multi-characteristics by Taguchi Method and Utility Concept

Taguchi method is usually focused on off-line experiments by considering single quality characteristic, performance or response. For several responses, Taguchi method may not provide further desired results at the same time.

Outcome of any process is judged by quality of final product. For example, in Platit PVD coating, surface roughness is "lower the best" type of quality characteristic whereas hardness of coating is "higher the best" type. To meet several requirements and optimize several responses at once, multi-characteristics response method using Taguchi methods and utility concept may provide a better solution.

Figure 6.1 shows the fishbone diagram for Platit PVD coating process quality. In Platit PVD coating process, the characteristics or qualities are surface roughness Ra value, adhesion, coating thickness and wear of resistance.
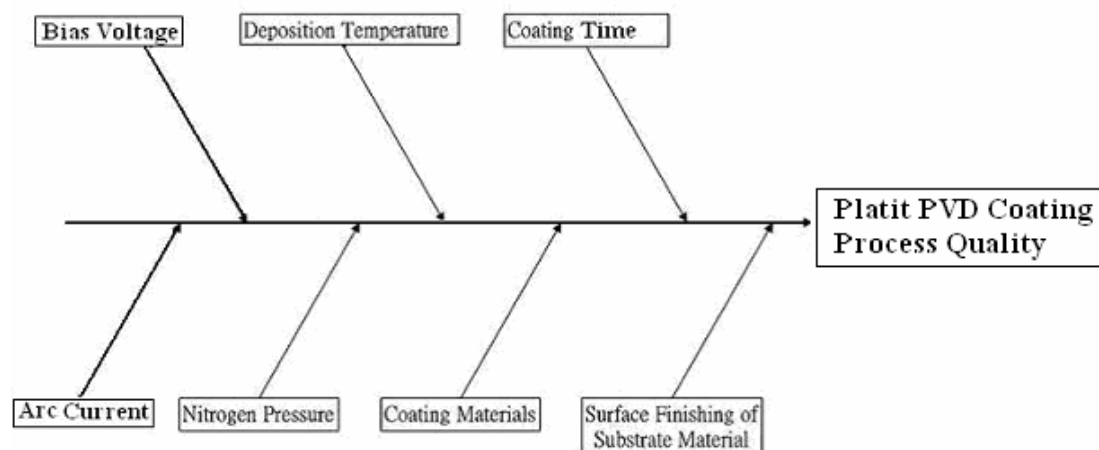
Figure 6.1 Fishbone diagram for Platit PVD coating process quality.

To evaluate a product based on a number of diverse qualitative characteristics. To be able to make a rational choice, the evaluations of various characteristics should be combined to give a composite index. This composite index represents the utility of a product. The overall utility of a product measures the usefulness of that product. However, the utility of a product with respect to a particular characteristic measures the usefulness of the particular characteristic only (Kumar *et al.*, 2000).

A joint function can express the overall utility of a product quality characteristic (Kumar *et al.*, 2000):

$$U(X_1, X_2, \dots X_n) = f(U_1(X_1), U_2(X_2), \dots, U_n(X_n)) \qquad (6\text{-}1)$$

where X_i is the measure of effectiveness of characteristic or response, i and n are characteristic or responses evaluating the outcome space.

Assuming that the characteristics are independent and have no interactions between them, and the overall utility function is a linear sum of individual utilities, the overall utility function becomes (Kumar *et al.*, 2000):

$$U(X_1, X_2, \dots X_n) = \sum_{i=1}^{n} U_i(X_i) \qquad (6\text{-}2)$$

Depending on the product requirement, the characteristics or attributes may be given

priorities or weights. Thus, the general or weighted form of Equation (6-2) can be expressed as:

$$U(X_1, X_2, \ldots, X_n) = \sum_{i=1}^{n} W_i U_i(X_i) \qquad (6\text{-}3)$$

To determine the utility value for a number of quality characteristics, a preference order is considered. These orders are weighted to obtain the overall utility.

The sum of attributes is equal to 1. If the overall utility is maximized, the qualitative characteristics are considered to be automatically maximized or minimized.

A preference scale for each characteristic is created to determine the utility value for quality characteristic. The scale which depends on the quality characteristics is set from minimum acceptable at 0 to the best quality at 9. If a log scale is chosen, the preference number P_i is (Kumar *et al.*, 2000):

$$P_i = A \log \frac{X_i}{X_i'} \qquad (6\text{-}4)$$

where X_i is the value of quality characteristic, X_i' is the minimum acceptable value of the quality characteristic i and A is a constant. One may choose $P_i = 9$ at $X_i = X^*$, where X^* is the optimum value of X_i assuming such a number exists.

The weight shall be assigned as $\sum_{i=1}^{n} W_i = 1$ and W_i is the weight assigned to attribute i.

The overall utility can be calculated as:

$$U = \sum_{i=1}^{n} W_i P_i \qquad \text{(6-5)}$$

The sum of the overall utility function can be calculated as:

$$U(n, R) = P_1(n, R)xW_1 + P_{2(}n, R)xW2 + \ldots + P_i(n, R)xW_i \qquad \text{(6-6)}$$

where n is the number of trail, and R is the repetition number.

After finding the utility value, the predicted optimal value in means will be found out by further calculation.

This multi-characteristic consideration method can be used to find out the optimal setting when considering several characteristics at the same time. If further experiments can be done, it can be used to find the best settings for optimal wear resistance, surface roughness, friction, and internal stress.

Although this method is first proposed by Kumar *et al.* at 2000, which was suggested before the starting date of this study, the company resources limited the research opportunities. In this stage, the company wants to mainly concern the surface roughness of the customer requirement. In the future, if the resources can be improved and increased, other characteristics of coating may be considered.

6.4.3. Nano-composite Coating

The first industry size nano-composite coating machine is provided by Platit AG in 2002. This is a new trend in this century. Nano-composite coating is just being started to provide better tool life and heat resistance to cutting tools (Nakonechna, 2004). However, no study is carried out on the mold application. The application of nano-composite will be a great value to the industry.

Figure 6.2: The latest PLATIT π80 PVD coating machine for nano-composite coating (PLATIT).

CHAPTER 7 CONCLUSIONS

A comprehensive literature review on different coatings, coating processes, and optimization method were carried out in the study. Taguchi Method and Response Surface Method (RSM) were used to investigate surface roughness R_a value of the titanium nitride and chromium nitride coatings.

The coating machine is the PLATIT PL 50 of PLATIT AG cathodic arc deposition system. After coating, surface profilometer is used to analyze the mean roughness value (R_a). The Daimler-Benz Rockwell-C adhesion test method is used to investigate the adhesion of the coating. And Scanning Electron Microscope (SEM) is used to analyze the surface morphology of the coating.

By using the cause-and-effect diagram, the coating parameters that affect the coatings were identified. They are bias voltage, arc current, nitrogen pressure and coating time.

After analyzing with the Taguchi Method, it is found that the main effect is factor A, the bias voltage. When bias voltage = –110V, arc current = 120, nitrogen pressure = 8.0 x 10 E-03mbar and coating time = 50mins., the optimal condition can be obtained in titanium nitride coating process. After further investigation by using RSM, it is found that optimal conditions with a R_a value 0.23μm can be reached when the bias voltage = -115V and the nitrogen pressure = 9.54 x 10E-03mbar.

For chromium nitride coating, after analyzing with the Taguchi Method, it is found that the main effect is factor C, the nitrogen pressure. When bias voltage = –80V, arc

current = 110A, nitrogen pressure = 10 x 10E-03mbar, and coating time = 57mins., the optimal condition can be obtained in the coating process. After further investigation by using RSM, it is found that optimal conditions with a R_a value 0.25μm can be reached when the bias voltage = -121V and the nitrogen pressure = 9.46 x 10E-03mbar.

For future work, evolutionary solution is suggested to run RSM in a real production size and practice. Furthermore, a multi-characteristic response method using Taguchi method and utility concept together can help to find out the optimal condition when several characteristics are needed to consider at the same time.

REFERENCES

1. André, I.K. and John, A. C., Response Surfaces: Designs and Analyses, Marcel Dekker, 1996.

2. Attar, F. and Johannesson, T., "Adhesion evaluation of thin ceramic coating on tool steel using the scratch testing technique" Surface and Coating Technology, Vol. 78, p.87-102, 1996.

3. Babu, M.V., Kumar, R.K், Prabhakar, O., and Shankar, N.G., "Simultaneous optimization of flame spraying process parameters for high quality molybdenum coatings using Taguchi methods", Surface and Coatings Technology, Vol.79, p.276-288, 1996.

4. Baouchi, A.W. and Perry, A.J., "A study of the macroparticle distribution in Cathodic arc evaporated TiN films", Surface and Coatings Technology, Vol. 49, p.253-257, 1991.

5. Beckford, J., Quality: A Critical Introduction, Routledge, 1998.

6. Bliznakovska, B. and Milosevski, M., Analysis methods and techniques for hard thin layer – coatings characterization – in particular on Titanium Nitride, Forschungszentrum Julich GmbH, 1993.

7. Box, G.E.P., "Evolutionary operation: A method for increasing industrial productivity", Applied Statistics, Vol. 6 (1), p.81-101, 1957.

8. Cheng, C.C., Young, M.S., Chuang, C.L., and Chang, C.C., "Fabrication optimization of carbon fiber electrode with Taguchi method", Biosensors and Bioelectronics, Vol.18, p.847-855, 2003.

9. Chou, W.J., Sun, C.H., Yu, G.P, and Huang, J.H., "Optimization of the deposition process of ZrN and TiN thin films on Si(1 0 0) using design of experiment method", Materials Chemistry and Physics, Vol.82, p.228-236, 2003.

10. Daimler–Benz Adhesion Test, Verein Deutscher Ingenieure (VDI), Richlinie 3198, p.7, 1992.

11. Donald, M.M., Handbook of Physical Vapor Deposition (PVD) Processing: Film Formation, Adhesion, Surface Preparation and Contamination Control, Noyes Publications, 1998.

12. Dynamic Ceramic, http://www.dynacer.com/coatings.htm#Plasma.

13. Gell, M., Xie, L., Ma, X., Jordan, E.H., and Padture, N.P., "Highly durable thermal barrier coatings made by the solution precursor plasma spray process", Surface and Coatings Technology, Vol.177-178, p.97-102, 2004.

14. Ghani, J.A., Choudhury, I.A., and Hassan, H.H., "Application of Taguchi method in the optimization of end milling parameters", Journal of Material Processing Technology, Vol.145, p. 84-92, 2003.

15. Graham, T., Industrial Metrology: Surfaces and Roundness, Springer, 2002.

16. Gupta, T.K., Handbook of thick- and thin-film hybrid microelectronics, John Wiley, 2003.

17. Guzman, L., Bonelli, M., Miotello, A., and Kothari, D.C., "Process parameters optimization for TiN and TiC formation using reactive ion beam assisted deposition", Surface and Coatings Technology, Vol.100-101, p.500-502, 1998.

18. Hajjaji, S.E., Lgamri, A., Puech-Costes, E., Guenbour, A., Ben Bachir, A., and Aries, L., "Optimization of conversion coatings: Study of the influence of parameters with experimental designs", Applied Surface Sciences, Vol.165, p.184-192, 2000.

19. Harris, S.G., Doyle, E.D., Wong, Y.C., Munroe, P.R., Cairney, J.M., and Long, J.M., "Reducing the macroparticle content of Cathodic arc evaporated TiN coatings", Surface and Coatings Technology, Vol. 183, p.283-294, 2004.

20. Hofmann, D., Hensel, B., Yasuoka, M., and Kato, N., "New multilayer PVD-coating technique for cutting tools", Surface & Coating Technology, Vol.61, p. 326-330, 1993.

21. Hong Kong Productivity Council, http://www.hkpc.org.hk.

22. Hu, C.C., Tsay, C.H., and Bai, A., "Optimization of the hydrogen evolution activity on zinc-nickel deposits using experimental strategies", Electrochimica Acta, Vol.48, p.907-918, 2003.

23. Huang, S., Neural Network Control: Theory and Applications, Research Studies Press, 2004.

24. Jacobsson, R., Measurement of the adhesion of thin films, Thin Solid Films, Vol. 34, p.191-199, 1976.

25. Jeffrey, H.A., Ionized Physical Vapor Deposition, Academic Press, 2000.

26. Jing Mei Group of Companies, http://www.jmi.com.hk.

27. John, M.E., Physical Vapor Deposition of Thin Films, John Wiley & Sons, 2000.

28. Kelly, P.J. and Arnell, R.D., "The influence of substrate temperature on the properties of Al, Zr and W coatings deposited by closed-field unbalanced magnetron sputtering", Surface and Coatings Technology, Vol.49, p.43-47, 1998.

29. Knotek, O., Loffler, F., and Bosserhoff, B., "PVD coating for die casting moulds", Surface & Coating Technology, Vol.62, p. 630-634, 1993.

30. Kumar, P., Barua, P.B., and Gaindhar, J.L., "Quality optimization (multi-characteristics) through Taguchi's technique and utility concept", Quality and Reliability Engineering International, Vol.16, p.475-485, 2000.

31. Lai, J.F., Liao, H., Normand, B., Cordier, C., Maurin, J., Foct, G., and Coddet, C., "Uniform design method for optimization of process parameters of plasma sprayed TiN coatings", Surface and Coatings Technology, Vol.176, p.1-13, 2003.

32. Li, D.J. and Gu, H.Q., "Cell attachment on diamond-like carbon coating", Bulletin of Material Science, Vol. 25, p.7-13, No.1, February, 2003.

33. Lin, K.L., Hwang, M.Y., and Wu, C.D., "The deposition and wear properties of cathodic arc plasma deposition TiAlN deposits", Materials Chemistry and Physics, Vol.46, p.77-83, 1999.

34. Lin, T.R., "Experimental design and performance analysis of TiN-coated carbide tool in face milling stainless steel", Journal of Material Processing Technology, Vol.127, p.1-7, 2002.

35. Liu, P., Fuzzy Neural Network Theory and Application, River Edge, 2004.

36. Lossen, J., Klein, S. and Finger, F., "Optimization of the filament arrangement at constant radiant heat in HW-CVD for the preparation of compact (c-Si:H at high deposition rates)", Thin Solid Films, Vol.451-452, p.531-535, 2004.

37. Meijer, M.D., "Analysis of the wet adhesion of coatings on wood", Adhesion Aspects of Polymeric Coatings, Vol. 2, p. 183-201, 2003.

38. Mittal, K.L., Adhesion measurement of films and coatings, VSP, 1995.

39. Montgomery, D.C., Design and Analysis of Experiments, John Wiley & Sons, 2005.

40. Montgomery, D.C., Introduction to Statistical Quality Control, John Wiley & Sons, 1985.

41. Mouche, M.J., Mermet, J.L., Pires, F., Richard, E., Torres, J., Palleau, J., and Braud, F., "Process optimization of copper MOCVD using modeling experimental design", Applied Surface Science, Vol.91, p.129-133, 1955.

42. Mudali, U.K., Sridhar, T.M., and Raj, B., "Corrosion of bio implants", Sadhana, Vol. 28, Part 3 & 4, p. 601-637, June / August 2003.

43. Nalwa, H.S., Handbook of thin film materials - Volume 1 – Deposition and processing of thin films, Academic Press, 2002.

44. Nakonechna, O., Cselle, T., Morstein, M., and Karimi, A., "On the behaviour of indentation fracture in TiAlSiN hard thin films", Thin Solid Films, Vol. 447-448, p.406-412, 2004.

45. George, P.M., Raghunath, B.K., Manocha, L.M., and Warrier, A.M., "EDM machining of carbon-carbon composite – a Taguchi approach'', Journal of Materials Processing Technology, Vol.145, p.66-71, 2004.

46. Phillip, R.J., Taguchi techniques for quality engineering: Loss Function, Orthogonal Experiments, Parameter and Tolerance Design, McGraw-Hill, 1996.

47. PLATIT AG, http://www.platit.com.

48. Ryan, T.P., Statistical Methods for Quality Improvement, John Wiley & Sons, 2000.

49. Ryntz, R.A., "Attaining adhesion / cohesion within painted plastics", Adhesion Aspects of Polymeric Coatings, Vol. 2, p. 29-43, 2003.

50. Sarwar, M., Zhang, X.Y., and Gilliband, D., "Performance of titanium nitride-coated carbide-tipped circular saws when cutting stainless steel and mild steel", Surface & Coating Technology, Vol.94-95, p. 617-621, 1997.

51. Sato, K., Ichimiya, Kondo, N.A., and Tanaka, Y., "Microstructure and mechanical properties of cathodic arc ion-plated (Al,Ti)N coatings", Surface and Coatings Technology, Vol.163-164, p.135-143, 2003.

52. Schulz, A., Stock, H.R., Mayr, P., Staeves, J., and Schmoeckel, D., "Deposition and investigation of TiN PVD coatings on cast steel forming tools", Surface and Coatings Technology, Vol.94-95, p.446-450, 1997.

53. SHM, http://www.shm-cz.cz/eng/index.html.

54. Soković, M. and Bahor, M., "On the inter-relationships of some machinability parameters in finish machining with cermet TiN (PVD) coated tools", Journal of Material Processing Technology, Vol.176, p.213-221, 1998.

55. Stuart, P.G., Taguchi Methods: A Hand-on Approach, Addison-Wesley Publishing Company, 1993.

56. Su, Y.L., Yao, S.H., Wei, C.S. and Wu, C.T., "Analysis and design of a WC milling cutter with TiCN coating", Wear, Vol.215, p.59-66, 1998.

57. Su, Y.L., Yao, S.H., Wei, C.S., Wu, C.T., and Kao, W.H., "Design of a titanium nitride-coated WC milling cutter", Journal of Material Processing Technology, Vol.86, p.233-236, 1998.

58. The Hong Kong Polytechnic University Materials Research Centre (MRC), http://www.polyu.edu.hk/mrc.

59. Tsao, C.C. and Hong, H.C., "Comparison of the tool life of tungsten carbides coated by multi-layer TiCN and TiAlCN for end mills using the Taguchi method", Journal of Material Processing Technology, Vol.123, p.1-4, 2000.

60. Valli, J., "A review of adhesion test methods for thin hard coatings", Journal of Vacuum Science and Technology A (Vacuum, Surfaces, and Films), Vol. 4 (6), p.3007 - 3014, 1986.

61. Villiger, P., Sprecher, C., and Peters, J.A., "Parameter optimization of Ti-DLC coatings using statistically based methods", Surface and Coatings Technology, Vol.116-119, p.585-590, 1999.

62. Wu, Y. and Wu, A., Taguchi Methods for Robust Design, Three Park Avenue, 2000.

63. Zhitomirsky, V.N., Grimberg, I., Rapoport, L., Boxman, R.L., Travitzky, N.A., Goldsmith, S., and Weiss, B.Z., "Bias voltage and incidence angle effects on the structure and properties of vacuum arc deposited TiN coating", Surface and Coating Technology, Vol.133-134, p.114-120, 2000.

64. Zhou, J.G., Herscovici, D., and Chen, C.C., "Parametric process optimization to improve the accuracy of rapid prototyped stereolithography parts", International Journal of Machine Tools and Manufacture, Vol.40, p. 363-379, 2000.

65. Zircotec, http://www.zircotec.com/ortho.html.

APPENDIX A

Full factorial design for four factors with three levels will take 81 runs. Three levels are represented by '-1', '0' and '1'(Montgomery, 2005).

Run Order	A	B	C	D
1	-1	-1	-1	-1
2	-1	-1	-1	0
3	-1	-1	-1	1
4	-1	-1	0	-1
5	-1	-1	0	0
6	-1	-1	0	1
7	-1	-1	1	-1
8	-1	-1	1	0
9	-1	-1	1	1
10	-1	0	-1	-1
11	-1	0	-1	0
12	-1	0	-1	1
13	-1	0	0	-1
14	-1	0	0	0
15	-1	0	0	1
16	-1	0	1	-1
17	-1	0	1	0
18	-1	0	1	1
19	-1	1	-1	-1
20	-1	1	-1	0
21	-1	1	-1	1
22	-1	1	0	-1
23	-1	1	0	0
24	-1	1	0	1
25	-1	1	1	-1
26	-1	1	1	0
27	-1	1	1	1
28	0	-1	-1	-1
29	0	-1	-1	0
30	0	-1	-1	1

31	0	-1	0	-1
32	0	-1	0	0
33	0	-1	0	1
34	0	-1	1	-1
35	0	-1	1	0
36	0	-1	1	1
37	0	0	-1	-1
38	0	0	-1	0
39	0	0	-1	1
40	0	0	0	-1
41	0	0	0	0
42	0	0	0	1
43	0	0	1	-1
44	0	0	1	0
45	0	0	1	1
46	0	1	-1	-1
47	0	1	-1	0
48	0	1	-1	1
49	0	1	0	-1
50	0	1	0	0
51	0	1	0	1
52	0	1	1	-1
53	0	1	1	0
54	0	1	1	1
55	1	-1	-1	-1
56	1	-1	-1	0
57	1	-1	-1	1
58	1	-1	0	-1
59	1	-1	0	0
60	1	-1	0	1
61	1	-1	1	-1
62	1	-1	1	0
63	1	-1	1	1
64	1	0	-1	-1
65	1	0	-1	0
66	1	0	-1	1
67	1	0	0	-1

68	1	0	0	0
69	1	0	0	1
70	1	0	1	-1
71	1	0	1	0
72	1	0	1	1
73	1	1	-1	-1
74	1	1	-1	0
75	1	1	-1	1
76	1	1	0	-1
77	1	1	0	0
78	1	1	0	1
79	1	1	1	-1
80	1	1	1	0
81	1	1	1	1

Table A-1: Full factorial table for four factors and three levels.

APPENDIX B
<u>Techmart Platit Process Flow Chart</u>

Receipt of goods

<u>Data Processing</u>
Order no., customer data, type of tools, amount, dimension, material, and date of delivery

In Quality Control

Fail

Pass

Storage

Non-coatable and inform representatives

Demagnetize

Loading for cleaning

Packing and Shipping return to customers

Loading

Cleaning Process

Loading for coating

Coating Process

Rework of coating

Fail

Out Quality Control

Fail

Non-coatable and information representatives

Pass

Packing and Shipping to customers

Figure B-1: Techmart Platit process flow chart

APPENDIX C

Substrate cleaning is very importance for PVD coating process. It is to make sure that a "true" surface for coating layer is provided. Any residuals, dirt and oils leave on the coating surface will cause peel off of coating.

The cleaning process for substrate includes:

   a. Ultrasonic cleaning by cleaning solvent for 10 minutes,

   b. Pure water rinsing for 5 minutes,

   c. Ultrasonic cleaning by cleaning solvent for 10 minutes,

   d. Pure water rinsing for 5 minutes,

   e. Pure water rinsing for 3 minutes and

   f. Dry out substrates by dryer for 30 minutes to 1 hours, which will depend on the size of substrates.

Techmart Platit Cleaning Line Process Flow

```
┌─────────────────────────────┐
│  Ultrasonic cleaning to remove │
│            dirts              │
│        (10 minutes)          │
└─────────────────────────────┘
              │
              ▼
┌─────────────────────────────┐
│    Rinsing by pure water     │
│        (10 minutes)          │
└─────────────────────────────┘
              │
              ▼
┌─────────────────────────────┐
│  Ultrasonic cleaning to remove │
│             oil              │
│        (10 minutes)          │
└─────────────────────────────┘
              │
              ▼
┌─────────────────────────────┐
│    Rinsing by pure water     │
│         (5 minutes)          │
└─────────────────────────────┘
              │
              ▼
┌─────────────────────────────┐
│    Rinsing by pure water     │
│         (3 minutes)          │
└─────────────────────────────┘
              │
              ▼
┌─────────────────────────────┐
│       Dry out by dryer       │
│  (30 minutes to 1 hour, depend │
│     on the substrates size)  │
└─────────────────────────────┘
```
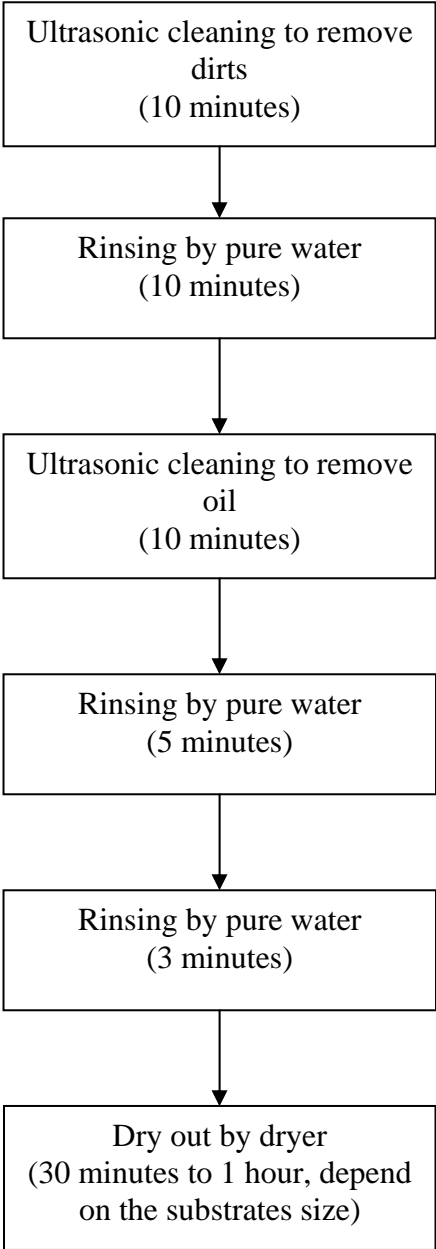
Figure C-1 Cleaning workflow for substrate.

APPENDIX D

F Values of Degree of Freedom for Denominator from 1 - 10

Degrees of Freedom for Denominator	Alpha	Degrees of Freedom for Numerator														
		1	2	3	4	5	6	7	8	9	10	11	12	13	14	15
1	0.25	5.83	7.50	8.20	8.58	8.82	8.98	9.10	9.19	9.26	9.32	9.37	9.41	9.44	9.47	9.49
	0.10	39.86	49.50	53.59	55.83	57.24	58.20	58.91	59.44	59.86	60.20	60.47	60.71	60.90	61.07	61.22
	0.05	161.45	199.50	215.71	224.58	230.16	233.99	236.77	238.88	240.54	241.88	242.98	243.91	244.69	245.36	245.95
	0.01	4052.18	4999.50	5403.13	5624.58	5763.65	5858.99	5928.36	5981.07	6022.47	6055.85	6083.32	6106.32	6125.86	6142.67	6157.28
2	0.25	2.57	3.00	3.15	3.23	3.28	3.31	3.34	3.35	3.37	3.38	3.39	3.39	3.40	3.41	3.41
	0.10	8.53	9.00	9.16	9.24	9.29	9.33	9.35	9.37	9.38	9.39	9.40	9.41	9.41	9.42	9.42
	0.05	18.51	19.00	19.16	19.25	19.30	19.33	19.35	19.37	19.38	19.40	19.41	19.41	19.42	19.42	19.43
	0.01	98.50	99.00	99.16	99.25	99.30	99.33	99.36	99.37	99.39	99.40	99.41	99.42	99.42	99.43	99.43
3	0.25	2.02	2.28	2.36	2.39	2.41	2.42	2.43	2.44	2.44	2.44	2.45	2.45	2.45	2.45	2.46
	0.10	5.54	5.46	5.39	5.34	5.31	5.28	5.27	5.25	5.24	5.23	5.22	5.22	5.21	5.20	5.20
	0.05	10.13	9.55	9.28	9.12	9.01	8.94	8.89	8.85	8.81	8.79	8.76	8.74	8.73	8.71	8.70
	0.01	34.12	30.82	29.46	28.71	28.24	27.91	27.67	27.49	27.35	27.23	27.13	27.05	26.98	26.92	26.87
4	0.25	1.81	2.00	2.05	2.06	2.07	2.08	2.08	2.08	2.08	2.08	2.08	2.08	2.08	2.08	2.08
	0.10	4.54	4.32	4.19	4.11	4.05	4.01	3.98	3.96	3.94	3.92	3.91	3.90	3.89	3.88	3.87
	0.05	7.71	6.94	6.59	6.39	6.26	6.16	6.09	6.04	6.00	5.96	5.94	5.91	5.89	5.87	5.86
	0.01	21.20	18.00	16.69	15.98	15.52	15.21	14.98	14.80	14.66	14.55	14.45	14.37	14.31	14.25	14.20
5	0.25	1.69	1.85	1.88	1.89	1.89	1.89	1.89	1.89	1.89	1.89	1.89	1.89	1.89	1.89	1.89
	0.10	4.06	3.78	3.62	3.52	3.45	3.40	3.37	3.34	3.32	3.30	3.28	3.27	3.26	3.25	3.24
	0.05	6.61	5.79	5.41	5.19	5.05	4.95	4.88	4.82	4.77	4.74	4.70	4.68	4.66	4.64	4.62
	0.01	16.26	13.27	12.06	11.39	10.97	10.67	10.46	10.29	10.16	10.05	9.96	9.89	9.82	9.77	9.72
6	0.25	1.62	1.76	1.78	1.79	1.79	1.78	1.78	1.78	1.77	1.77	1.77	1.77	1.77	1.76	1.76
	0.10	3.78	3.46	3.29	3.18	3.11	3.05	3.01	2.98	2.96	2.94	2.92	2.90	2.89	2.88	2.87
	0.05	5.99	5.14	4.76	4.53	4.39	4.28	4.21	4.15	4.10	4.06	4.03	4.00	3.98	3.96	3.94
	0.01	13.74	10.92	9.78	9.15	8.75	8.47	8.26	8.10	7.98	7.87	7.79	7.72	7.66	7.60	7.56
7	0.25	1.57	1.70	1.72	1.72	1.71	1.71	1.70	1.70	1.69	1.69	1.69	1.68	1.68	1.68	1.68
	0.10	3.59	3.26	3.07	2.96	2.88	2.83	2.79	2.75	2.72	2.70	2.68	2.67	2.65	2.64	2.63
	0.05	5.59	4.74	4.35	4.12	3.97	3.87	3.79	3.73	3.68	3.64	3.60	3.57	3.55	3.53	3.51
	0.01	12.25	9.55	8.45	7.85	7.46	7.19	6.99	6.84	6.72	6.62	6.54	6.47	6.41	6.36	6.31
8	0.25	1.54	1.66	1.67	1.66	1.66	1.65	1.64	1.64	1.64	1.63	1.63	1.62	1.62	1.62	1.62
	0.10	3.46	3.11	2.92	2.81	2.73	2.67	2.62	2.59	2.56	2.54	2.52	2.50	2.49	2.48	2.46
	0.05	5.32	4.46	4.07	3.84	3.69	3.58	3.50	3.44	3.39	3.35	3.31	3.28	3.26	3.24	3.22
	0.01	11.26	8.65	7.59	7.01	6.63	6.37	6.18	6.03	5.91	5.81	5.73	5.67	5.61	5.56	5.52
9	0.25	1.51	1.62	1.63	1.63	1.62	1.61	1.60	1.60	1.59	1.59	1.58	1.58	1.58	1.57	1.57
	0.10	3.36	3.01	2.81	2.69	2.61	2.55	2.51	2.47	2.44	2.42	2.40	2.38	2.36	2.35	2.34
	0.05	5.12	4.26	3.86	3.63	3.48	3.37	3.29	3.23	3.18	3.14	3.10	3.07	3.05	3.03	3.01
	0.01	10.56	8.02	6.99	6.42	6.06	5.80	5.61	5.47	5.35	5.26	5.18	5.11	5.05	5.01	4.96
10	0.25	1.49	1.60	1.60	1.59	1.59	1.58	1.57	1.56	1.56	1.55	1.55	1.54	1.54	1.54	1.53
	0.10	3.28	2.92	2.73	2.61	2.52	2.46	2.41	2.38	2.35	2.32	2.30	2.28	2.27	2.26	2.24
	0.05	4.96	4.10	3.71	3.48	3.33	3.22	3.14	3.07	3.02	2.98	2.94	2.91	2.89	2.86	2.85
	0.01	10.04	7.56	6.55	5.99	5.64	5.39	5.20	5.06	4.94	4.85	4.77	4.71	4.65	4.60	4.56

Table D-1: F Values of degree of freedom for denominator from 1 – 10 (Montgomery, 2005).